Supporting Information

Pure Blue Phosphorescent Platinum(II) Emitters Supported by NHC-Based Pincer Type Ligands with Unitary Emission Quantum Yields

Jie Liu,†[a] Tsz-Lung Lam,†[ab] Man-Ki Sit,[a] Qingyun Wan,[a] Chen Yang,[a] Gang Cheng,*[abc] Chi-Ming Che*[abc]

[a] State Key Laboratory of Synthetic Chemistry, Department of Chemistry, The University of Hong Kong, Pokfulam Road, Hong Kong SAR, P. R. China.

[b] Hong Kong Quantum AI Lab Limited, Units 909–915, Building 17W, 17 Science Park West Avenue, Hong Kong Science Park, Pak Shek Kok, Hong Kong SAR, P. R. China.

[c] HKU Shenzhen Institute of Research and Innovation, Shenzhen, Guangdong 518057, P. R. China.

Experimental Section

1,3-dibromo-5-(trifluoromethyl)benzene, 1,3-dibromo-4,6-bis(trifluoromethyl)benzene and other starting materials were purchased from commercial sources. Solvents used for photophysical measurements were of HPLC grade. Unless specified, solvents of analytical grade were used for syntheses. Anhydrous DCM was distilled over calcium hydride under N_2 atmosphere prior to use. Anhydrous DMF for cyclic voltammetry was purchased from Sigma-Aldrich. ^{1}H NMR (400 MHz or 500 MHz) spectra were recorded on Avance400 Bruker and DRX-500 FT-NMR spectrometers. UV-vis spectra were recorded on a Perkin-Elmer Lambda 19 UV/vis spectrophotometer. Elemental analyses were performed by the Institute of Chemistry at the Chinese Academy of Sciences, Beijing.

X-ray crystal-structure determination

The X-ray diffraction data were collected on a Bruker X8 Proteum diffractometer. The crystal was kept at 100 K during data collection. The diffraction images were interpreted, and the diffraction intensities were integrated by using the program SAINT. Multi-scan SADABS was applied for absorption correction. By using Olex2, the structure was solved with the ShelXS structure solution program using direct Methods and refined with the XL refinement package using Least Squares minimization. The positions of the H atoms were calculated on the basis of the riding mode with thermal parameters equal to 1.2 times that of the associated C atoms and these positions participated in the calculation of the final R indices. In the final stage of least-squares refinement, all non-hydrogen atoms were refined anisotropically. Crystallographic parameters are summarized in Table. S2. CCDC 1858581 (complex **6**), 1858579 (complex **7**), 1858582 (complex **10**), and 1858580 (complex **11**) contain the supplementary crystallographic data for this paper. The data can be obtained free of charge from The Cambridge Crystallographic Data enter via www.ccdc.cam.ac.uk/data_request/cif.

Photophysical measurement

Steady-state emission and excitation spectra and were obtained on a Spex Flurolog-3 Model FL3-21 spectrophotometer equipped with a Hamamatsu R928 PMT detector. Solid-state samples and glassy solutions (dissolved in a mixed solvent of DCM: MeOH: EtOH = 1: 1: 4) for photophysical studies were placed in a 5 mm-diameter quartz tube. The emission spectra of glassy solutions and solid state at 77 K were recorded by placing the quartz tube into a liquid-nitrogen Dewar equipped with quartz windows. Photoluminescence data of thin-film (with samples dispersing into an inert polymer matrix in 2wt–60 wt%, poly (methyl methacrylate) (PMMA) and coating on quartz plate) was recorded by Hamamatsu Absolute PL Quantum Yield Spectrometer C11347. Fast atom bombardment (FAB) mass spectra were obtained on a Finnigan Mat 95 mass spectrometer. All solutions for photophysical measurements, except stated otherwise, were degassed in a high-vacuum line with at least five freeze-pump-thaw cycles. Emission lifetimes were measured with a Quanta-Ray Q-switch DCR-3 Nd:YAG pulsed laser system. Emission quantum yields of solutions were calculated by $\Phi_s = \Phi_r (B_r/B_s)(n_s/n_r)^2(D_s/D_r)$ by using a reference solution of quinine hemisulfate salt monohydrate in 0.5 M H_2SO_4 ($\Phi_r = 0.546$), where the subscripts *s* and *r* refer to sample and reference standard solution respectively, *n* is the refractive index of solvents, *D* is the integrated intensity, and Φ is luminescence quantum yield. The quantity *B* is calculated by $B = 1–10^{-AL}$, where *A* is the absorbance at excitation wavelength and *L* is the optical path length. Errors for wavelength values (1 nm) and Φ (10%) are estimated. Nanosecond time-resolved absorption and emission measurements were performed using a LP920-KS Laser Flash Photolysis Spectrometer (Edinburgh Instruments Ltd, Livingston, UK). The excitation source was 355 nm output from a Nd:YAG laser. Femtosecond time-resolved transient absorption (fs-TA) measurements were performed on a HELIOS setup equipped with a femtosecond regenerative amplified Ti:sapphire laser system (Spitfire Pro) in which the amplifier was seeded with the 120 fs laser pulses from an

oscillator laser system (1k Hz). The laser probe pulse was produced by utilizing about 100 mW of the amplified 800 nm laser pulses to generate a white-light continuum (430–750 nm) in a sapphire crystal and then this probe beam was split into two 4 parts before traversing the sample. One part of the probe laser beam goes through the sample while the other part of the probe laser beam goes to the reference spectrometer. For the present experiments, sample solutions were excited by a 400 nm pump beam (the second harmonic of the fundamental 800 nm, 50 mW) in a 2 mm path-length cuvette. The maximum time window is 3300 ps. Signals for each measurement were averaged for 1 s. Femtosecond time-resolved emission (fs-TRE) measurements were performed on the same setup as fs-TA. The output 800 nm laser pulse (200 mW) is used as gate pulse while the 400 nm laser pulse (10 mW) (second harmonic) is used as the pump laser. After excitation by the pump laser, the sample fluorescence is focused into the nonlinear crystal (BBO) mixing with the gate pulse to generate the sum frequency signal. Broadband fluorescence spectra were obtained by changing the crystal angles and the spectra were detected by the air-cooled CCD. For the measurement of the orientation of emitting dipole of complex **11** in CzSi hosted film, a setup RSQX-01 made by the Changchun Ruoshui Technology Development Co., Ltd. was used. The dipole orientations of the 6 wt% **11**-doped films was determined by angle-resolved and polarization resolved PL on a half quartz cylinder prism. A continuous-wave He:Cd laser (325 nm) with a fixed angle of 45° to the substrate was employed as excitation source. p-Polarized emitted light was detected at the peak wavelength of the PL spectrum of the film sample.

Cyclic voltammetry

Cyclic voltammetry measurements were performed on a Princeton Applied Research Model 273A potentiostat. The glassy-carbon electrode was polished with 0.05 μm alumina on a microcloth, sonicated for 5 min in deionized water, and rinsed with acetonitrile before use. Saturated Calomel Electrode (SCE) was used as reference electrode and a platinum wire as counter electrode. All solutions of samples were prepared in DMF containing 0.1 M tetra(n-butyl)ammonium hexafluorophosphate ($^{n}Bu_4NPF_6$) as supporting electrolyte. The solutions were purged and maintained under Argon atmosphere. Scan rates were 100 mV s^{-1} or 10 mV s^{-1} and the potentials were reported with respect to the potential of SCE. Ferrocene was used as internal reference and recorded with the potential for ferrocenium/ferrocene (Cp_2 $Fe^{+/0}$) vs SCE in the range of 0.48–0.50 V in DMF solution.

Computational details

Optimization of **2** and **11** at S_0 by DFT and T_1 states by TDDFT method , and the FC factor calculations were performed using the Gaussian09 program package.[1] The real vibrational frequencies of these optimized structures were computed to confirm that all the optimized structures are potential energy minima. Hybrid functional PBE0[2] with dispersion corrections in revision three (D3)[3] was employed. The LANL2DZ basis set and corresponding effective core potentials (ECPs) proposed by Hay and Wadt[4,5] were employed for the valence atomic orbitals of Pt. The 6-31G* basis set[6,7] was used for other atoms. Solvent effects were taken into account using the polarizable continuum model (PCM) with CH_2Cl_2 as solvent.[8] Half-Width at Half-Maximum for the convolution of the phosphorescence spectrum using a Gaussian distribution was set as 270 cm^{-1}.

Calculations of the SO electronic transition and SOCME

The calculations of SO electronic transitions were performed by the TDDFT methods in the ADF2019 package[9,10] at the level of ZORA (Zeroth Order Regular Approximation)[11-13]-PBE0/TZP for Pt and DZP for other atoms[14] at the optimized T_1 structure. Representations of molecular orbitals were drawn by ADF view. Environmental effects were included via COSMO continuum solvation using dichloromethane parameters. The TDDFT

calculations are first performed to determine the lowest single group excited states and the spin-orbit coupling operator (as a perturbation in the pSOC-TDDFT method) is applied to these single-group excited states to obtain the excitation energies with spin-orbit coupling effects included. The calculated total radiative lifetime is an average over the three substates under the assumption of fast thermalization[15]:

$$\tau_{av} = \frac{1}{k_{av}} = \frac{3}{k_I + k_{II} + k_{III}}$$

OLED fabrication

Indium-tin-oxide (ITO) coated glass with a sheet resistance of 10 Ω/sq was used as the anode substrate. Before film deposition, patterned ITO substrates were cleaned with detergent, rinsed in de-ionized water, acetone, and isopropanol, and then dried in an oven for 1 h in a cleanroom. The slides were then treated in an ultraviolet-ozone chamber for 5 min. The OLEDs were fabricated in a Kurt J. Lesker SPECTROS vacuum deposition system with a base pressure of 10^{-7} mbar. In the vacuum chamber, organic materials were thermally deposited in sequence at a rate of 0.5 Å s^{-1}. The doping process in the EMLs was realized using co-deposition technology. Afterward, LiF (1.2 nm) and Al (100 nm) were thermally deposited at rates of 0.02 and 0.2 nm s^{-1}, respectively. The film thicknesses were determined *in situ* with calibrated oscillating quartz-crystal sensors.

Current density-brightness-voltage characteristics, EL spectra, and EQE of EL device were obtained by using a Keithley 2400 source-meter and an absolute external quantum efficiency measurement system (C9920-12, Hamamatsu Photonics). All devices were encapsulated in a 200-nm-thick Al_2O_3 thin film deposited by atomic layer deposition (ALD) in a Kurt J. Lesker SPECTROS ALD system before measurements.

Device lifetime evaluation

Device structure: ITO/BPBPA (80 nm)/mCBP (10 nm)/emitter(s): mCBP (20 nm)/SF3-TRz (5 nm)/ SF3-TRz: Liq (1:1, 25 nm)/Liq(2 nm)/Al (100 nm)

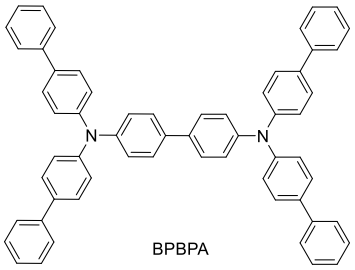

BPBPA

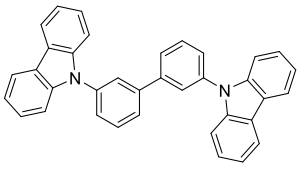

mCBP

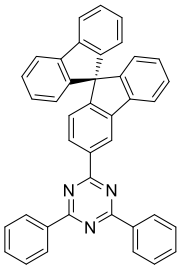

SF3-TRZ

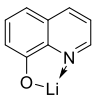

Liq

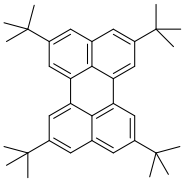
TBPe

Synthesis and characterization of ligands and platinum complexes

General procedures

The 1,3-bis(1-butylimidazolium-3-yl)benzene dibromide ligand precursors were synthesized according to the literatures.[16,17] All Pt(C_{NHC}^C_{Ar}^C_{NHC})Cl complexes were prepared by transmetallation with $Zr(NMe_2)_4$,[18] in which [Pt(cod)Cl_2] was added to react with the in-situ generated [Zr(C^C^C)] species. Complexes **6**, **7**, **10** and **11** were prepared according to the literature methods.[19]

3',5'-dibromo-2,6-dimethyl-1,1'-biphenyl

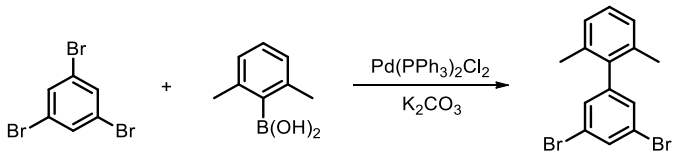

To a two-neck round-bottom flask fitted with a condenser was charged with 2,6-dimethylphenylboronic acid (5.0 g, 33.3 mmol), 1,3,5-tribromobenzene (10.5 g, 33.3 mmol), $PdCl_2(PPh_3)_2$ (1.17 g, 1.67 mmol) and K_2CO_3 (9.21 g, 66.7 mmol). The setup was evacuated and backfilled with argon (3 times). A mixture of degassed toluene/H_2O (1:1, 333 mL) was added. The resultant mixture was refluxed at 120 ºC and stirred for 16 h. The reaction turned brown and finally yellowish brown. When the reaction mixture was cooled down, the organic layer was separated. The aqueous phase was extracted with hexane (3 × 30 mL). The combined organic layer was concentrated under reduced pressure. The crude was concentrated under reduced pressure and purified by column chromatography (silica gel, 0 → 3.2% EtOAc in hexane) to give 3',5'-dibromo-2,6-dimethyl-1,1'-biphenyl as white solid.
Yield: 5.7 g (50%). ^{1}H NMR (500 MHz, $CDCl_3$) δ 7.72 (t, *J* = 1.8 Hz, 1H), 7.32 (d, *J* = 1.8 Hz, 2H), 7.23 (dd, *J* = 8.2 Hz, *J* = 6.9 Hz, 1H), 7.14 (d, *J* = 7.6 Hz, 2H), 2.10 (s, 6H); ^{13}C NMR (126 MHz, $CDCl_3$) δ 144.83, 138.99, 135.76, 132.50, 131.02, 127.99, 127.62, 123.13, 20.90.

Synthesis of C_{NHC}^C_{Ar}^C_{NHC} ligand precursors

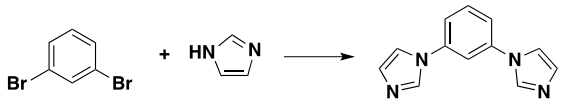

1,3-bis(imidazolyl)benzene: 1,3-dibromobenzene (2.5 mL, 21 mmol), imidazole (3.5 g, 52 mmol), K_2CO_3 (7.2 g, 52 mmol) and CuO (0.4 g, 5.2 mmol) were mixed and dissolved in DMSO (20 mL). The solution was heated at 150ºC for 48 h. The reaction was cooled, and the DMSO was removed by distillation under low-pressure, yielding an off-white solid. Chromatography on silica gel (25:1) eluting with CH_2Cl_2/MeOH (10:1) gave a white solid (3.3 g, 77%). Characterization data were reported elsewhere.[16,17]

The synthetic methods of following ligand precursors are the same as 1,3-bis(imidazolyl)benzene except respective substituted 1,3-dibromobenzenes were used.

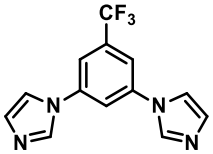

1,1'-(5-(trifluoromethyl)-1,3-phenylene)bis(1*H*-imidazole): Pale yellow solid. Yield: 66%. ^{1}H NMR (400 MHz, $CDCl_3$): δ = 7.96 (s, 2H), 7.65 (s, 2H), 7.63 (s, 1H), 7.37 (s, 2H), 7.29 (s, 2H). MS (+ESI) *m/z*: 278.1 $[M]^+$.

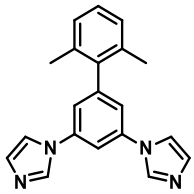

1,1'-(2',6'-dimethyl-[1,1'-biphenyl]-3,5-diyl)bis(1*H*-imidazole): Pale yellow solid. Yield: 60%. ^{1}H NMR (400 MHz, $CDCl_3$) δ 7.87 (s, 2H), 7.48 (t, *J* = 2.0 Hz, 1H), 7.34 (t, *J* = 1.2 Hz, 2H), 7.13 (d, *J* = 2.0 Hz, 2H), 7.05 (s, 2H), 7.04–6.95 (m, 3H), 2.00 (s, 6H); ^{13}C NMR (101 MHz, $CDCl_3$) δ 144.46, 138.75, 138.31, 135.11, 135.05, 130.26, 127.58, 127.18, 119.54, 117.56, 111.61, 20.37. MS (+ESI) *m/z*: 315.1601 $[M]^+$.

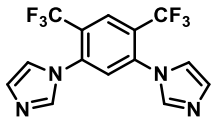

1,1'-(4,6-bis(trifluoromethyl)-1,3-phenylene)bis(1*H*-imidazole): Pale yellow solid. ^{1}H NMR (500 MHz, $CDCl_3$) δ = 8.30 (s, 1H), 7.71 (s, 2H), 7.53 (s, 1H), 7.27 (s, 2H), 7.20 (s, 2H). ^{19}F NMR (471 MHz, $CDCl_3$) δ = -59.37 (s, 6F). MS (+ESI) *m/z*: 347.0724 [M]+;

Synthesis of C_{NHC}^C_{Ar}^C_{NHC} ligands

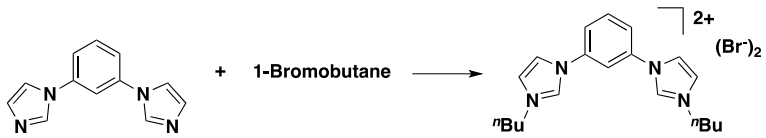

The suspension of C_{NHC}^C_{Ar}^C_{NHC} ligand precursor and 1-bromobutane or 1-chlorobutane in toluene (100 mL) was refluxed at 150°C for 48 hours, during which time oily solid is formed. The oily solid was filtered and washed with THF and diethyl ether. Product was obtained as off-white solid after drying under vacuum.

L1: Off-white solid. Isolated yield: 75%. Characterization data were reported elsewhere.[16,17]

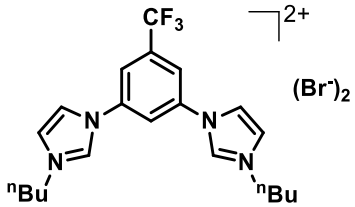

L2: Off-white solid. Isolated yield: 80%. ^{1}H NMR (400 MHz, CD_3CN) δ = 10.71 (s, 2H), 9.05 (s, 1H), 8.35 (t, *J*=1.8, 2H), 8.22 (s, 2H), 7.67 (s, 2H), 4.32 (t, *J* = 7.2, 4H), 2.05–1.96 (m, 4H), 1.48–1.37 (m, 4H), 0.98 (t, *J* = 7.4, 6H). ^{19}F NMR (377 MHz, CD_3CN) δ = -63.30 (s, 3F). MS (+ESI) *m/z*: 196.1086 $[M–2Br]^{2+}$.

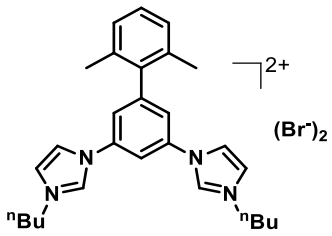

L3: Off-white solid. Isolated yield: 74 %; ^{1}H NMR (400 MHz, CD_3CN) δ 10.94 (d, *J* = 1.4 Hz, 2H), 8.83 (t, *J* = 2.1 Hz, 1H), 8.48–8.31 (m, 2H), 7.74 (t, *J* = 2.6 Hz, 2H), 7.70–7.63 (m, 2H), 7.29–7.21 (m, 1H), 7.21–7.09 (m, 2H), 4.33 (t, *J* = 7.2 Hz, 4H), 2.11 (s, 6H), 2.05–1.98 (m, 4H), 1.48–1.33 (m, 4H), 0.98 (t, *J* = 7.4 Hz, 6H). MS (+ESI) *m/z*: 214.1464 $[M–2Br]^{2+}$.

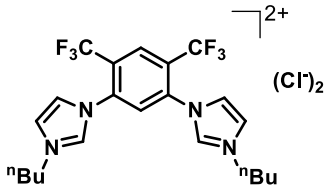

L4: Off white solid. Isolated yield: 60%. ^{1}H NMR (400 MHz, DMSO) δ = 9.83 (s, 2H), 8.76 (s, 1H), 8.70 (s, 1H), 8.20 (s, 2H), 8.17 (s, 2H), 4.39 (t, *J*=7.1, 4H), 1.93–1.82 (m, 4H), 1.37–1.25 (m, 4H), 0.93 (t, *J*=7.3, 6H). ^{19}F NMR (377 MHz, DMSO) δ = -58.04 (s, 6F). MS (+ESI) *m/z*: 230.1024 $[M–2Cl]^{2+}$.

Synthesis of [Pt(C_{NHC}^C_{Ar}^C_{NHC})Cl]

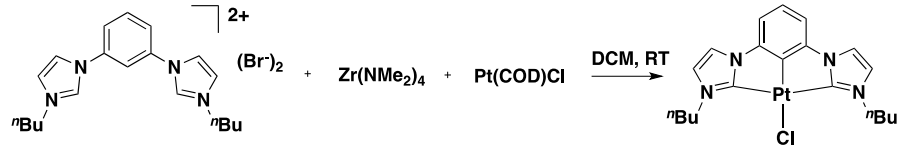

Complex 1:[18] 1,3-Bis(1-butylimidazolium-3-yl)benzene dibromide (200 mg, 0.4 mmol), Tetrakis(dimethylamino)zirconium (200 mg, 1.5 mmol) and anhydrous CH_2Cl_2 (~5.0 mL) were combined. The mixture was stirred for an hour at room temperature to afford a red solution. [Pt(cod)Cl_2] (155 mg, 0.4 mmol) was added, and the mixture was stirred at room temperature overnight. The mixture was settled for a while. Yellow solid was observed at the bottom of the flask. The red solution was removed, and the yellow solid was dissolved in 50 mL CH_2Cl_2 and filtered through Celite. The filtration was concentrated and precipitated by adding Et_2O. Yield: 130 mg (60%). ^{1}H NMR (400 MHz, $CDCl_3$) δ = 7.34 (d, *J* = 2.0 Hz, 2H), 7.12 (t, *J* = 7.8 Hz, 1H), 6.97 (d, *J* = 2.0 Hz, 2H), 6.87 (d, *J* = 7.9 Hz, 2H), 4.72 (t, *J* = 7.3 Hz, 4H), 1.89 (p, *J* = 7.5 Hz, 4H), 1.47 (sext, *J* = 7.4 Hz, 4H), 0.96 (t, *J* = 7.4 Hz, 6H). ^{13}C NMR (126 MHz, $CDCl_3$) δ = 173.23 (d, $^1J_{Pt\text{-}NHC}$ = 1170.3), 144.97 (d, *J* = 24.5), 134.73, 123.41, 120.61 (d, *J* =27.3), 114.98 (d, *J* = 43.1), 107.56 (d, *J* = 32.7), 49.42, 33.88, 19.89, 14.01.

The synthetic methods of following complexes are the same as **1**.

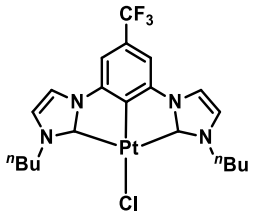

Complex 2: Yield: 154 mg (66%). ^{1}H NMR (400 MHz, $CDCl_3$) δ = 7.41 (d, *J* = 2.2 Hz, 2H), 7.15 – 7.11 (m, 2H), 7.03 (d, *J* = 2.2 Hz, 2H), 4.80 (t, *J* = 7.4 Hz, 4H), 1.90 (p, *J* = 7.6, 4H), 1.49 (sext, *J* = 7.4, 4H), 0.97 (t, *J* = 7.4 Hz, 6H). ^{13}C NMR (126 MHz, $CDCl_3$) δ = 173.29 (d, $^1J_{Pt\text{-}NHC}$ = 1168.6), 144.81 (d, *J* = 25.7), 140.28, 126.10, 125.86, 125.61, 123.94, 121.21 (d, *J* = 27.7), 115.08 (d, *J* = 42.3), 104.96 (d, *J* = 37.0), 104.94, 49.55, 33.81, 19.89, 13.98. ^{19}F NMR (377 MHz, $CDCl_3$) δ = -61.23. MS (+ESI) *m/z*: 584.2 $[M–Cl]^+$. Anal. Calcd for $C_{21}H_{24}ClF_3N_4Pt$: C, 40.68; H, 3.90; N, 9.04. Found: C, 40.74; H, 3.92; N, 8.83.

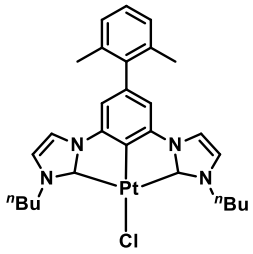

Complex 3： Yield: 130 mg (50%). ^{1}H NMR (500 MHz, $CDCl_3$) δ = 7.29 (s, 2H), 7.21–7.16 (m, 1H), 7.13 (s, 1H), 7.11 (s, 1H), 6.97 (s, 2H), 6.71–6.63 (m, 2H), 4.81 (t, *J* = 7.2 Hz, 4H), 2.09 (s, 6H), 1.91 (p, *J* = 7.3 Hz, 4H), 1.49 (sext *J* = 7.6 Hz,4), 0.97 (t, *J* = 7.3 Hz, 6H). ^{13}C NMR (126 MHz, CDCl3) δ 172.15 (d, $^{1}J_{Pt\text{-}NHC}$=1170.8), 144.94, 142.07, 137.09, 136.41, 128.84, 127.44, 127.40, 121.01, 114.83, 108.32, 50.19, 34.14, 20.98, 19.88, 14.06. MS (+ESI) *m*/*z*: 652.1 $[M–Cl]^+$. Anal. Calcd for $C_{22}H_{23}ClF_6N_4Pt$: C, 38.41; H, 3.37; N, 8.14. Found: C, 38.51; H, 3.38; N, 7.82.

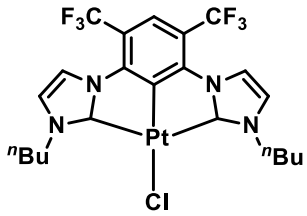

Complex 4: Yield: 65 mg (25%). ^{1}H NMR (500 MHz, CD_2Cl_2) δ = 7.86 (s, 1H), 7.81 (s, 2H), 7.10 (s, 2H), 4.80 (t, *J*=7.3, 4H), 1.96–1.82 (m, 4H), 1.52–1.41 (m, 4H), 0.98 (t, *J*=7.4, 6H). ^{13}C NMR (151 MHz, CD_2Cl_2) δ = 176.09 (d, $^{1}J_{Pt\text{-}NHC}$ = 1138), 145.12 (d, *J* = 30.4), 141.80 (d, *J* = 967.8), 123.62 (q, *J* = 272.0), 122.25 (d, *J* = 27.7), 120.83–120.52 (m), 119.12–118.87 (m), 111.41–110.59 (m), 49.69, 33.95, 20.11, 14.01. ^{19}F NMR (471 MHz, CD_2Cl_2) δ = -57.62 (s, 6F). ^{195}Pt NMR (108 MHz, CD_2Cl_2) δ = -4052.29. MS (+ESI) *m*/*z*: 652.1 $[M–Cl]^+$. Anal. Calcd for $C_{28}H_{33}ClN_4Pt$: C, 51.26; H, 5.07; N, 8.54. Found: C, 50.68; H, 5.00; N, 8.16.

Synthesis of [Pt(C_{NHC}^C_{Ar}^C_{NHC})C≡N]

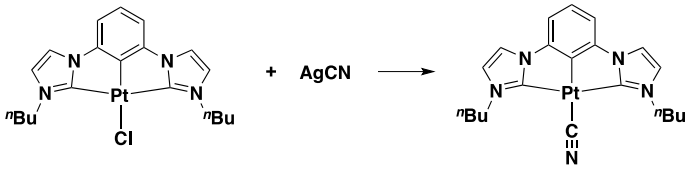

Complex 5: The mixture of Pt(C_{NHC}^C_{Ar}^C_{NHC})Cl (100 mg, 0.167 mmol) and silver cyanide (24.7 mg, 0.184 mmol) was stirred overnight in CH_2Cl_2 (25 mL). Removal of AgCl through Celite, the filtrate was collected. After removing the solvent in vacuum, greenish yellow solid was obtained.

Yield: 60 mg (66%). ^{1}H NMR (400 MHz, $CDCl_3$): δ = 7.35 (s, 2H), 7.15 (t, *J* = 7.8 Hz, 1H), 7.13–6.91(m, 4H), 4.57 (t, *J* = 7.2 Hz, 4H), 1.93 (quint, *J* = 7.5 Hz, 4H), 1.52 (sext, *J* = 7.5 Hz, 4H), 0.97 (t, *J* = 7.4 Hz, 6H). ^{13}C NMR (101 MHz, $CDCl_3$) δ = 170.72 (d, $^{1}J_{Pt\text{-}NHC}$ = 1136.7), 146.57 (d, *J* = 23.0), 145.53, 143.95, 125.37, 120.03 (d, *J* = 27.0), 115.70 (d, *J* = 40.8), 107.68 (d, *J* = 22.0), 51.50, 33.95, 19.83, 13.99. IR (KBr disc, cm^{-1}): $\nu_{C\equiv N}$ = 2106. MS (+FAB) *m*/*z*: 543.0 $[M\text{-}H]^+$. Anal. Calcd for $C_{21}H_{25}N_5Pt{\cdot}H_2O$: C, 45.00; H, 4.86; N, 12.44. Found: C, 45.02; H, 59; N, 12.55.

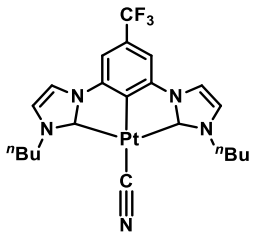

Complex 9: The procedure is the same as **5**.

Yield: 90 mg (91%). ^{1}H NMR (400 MHz, $CDCl_3$): δ = 7.41 (d, *J* = 3.2 Hz, 2H), 7.16 (t, *J* = 5.0 Hz, 2H), 7.03 (d, *J* = 3.2 Hz, 2H), 4.60 (t, *J* = 7.2 Hz,4H), 1.94 (quint, *J* = 7.4 Hz, 4H), 1.51 (sext, *J* = 7.5 Hz, 4H), 0.98 (t, *J* = 7.4 Hz, 6H). ^{13}C NMR (151 MHz, $CDCl_3$) δ = 171.07 (d, $^{1}J_{Pt\text{-}NHC}$ = 1135.4), 151.22 (d, *J* = 675.5), 146.46 (d, *J* = 23.1), 142.24 (d, *J* = 925.4), 127.77 (q, *J* = 32.4), 124.68 (q, *J* = 271.8), 120.59 (d, *J* = 27.2), 115.75 (d, *J* = 40.2), 105.23–104.71 (m), 51.72, 33.92, 19.83, 13.99. ^{19}F NMR (471 MHz, $CDCl_3$) δ = -61.33. IR (KBr disc, cm^{-1}): $\nu_{C\equiv N}$ = 2113. MS (+FAB) *m*/*z*: 610.9 $[M\text{-}H]^+$. Anal. Calcd for $C_{22}H_{26}N_5F_3Pt$: C, 43.14; H, 4.28; N, 11.43. Found: C, 43.03; H, 3.96; N, 11.33.

Synthesis of [Pt(C_{NHC}^C_{Ar}^C_{NHC})C≡N(BPh_3)]

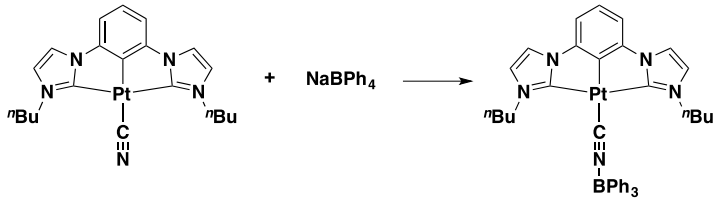

Complex 6: To a stirred suspension of Pt(C_{NHC}^C_{Ar}^C_{NHC})C≡N (50 mg, 0.092 mmol) in 20 mL mixed solvent of water and methanol (v:v = 1:1), 2 mL of hydrochloric acid (3.0 M) was added in dropwise. After 30 min, $NaBPh_4$ (65 mg, 0.190 mmol) was added. The resulting solution was stirred overnight at room temperature, during which a light-yellow solid gradually precipitated. The precipitate was then collected by filtration and washed with water and MeOH. Further purification was achieved by recrystallization from the slow diffusion of diethyl ether into concentrated CH_2Cl_2 solution of the complexes.

Yield: 60 mg (82%). ^{1}H NMR (500 MHz, $CDCl_3$): δ = 7.45 (d, *J* = 6.8 Hz, 6H), 7.32 (s, 2H), 7.18 (t, *J* = 7.4 Hz, 6H), 7.14–7.08 (m, 4H), 6.93–6.79 (m, 4H), 4.09 (t, *J* = 6.2 Hz, 4H), 1.42–1.31 (m, 4H), 0.97 (sext, *J* = 7.3 Hz, 4H), 0.67 (t, *J* = 7.3 Hz, 6H). ^{13}C NMR (126 MHz, CD_2Cl_2) δ = 169.89 (d, $^{1}J_{Pt\text{-}C}$ =1147.1), 154.67 (br, s), 146.71 (d, *J* = 23.8), 143.95 (d, *J* = 696.6), 141.43 (d, *J* = 980.3), 120.32 (d, *J* = 27.0), 116.39 (d, *J* = 40.9), 108.22 (d, *J* = 22.7), 51.53, 33.06, 19.53, 13.84. IR (KBr disc, cm^{-1}): $\nu_{C\equiv N}$ = 2162. MS (+FAB) *m*/*z*: 784.0 $[M\text{-}H]^+$. Anal. Calcd for $C_{39}H_{40}N_5BPt$: C, 59.70; H, 5.14; N, 8.93. Found: C, 59.10; H, 5.16; N, 8.79.

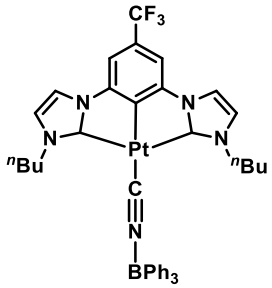

Complex 10: The procedure is the same as **6**.

Yield: 40 mg (57%). ^{1}H NMR (400 MHz, CD_3CN) δ = 7.63 (d, *J* = 3.2 Hz, 2H), 7.41 (t, *J* = 5.2 Hz, 2H), 7.35 (d, *J* = 6.8 Hz, 6H), 7.19 (t, *J* = 7.3 Hz, 6H), 7.06–7.13 (m, 5H), 4.12 (t, *J* = 6.5 Hz, 4H), 1.37 (quint, *J* = 6.8 Hz, 4H),

0.90 (sext, *J* = 7.5 Hz, 4H), 0.62 (t, *J* = 7.3 Hz, 6H). ^{13}C NMR (101 MHz, $CDCl_3$) δ = 169.44 (d, $^1J_{Pt\text{-}C}$ = 1147.2), 154.09, 149.03, 146.10 (d, *J* = 24.3), 138.52, 134.11, 128.09, 126.74, 125.78, 124.65, 123.23, 120.77 (d, *J* = 27.6), 115.99 (d, *J* = 40.2), 104.99, 51.53, 32.74, 19.23, 13.71. ^{19}F NMR (471 MHz, $CDCl_3$) δ = -61.42. IR (KBr disc, cm^{-1}): $\nu_{C\equiv N}$ = 2169. MS (+FAB) *m/z*: 851.0 $[M\text{-}H]^+$. Anal. Calcd for $C_{40}H_{39}N_5BF_3Pt\cdot(Et_2O)_{0.5}$: C, 56.70; H, 4.98; N, 7.87. Found: C, 56.95; H, 5.13; N, 7.93.

Synthesis of [Pt(C_{NHC}^C_{Ar}^C_{NHC})C≡N$B(C_6F_5)_3$]

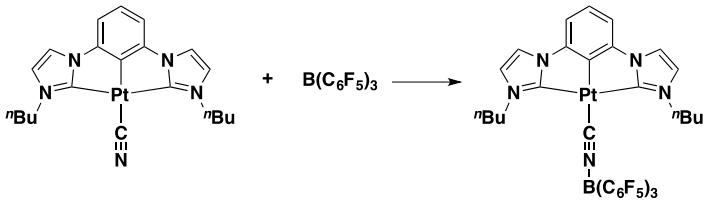

Complex 7：The mixture of Pt(C_{NHC}^C_{Ar}^C_{NHC})C≡N (58 mg, 0.107 mmol) and $B(C_6F_5)_3$ (60 mg, 0.117 mmol) was pump-filled for three times and the dry CH_2Cl_2 (10 mL) was added into the flask. The solution was stirred overnight at room temperature under argon. Yellow solid was obtained after solvent was removed in vacuum; yield 100 mg, 88.5%.

Yield: 100 mg (88.5%). ^{1}H NMR (500 MHz, $CDCl_3$): δ = 7.36 (s, 2H), 7.12 (t, *J* = 7.8 Hz, 1H), 6.96 (s, 2H), 6.93–6.86 (m, 2H), 4.13 (t, *J* = 6.6 Hz, 4H), 1.55–1.45 (m, 4H), 1.02 (sext, *J* = 7.6 Hz, 4H), 0.79 (t, *J* = 7.3 Hz, 6H). ^{13}C NMR (125 MHz, $CDCl_3$): δ = 169.0 (d, $^1J_{Pt\text{-}NHC}$ = 1156.7), 146.3, 146.2, 142.8, 148.06 (d, $^1J_{CF}$ = 242 Hz), 139.63 (d, $^1J_{CF}$ = 250 Hz), 137.0 (d, $^1J_{CF}$ = 260 Hz), 126.7, 120.0, 119.9, 116.1, 108.0, 50.8, 32.8, 19.2, 13.4. IR (KBr disc, cm^{-1}): $\nu_{C\equiv N}$ = 2173. MS (+FAB) *m/z*: 1083.2 $[M+CH_3OH\text{-}H]^+$. Anal. Calcd for $C_{39}H_{25}N_5BF_{15}Pt\cdot H_2O$: C, 43.67; H, 2.54; N, 6.53. Found: C, 43.64; H, 2.48; N, 6.42.

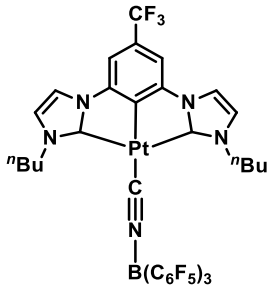

Complex 11: The procedure is the same as **7**.

Yield: 150 mg (81%). ^{1}H NMR (400 MHz, $CDCl_3$): δ = 7.45 (s, 2H), 7.45 (t, *J* = 5.36 Hz, 2H), 7.04 (s, 2H), 4.18 (t, *J* = 6.36 Hz, 4H), 1.54 (quint, *J* = 6.80 Hz), 1.04 (sext, *J* = 7.68 Hz, 2H), 0.79 (t, *J* = 7.40 Hz, 6H). ^{13}C NMR (151 MHz, CD_2Cl_2) δ = 169.53 (d, $^1J_{Pt\text{-}NHC}$ = 1149.2), 148.45 (dt, *J* = 241.7, 12.2), 148.30 (d, *J* = 711.7), 146.72 (d, *J* = 24.7), 146.16 (d, *J* = 1010.8), 140.09 (d, *J* = 248.9), 137.41 (ddd, *J* = 34.0, 19.0, 13.3), 129.37 (q, *J* = 32.6), 124.67 (q, *J* = 271.9), 121.14 (d, *J* = 27.0), 119.07 (s), 116.79 (d, *J* = 40.3), 106.00–105.69 (m), 51.26, 33.18, 19.62, 13.63. ^{19}F NMR (471 MHz, $CDCl_3$) δ = -61.72 (s), -133.21 (dd, *J*= 22.7, 6.4), -158.41 (t, *J* = 20.4), -164.39 (td, *J* = 23.5, 8.1). IR (KBr disc, cm^{-1}): $\nu_{C\equiv N}$ = 2186, 2171. MS (+FAB) *m/z*: 953.8 $[M\text{-}C_6F_5]^+$. Anal. Calcd for $C_{40}H_{24}N_5BF_{18}Pt\cdot(Et_2O)_{0.5}$: C, 43.50; H, 2.52; N, 6.04. Found: C, 43.09; H, 2.50; N, 6.16.

Synthesis and Characterization of [Pt(C_{NHC}^C_{Ar}^C_{NHC})Pz]

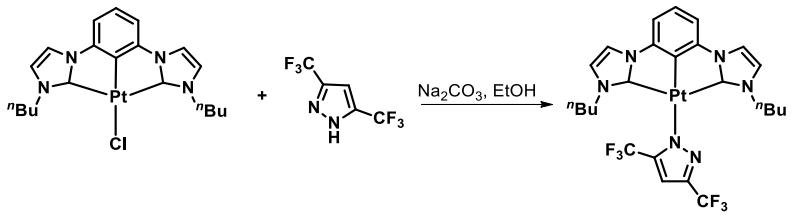

Complex 8: A mixture of Pt(C_{NHC}^C_{Ar}^C_{NHC})Cl (50 mg, 0.09 mmol), 3,5-bis(trifluoromethyl)pyrazole (20 mg, 0.098 mmol), an Na_2CO_3 (14.4 mg, 0.13 mmol) in EtOH (20 mL) was refluxed overnight in the dark, giving a light yellow solution. The light-yellow solution was evaporated to dryness under reduced pressure. The residue was recrystallized by diffusing pentane into the DCM solution, affording the product as a light yellow solid.

Yield: 55 mg (84%). ^{1}H NMR (500 MHz, CD_3CN, 298 K) δ = 7.61 (d, *J* = 2.1 Hz, 2H), 7.21 (t, *J* = 7.5 Hz, 1H), 7.13 (d, *J* = 2.1 Hz, 2H), 7.08 (d, *J* = 7.2 Hz, 2H), 7.05 (s, 1H), 3.45 (ddd, *J* = 13.3, 10.0, 5.4 Hz, 2H), 3.28 (ddd, *J* = 13.2, 10.0, 6.4 Hz, 2H), 1.39 - 1.56 (m, 4H), 1.11–0.92 (m, 4H), 0.77 ppm (t, *J* = 7.4 Hz, 6H). ^{13}C NMR (151 MHz, CD_2Cl_2) δ = 174.00 (d, $^1J_{Pt\text{-}NHC}$ = 1189.4), 146.37 (d, *J* = 23.7), 143.53 (q, *J* = 36.1), 140.93 (q, *J* = 35.3), 135.26 (d, *J* = 835.2), 124.82, 123.16 (q, *J* = 267.7), 122.52 (q, *J* = 268.3), 120.21 (d, *J* = 28.1), 116.00 (d, *J* = 43.1), 107.92 (d, *J* = 27.6), 104.17, 49.57, 33.61, 19.94, 13.63. ^{19}F NMR (471 MHz, CD_3CN) δ = -59.4, -60.85. MS (+ESI) *m*/*z*: 720.2 $[M+H]^+$. Anal. Calcd for $C_{25}H_{26}F_6N_6Pt$: C, 41.73; H, 3.64; N, 11.68. Found: C, 41.84; H, 3.69; N, 11.47.

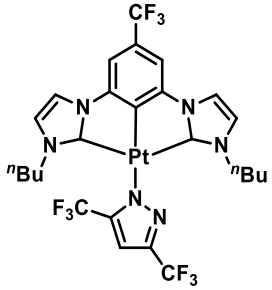

Complex 12: The procedure is the same as **8**.

Yield: 50 mg (81%). ^{1}H NMR (400 MHz, $CDCl_3$) δ = 7.40 (d, *J* = 1.9 Hz, 2H), 7.13 (t, *J* = 6.7 Hz, 2H), 6.99 (s, 1H), 6.94 (d, *J* = 1.9 Hz, 2H), 3.48–3.32 (m, 4H), 1.48–1.57 (m, 4H), 1.04 (sext, *J* = 7.4 Hz, 4H), 0.80 (t, *J* = 7.3 Hz, 6H). ^{13}C NMR (151 MHz, $CDCl_3$) δ = 173.88 (d, $^1J_{Pt\text{-}NHC}$ =1191.2), 145.83 (d, *J* = 23.2), 143.74 (q, *J* = 36.4), 141.15, 140.74 (q, *J* = 35.6), 126.93 (q, *J* = 32.5), 124.76 (q, *J* = 271.9), 122.55 (q, *J* =268.1), 122.03 (q, *J* = 268.7), 120.35 (d, *J* = 27.8), 115.67 (d, *J* = 42.3), 104.91 (d, *J* = 3.9), 104.08, 49.49, 33.31, 19.70, 13.49. ^{19}F NMR (471 MHz, $CDCl_3$) δ -59.17 (d, *J*=18.9), -60.55, -61.35. MS (+ESI) *m*/*z*: 788.2 $[M+H]^+$. Anal. Calcd for Anal. Calcd for $C_{26}H_{25}F_9N_6Pt$: C, 39.65; H, 3.20; N, 10.67. Found: C, 39.67; H, 3.19; N, 10.53.

Table S1. Selected bond lengths (Å) and angles (°) for complexes **6**, **7**, **10** and **11**.

Complex	Bond length (Å)		Bond angles (°)	
6	Pt1–C1	2.033(4)	C1–Pt1–C4	77.58(16)
	Pt1–C4	1.990(4)	C1–Pt1–C12	155.17(16)
	Pt1–C12	2.050(4)	C1–Pt1–C39	102.60(16)
	Pt1–C39	2.016(4)	C12–Pt1–C39	102.08(16)
	C39–N5	1.145(6)	C4–Pt1–C12	77.90(16)
	N5–B1	1.584(6)	C4–Pt1–C39	177.21(15)
7	Pt1–C1	2.044 (7)	C1–Pt1–C4	77.7(3)
	Pt1–C4	1.982 (7)	C1–Pt1–C10	155.4(3)
	Pt1–C10	2.050 (7)	C10–Pt1–C21	101.3(3)
	Pt1–C21	1.998 (7)	C1–Pt1–C21	103.6(3)
	N5–C21	1.159 (9)	C4–Pt1–C10	77.7(3)
	N5–B1	1.556 (9)	C4–Pt1–C21	177.9(3)
10	Pt1–C1	2.056 (4)	C1–Pt1–C4	77.92 (14)
	Pt1–C4	1.977 (4)	C1–Pt1–C10	155.43 (15)
	Pt1–C10	2.056 (4)	C1–Pt1–C22	100.55 (15)
	Pt1–C22	2.029 (4)	C10–Pt1–C22	103.35 (15)
	N5–C22	1.143 (5)	C10–Pt1–C4	77.81 (15)
	N5–B1	1.597 (5)	C4–Pt1–C22	175.43 (14)
11	Pt1–C1	2.045(7)	C1–Pt1–C22	102.0(3)
	Pt1–C9	1.988(7)	C1–Pt1–C9	77.6(3)
	Pt1–C10	2.061(7)	C1–-Pt1–C10	155.9(3)
	Pt1–C22	2.013(7)	C10–Pt1–C22	102.1(3)
	N5–C22	1.142(9)	C10–Pt1–C9	78.4(3)
	N5–B2	1.556(8)	C9–Pt1–C22	175.2(3)

Table S2. Crystal data and structure refinement for crystals of complexes **6**, **7**, **10** and **11**.

Complex	6	7	10	11
Empirical formula	$C_{39}H_{40}BN_5Pt$	$C_{39}H_{25}BF_{15}N_5Pt\cdot(CHCl_3)_{0.11}$	$C_{40}H_{39}BF_3N_5Pt\cdot(C_5H_{12})_{0.5}$	$C_{40}H_{24}BF_{18}N_5Pt$
Formula weight	784.66	1067.8	888.73	1122.54
Temperature/K	100	100	100	296.15
Crystal system	monoclinic	monoclinic	triclinic	triclinic
Space group	$P2_1/n$	$P2_1/c$	P-1	P-1
a/Å	9.3296(4)	31.0734(13)	11.0102(6)	14.8125(18)
b/Å	18.5086(9)	18.7239(8)	14.6614(8)	18.029(2
c/Å	19.5455(9)	19.9820(9)	24.5850(13)	18.136(2)
α/°	90	90	80.399(2)	117.285(2)
β/°	102.7823(10)	93.2010(14)	78.892(2)	100.039(3)
γ/°	90	90	77.090(2)	105.794(3)
Volume/Å^3	3291.4(3)	11607.7(9)	3763.9(4)	3880.3(8)
Z	4	12	4	4
ρ_{calc}g/cm^3	1.583	1.833	1.568	1.922

μ/mm^{-1}	8.244	8	7.402	7.925
F(000)	1568	6221	1780.0	2176.0
Crystal size/mm^3	0.25 × 0.25 × 0.25	0.4 × 0.2 × 0.2	0.6 × 0.03 × 0.03	0.6 × 0.05 × 0.04
Radiation	CuKα (λ = 1.54178)	CuKα (λ = 1.54178)	CuKα (λ = 1.54178)	CuKα (λ = 1.54178)
2Θ range for data collection/	9.28 to 135.142	2.848 to 134.794	3.694 to 131.762	5.736 to 133.386
Index ranges	-10 ≤ h ≤ 11, -21 ≤ k ≤ 22, -23 ≤ l ≤ 23	-36 ≤ h ≤ 37, -22 ≤ k ≤ 22, -23 ≤ l ≤ 23	-13 ≤ h ≤ 8, -16 ≤ k ≤ 17, -29 ≤ l ≤ 27	-17 ≤ h ≤ 17, -21 ≤ k ≤ 21, -21 ≤ l ≤ 21
Reflections collected	35017	139155	87215	61739
Independent reflections	5852	20596	12829	13358
Data/restraints/parameters	5852/0/417	20596/67/1398	12829/858/946	13358/1028/1188
Goodness-of-fit on F^2	1.128	1.026	1.079	1.139
Final R indexes [I>=2σ (I)]	R_1 = 0.0397, wR_2 = 0.1056	R_1 = 0.0553, wR_2 = 0.1461	R_1 = 0.0309, wR_2 = 0.0808	R1 = 0.0410, wR2 = 0.1113
Final R indexes [all data]	R_1 = 0.0397, wR_2 = 0.1057	R_1 = 0.0604, wR_2 = 0.1515	R_1 = 0.0332, wR_2 = 0.0828	R1 = 0.0425, wR2 = 0.1120
Largest diff. peak/hole/e $Å^{-3}$	1.50/-2.03	1.97/-1.57	2.28/-0.77	1.56/-1.63

[a] $R_1 = \sum||F_o|-|F_c|| / \sum|F_o|$; [b] $wR_2 = [\sum w(|F_o|-|F_c|)_2 / \sum w|F_o|_2]^{1/2}$

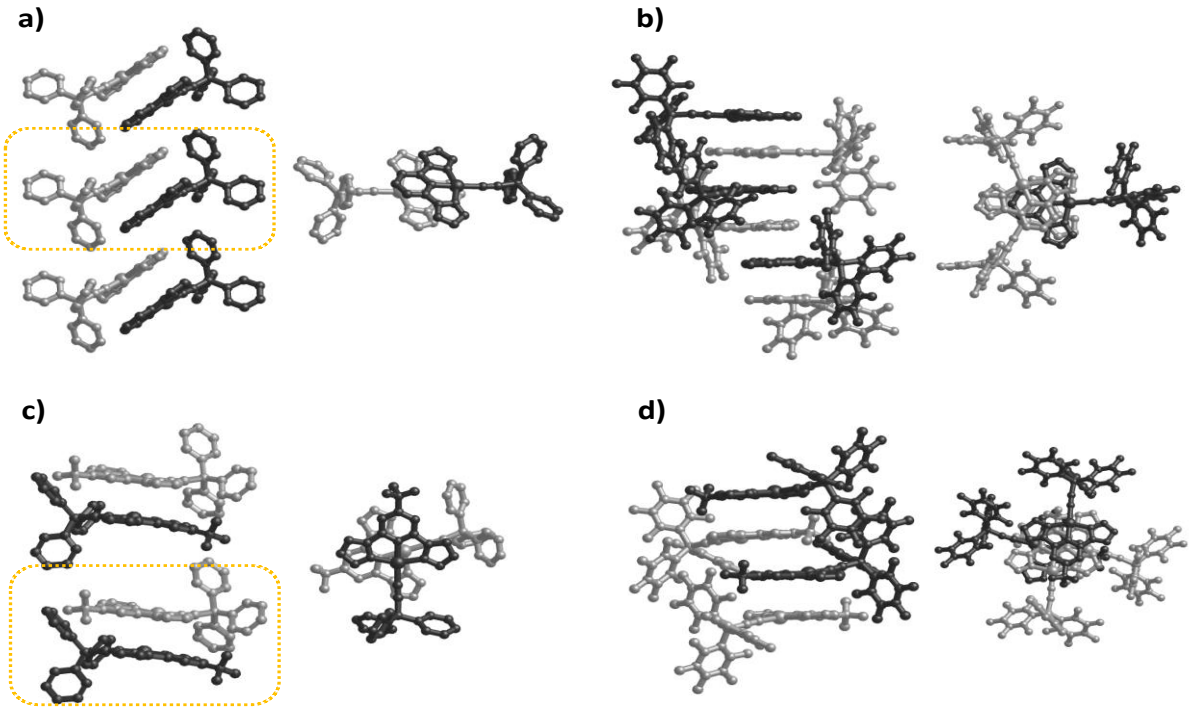

Figure S1. Crystal packing diagrams of (a) **6**, (b) **7**, (c) **10** and (d) **11**.

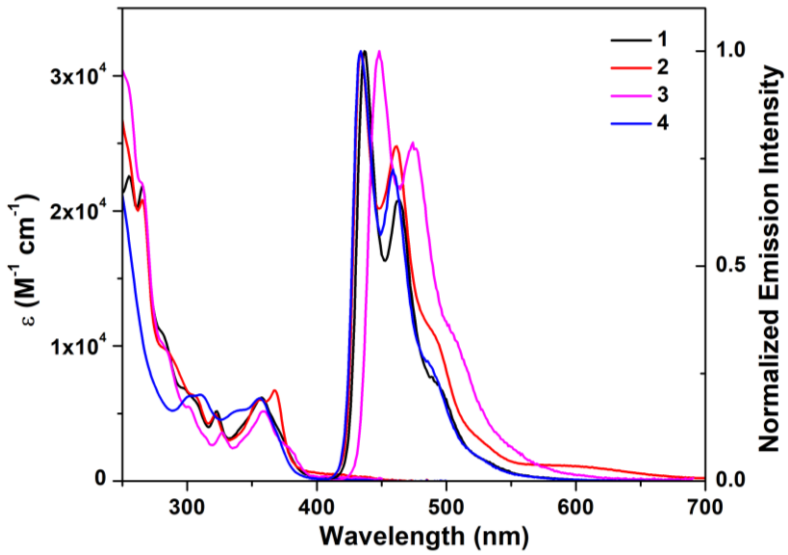

Figure S2. UV-vis absorption and emission spectra of **1**–**4** in CH_2Cl_2.

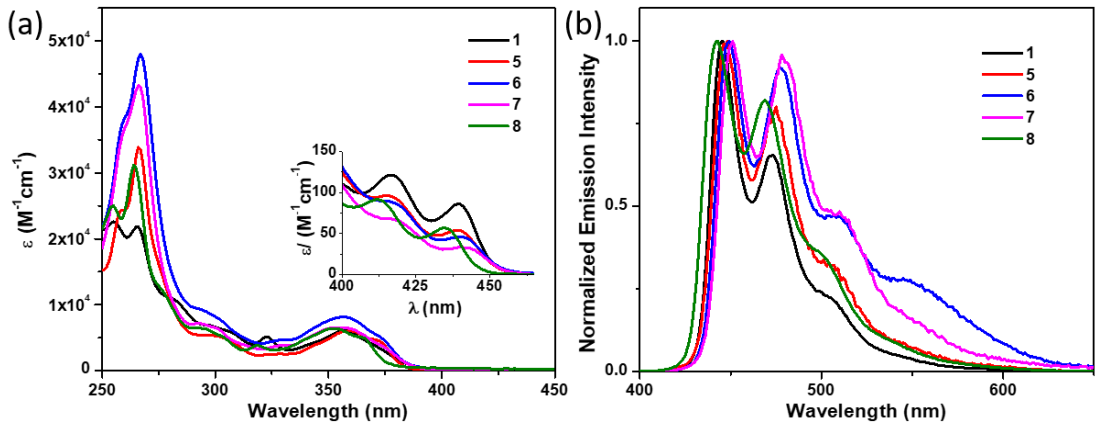

Figure S3. (a) UV-vis absorption and (b) emission spectra of **1** and **5**–**8** in CH_2Cl_2.

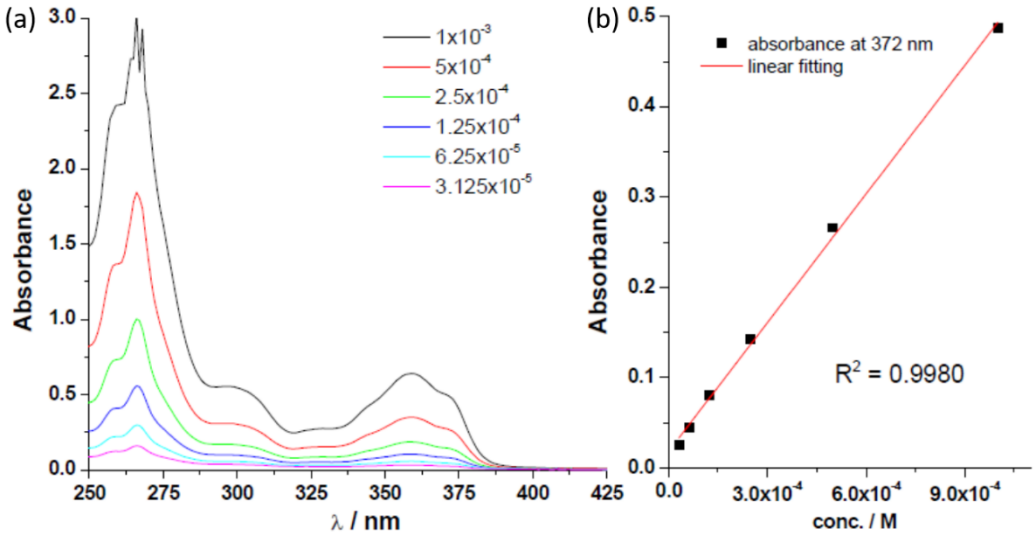

Figure S4. (a) UV-vis absorption spectra of **5** at different concentrations (path length of cuvette = 1 mm) in CH_2Cl_2 and (b) plot of absorbance at 372 nm versus concentration and the linear fit.

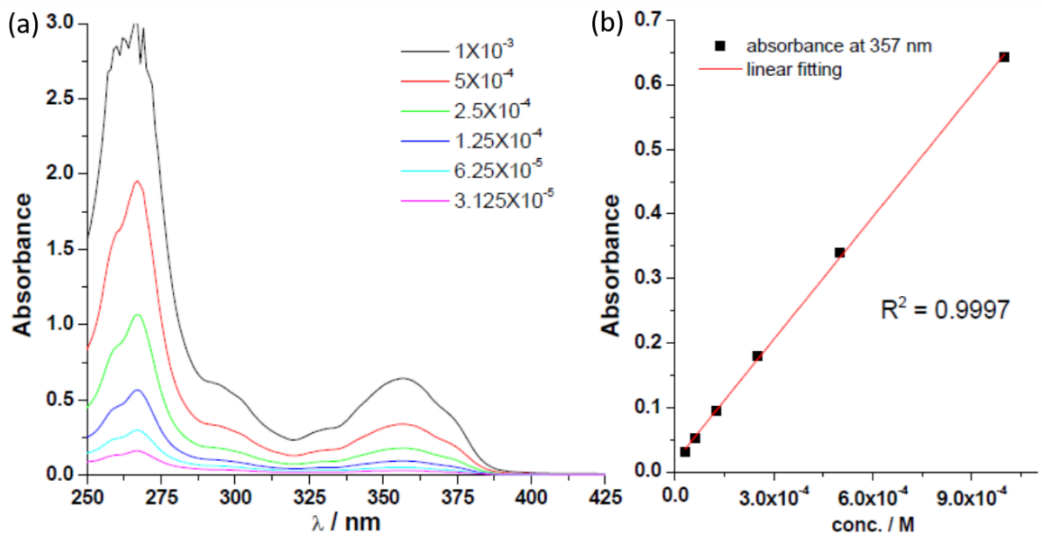

Figure S5. (a) UV-vis absorption spectra of **6** at different concentrations (path length of cuvette = 1 mm) in CH_2Cl_2 and (b) plot of absorbance at 357 nm versus concentration and the linear fit.

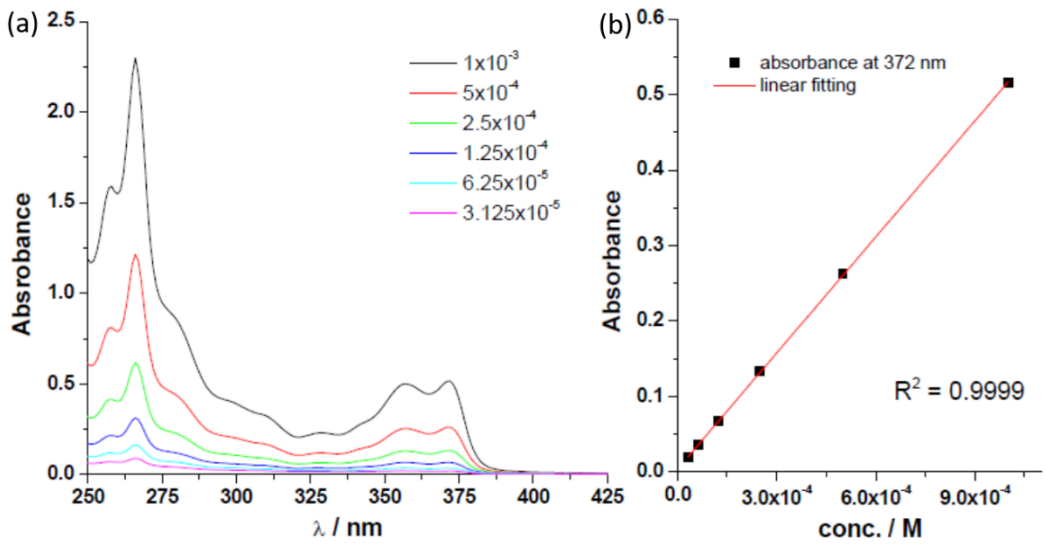

Figure S6. (a) UV-vis absorption spectra of **9** at different concentrations (path length of cuvette = 1 mm) in CH_2Cl_2 and (b) plot of absorbance at 372 nm versus concentration and the linear fit.

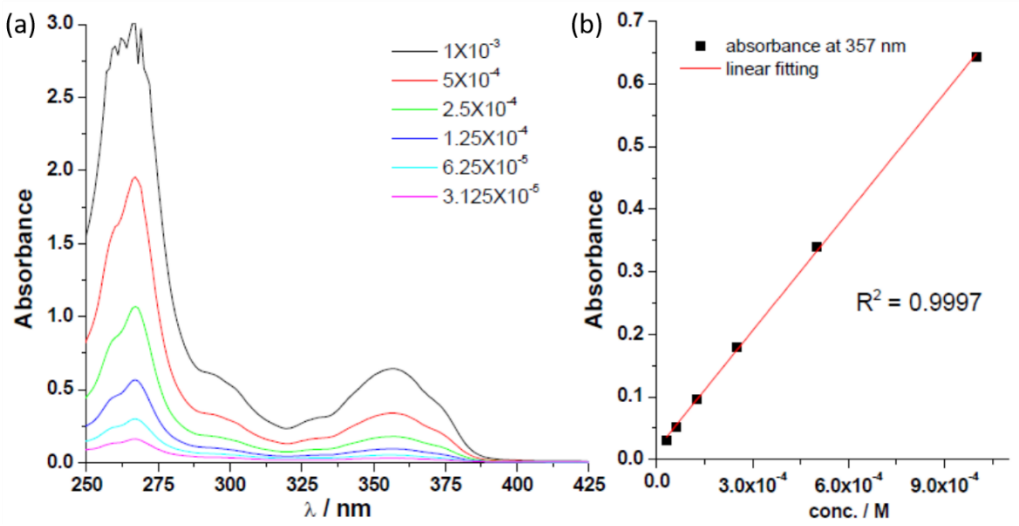

Figure S7. (a) UV-vis absorption spectra of **10** at different concentrations (path length of cuvette = 1 mm) in CH_2Cl_2 and (b) plot of absorbance at 357 nm versus concentration and the linear fit.

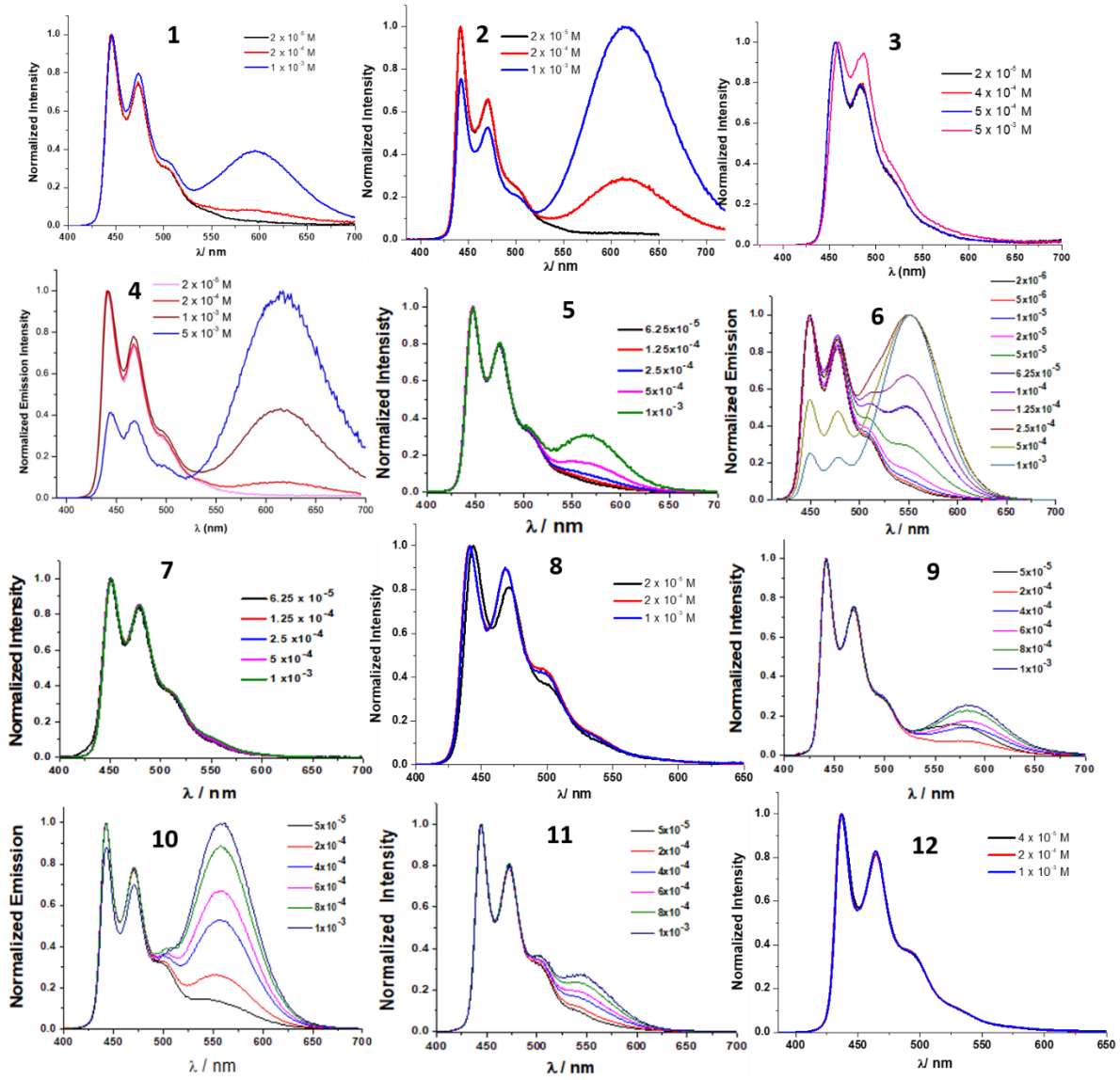

Figure S8. Emission spectra of **1**–**12** at different concentrations in CH_2Cl_2.

Table S3. Photophysical data of **1, 2** and **5**–**12** in solid state at 298 and 77K and in EtOH/MeOH (*v*/*v* = 4:1) glassy solution at 77K.

	Emission λ_{max} [nm], (τ [μs])		
	Solid 298K	Solid 77K	EtOH/MeOH (*v*/*v* = 4:1) 77K
1	447, 468, 496 (0.6)	439, 465, 496	439, 469, 501 (5.8)
2	451, 473, 498 (1.8)	444, 470, 496	436, 466, 492 (6.6)
5	446, 473, 504 (2.5)	440, 469, 502	441, 471, 502 (9.0)
6	452, 480, 512, 580 (2.3)	447, 478, 510	442,470, 502 (8.1)
7	455, 479, 513 (3.2)	455, 481, 518	446,475, 508, 548 (10.2)
8	446, 469, 498 (6.1)	440, 469, 501	437, 466, 497 (7.7)
9	448, 473, 502 (3.3)	443, 472, 497	436, 465, 495 (8.9)
10	561 (1.0)	570	436, 465, 495 (9.7)
11	444, 470, 499 (3.4)	442, 471, 499	439, 469, 498 (10.6)
12	437, 463, 489 (3.9)	434, 462, 490	432, 461, 489 (8.7)

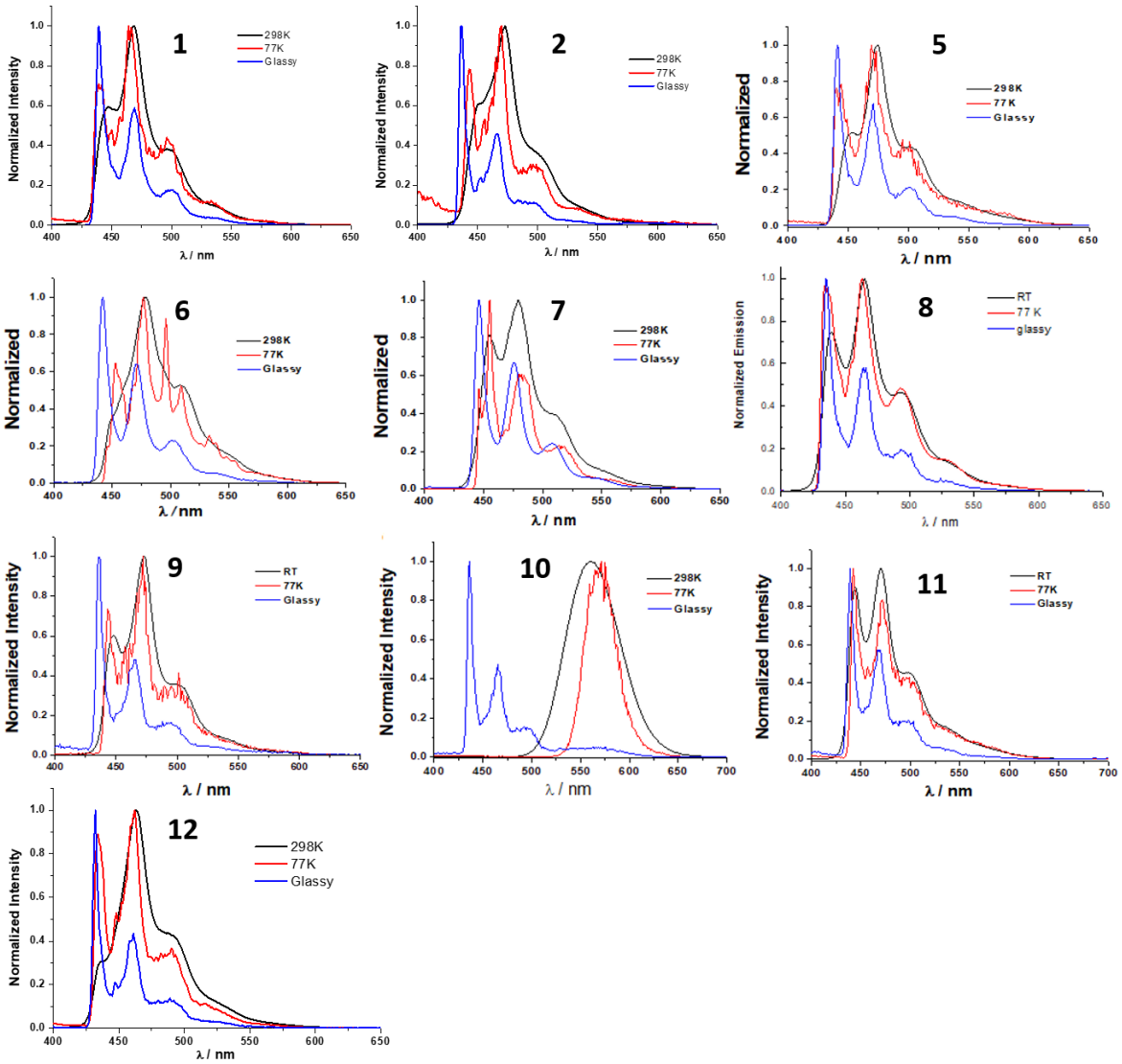

Figure S9. Emission spectra of **1**, **2** and **5**–**12** in solid state at 298K and 77K and in EtOH/MeOH (*v*/*v* = 4:1) glassy solution at 77K.

Table S4. Photophysical properties of **11** in different solvents.

	UV-Vis absorption	Emission		
	λ_{max} [nm] ($\varepsilon \times 10^3$ [M^{-1} cm^{-1}])	λ_{max} [nm]	Φ	τ [µs]
CH_2Cl_2	259 (28.9), 265 (36.6), 293 (6.6), 303 (5.7), 328 (3.7), 353 (5.7), 372 (4.1)	440, 469, 502	0.03	0.4
toluene	303 (5.3), 311 (5.1), 328 (4.1), 355 (5.8), 371 (4.8)	441, 469, 502	0.04	0.3
EtOAc	365 (37.3), 292 (5.5), 301 (4.8), 328 (3.4), 350 (5.8), 373 (4.0)	441, 470, 504	0.04	0.5
THF	259 (32.0), 266 (39.2), 282 (6.9), 303 (6.0), 328 (3.9), 351 (6.2), 371 (4.4)	441, 470, 504	0.05	0.6
MeCN	259 (27.9), 265 (36.6), 291 (5.7), 302 (4.8), 328 (3.4), 350 (5.8), 372 (4.1)	443, 472, 506	0.04	0.6
EtOH	259 (29.1), 265 (36.6), 291 (5.7), 302 (4.8), 328 (3.4), 350 (5.8), 372 (4.1)	442, 471, 505	0.04	0.5

Table S5. Photophysical properties of **1**–**12** at various concentrations in PMMA thin films.

	Emission λ_{max} [nm], (τ [µs]); Φ							
	2 wt%	5 wt%	10 wt%	15 wt%	20 wt%	25 wt%	40 wt%	60 wt%
1	443 (3.6), 471, 505; 0.56	443 (4.0), 472, 505; 0.65	445 (3.5), 473, 507; 0.60	445 (3.5), 472, 506; 0.63	444 (0.5, 3.5), 472, 506; 0.49	444 (0.4, 3.4), 471, 505; 0.47	445 (1.3), 472, 504, 586 (2.1); 0.31	441 (0.4), 469, 498, 589 (1.5); 0.12
2	441 (4.0), 469, 504; 0.60	441 (4.0), 469, 504; 0.64	441 (3.2), 469, 504, 601; 0.64	441 (2.5), 469, 504, 601; 0.61	441 (1.6), 469, 504, 601; 0.63	441 (0.4, 1.5), 469, 504, 601; 0.61	442 (0.6), 470, 597 (2.0); 0.61	441 (0.3), 468, 599 (1.7); 0.47
3	453 (4.1), 481, 519; 0.56	/	454 (4.0), 481, 519; 0.40	/	/	456, 482 (2.2); 0.15	/	/
4	441 (3.6), 468, 503; 0.54	441 (3.3), 468, 503, 601 2.9); 0.61	441 (2.2), 468, 503, 601 (2.5); 0.68	441 (1.5), 468, 503, 601 (2.3); 0.69	441 (1.1), 468, 503, 601 (2.2); 0.66	441 (0.3), 468, 503, 601 (2.1); 0.62	/	/
5	445 (4.2), 473, 505, 552 (3.3); 0.76	445 (3.8), 473, 504, 558 (3.1); 0.73	446 (3.0), 473, 560 (2.2); 0.85	446 (2.7), 474, 561 (2.1); 0.84	446 (2.2), 474, 561 (1.9); 0.90	446 (2.2), 474, 562 (1.8); 0.95	446 (2.1), 474, 562 (1.8); 0.90	448 (3.0), 474, 505; 0.87
6	446 (7.4), 473, 509; 0.81;	447 (7.1), 475, 507; 0.83	447 (6.0), 476, 507, 544 (4.46); 0.95	448 (4.9), 476, 510, 545 (3.91); 0.93	448 (4.4), 476, 513(sh), 540 (3.80); 0.90	449 (3.1), 476, 509, 542 (3.31); 0.97	448 (2.0), 476, 545 (2.68); 0.96	448 (1.5), 476, 545 (2.14); 0.86
7	448 (8.3), 476, 507;	449 (8.1), 476, 508; 0.79	449 (8.00), 476, 508; 0.82	449 (7.7), 476, 508;	450 (7.5), 477, 510;	450 (7.1), 478, 511;	451 (6.7), 478, 511;	452 (5.1), 478, 511;

	0.80						0.79		0.75		0.77		0.69		0.56					
8	439	(4.9),	439	(4.9),	439	(5.3),	439	(4.7),	439	(4.9),	439	(4.9),	440	(4.4),	442	(3.5),				
	466,	495;	467, 495; 0.87		467, 495; 0.89		467,	495;	467,	495;	467,	495;	467,	495;	467,	497;				
	0.78						0.91		0.92		0.93		0.56		0.38					
9	440	(3.4),	440	(1.8),	440	(1.0),	441	(0.7),	440	(0.3),	440	(0.2),	440	(0.2),	440	(0.2),				
	468,	572	468,	572	468,	572	469,	569	469,	569	469,	569	468,	572	462,	572				
	(2.4); 0.65		(1.9); 0.82		(2.1); 0.91		(2.0); 0.90		(2.0); 0.95		(1.9); 0.95		(1.8); 0.96		(2.2); 0.88					
10	442	(8.4),	441	(7.3),	442	(4.9),	442	(3.9),	442	(2.6),	442	(1.8),	440	(0.9),	441	(0.5),				
	470,	501;	470, 499, 542;		470, 505, 545		470,	546	470,	545	471,	546	470,	545	470,	546				
	1.00		1.00		(3.6); 1.00		(3.6);1.00		(2.7); 1.00		(2.5); 1.00		(2.1); 1.00		(1.8); 1.00					
11	442	(8.6),	443	(8.2),	442	(7.7),	443	(7.5),	443	(9.0),	443	(7.4),	443	(6.7),	444	(5.3),				
	470,	500;	470, 500; 0.82		470, 502; 0.85		470,	501;	471,	501;	472,	503;	472,	502;	472,	503,				
	0.75;						0.83		0.83		0.80		0.77		540; 0.70					
12	436	(6.7),	436	(6.9),	436	(6.6),	436	(6.6),	436	(5.8),	436	(5.4),	437	(4.7)	438	(2.0),				
	464,	490;	464, 490; 1.00		464, 490; 0.98		464,	491;	464,	491;	464,	491;	463,	492;	464,	493;				
	0.98						0.99		0.80		0.79		0.58		0.38					

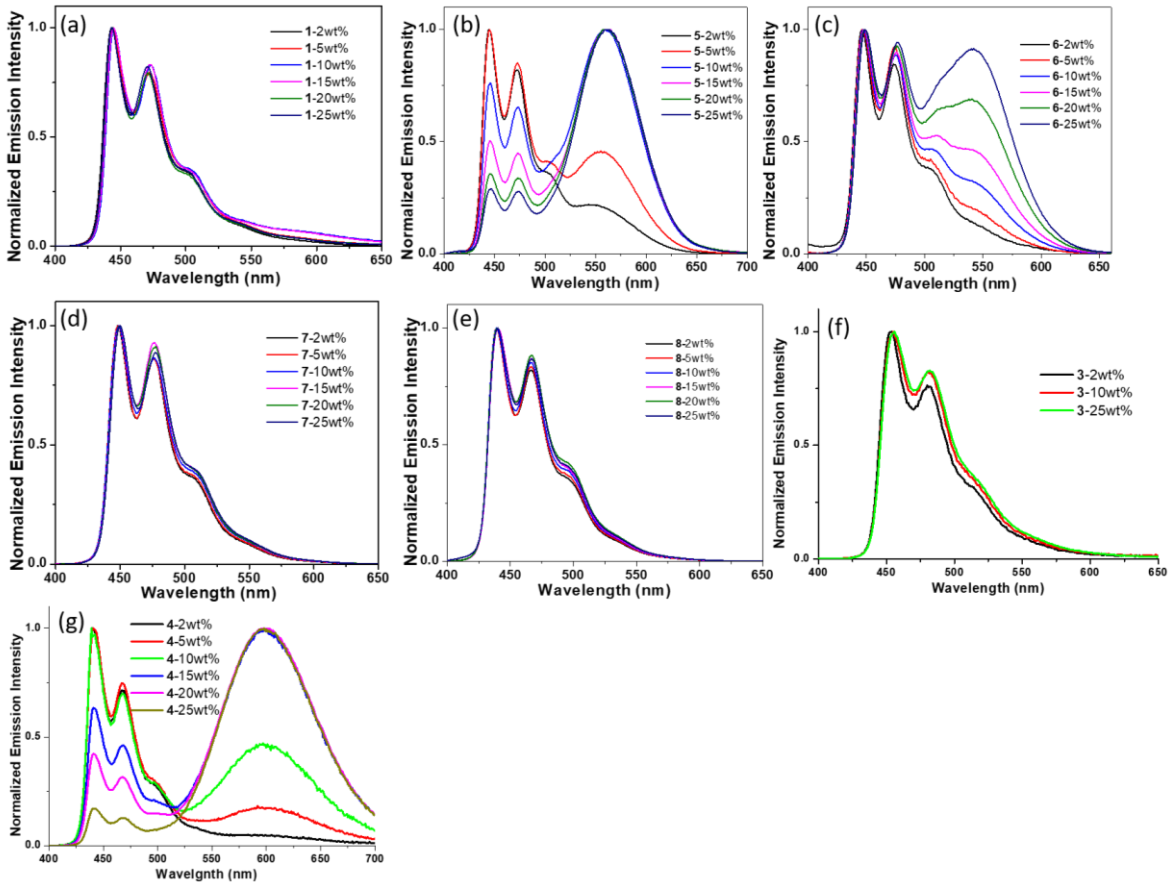

Figure S10. Emission spectra of (a) **1**, (b) **5**, (c) **6**, (d) **7**, (e) **8**, (f) **3** and (g) **4** dispersed in PMMA films at difference dopant concentrations (2–25wt%).

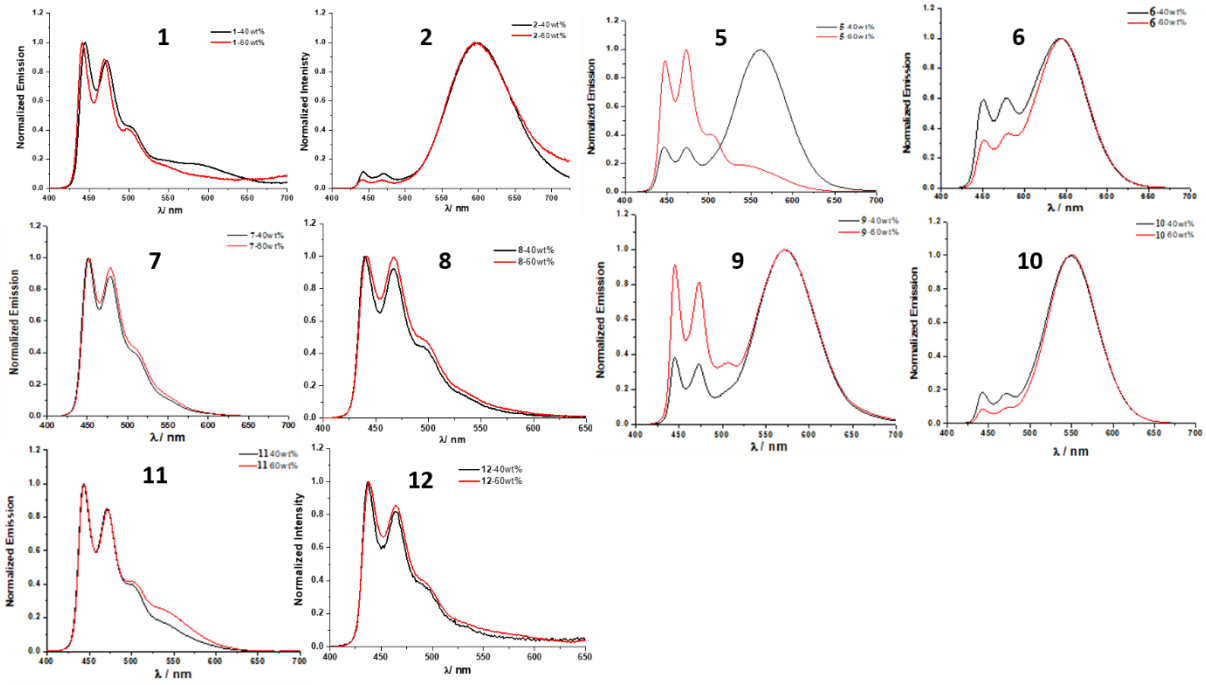

Figure S11. Emission spectra of complexes **1**, **2** and **5**–**12** dispersed in PMMA with 40 and 60 wt% dopant concentration.

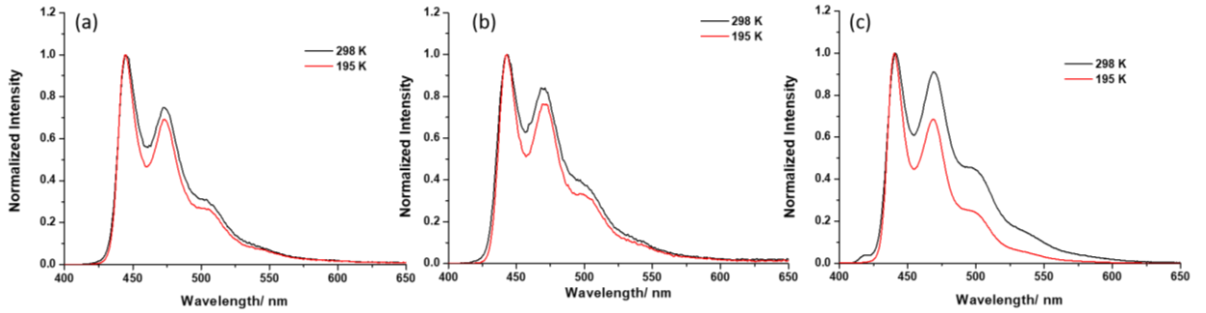

Figure S12. Emission spectra of (a) **1** in CH_2Cl_2 and (b) **8** and (c) **11** in toluene at 2×10^{-5} M at 298 and 195 K.

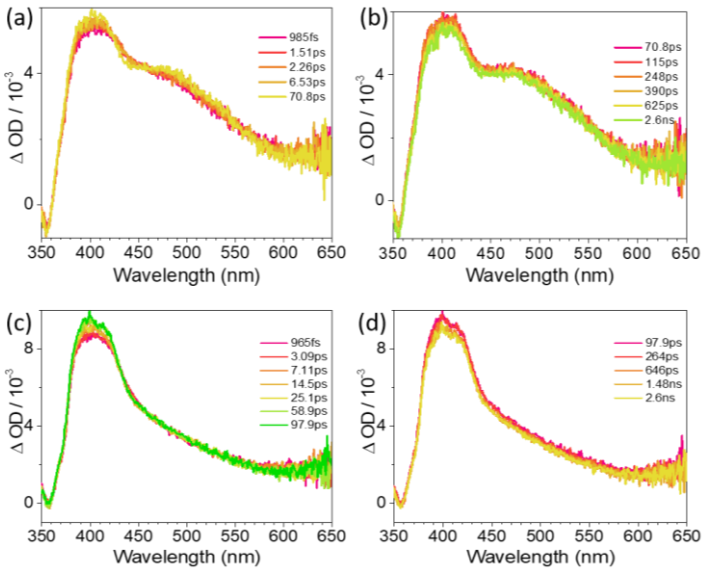

Figure S13. Femtosecond transient absorption difference spectra of (a, b) **1** and (c, d) **5** in CH_2Cl_2.

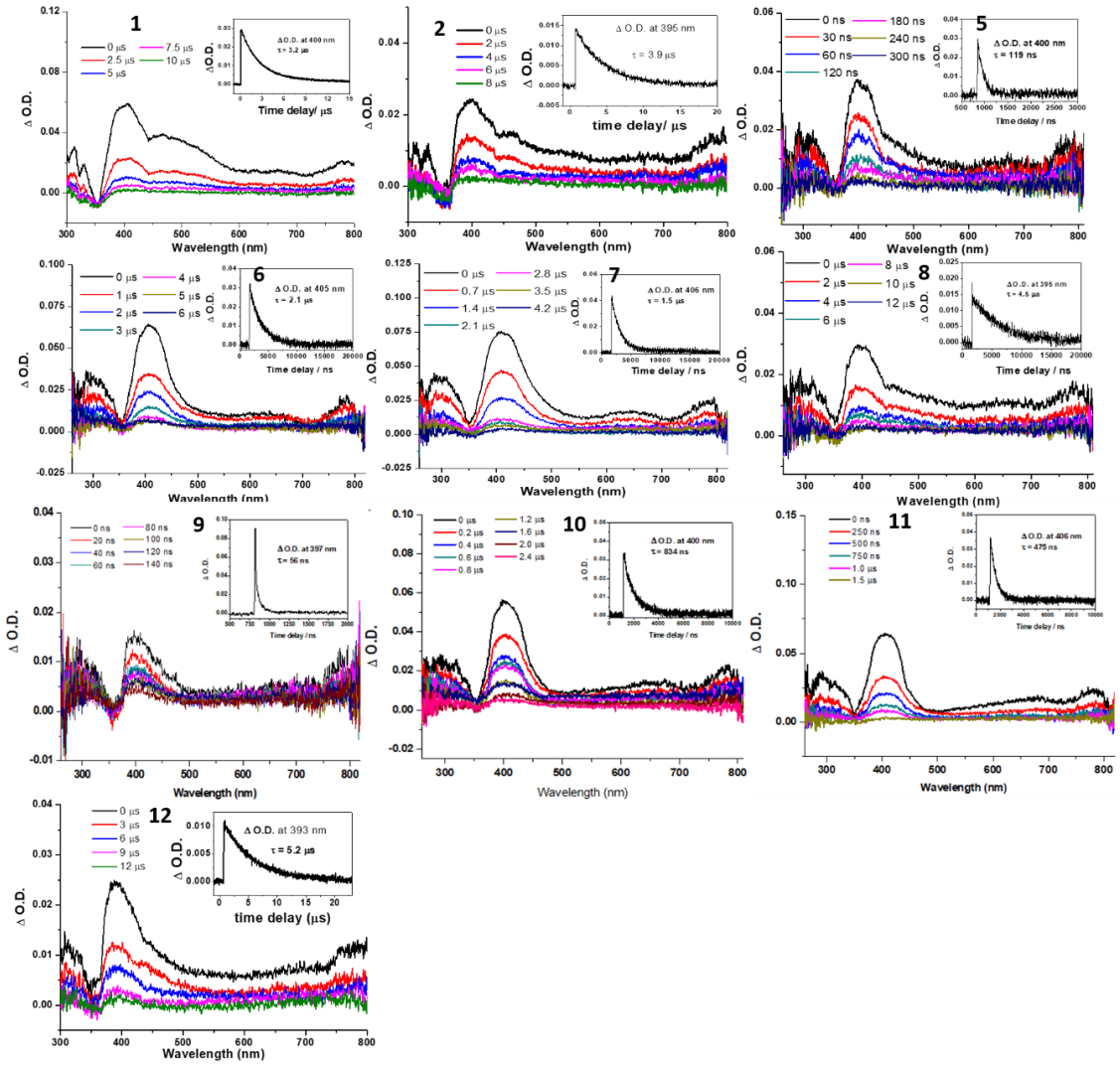

Figure S14. ns-TA spectra of **1**, **2** and **5**–**12** in degassed CH_2Cl_2 at 5×10^{-5} M.

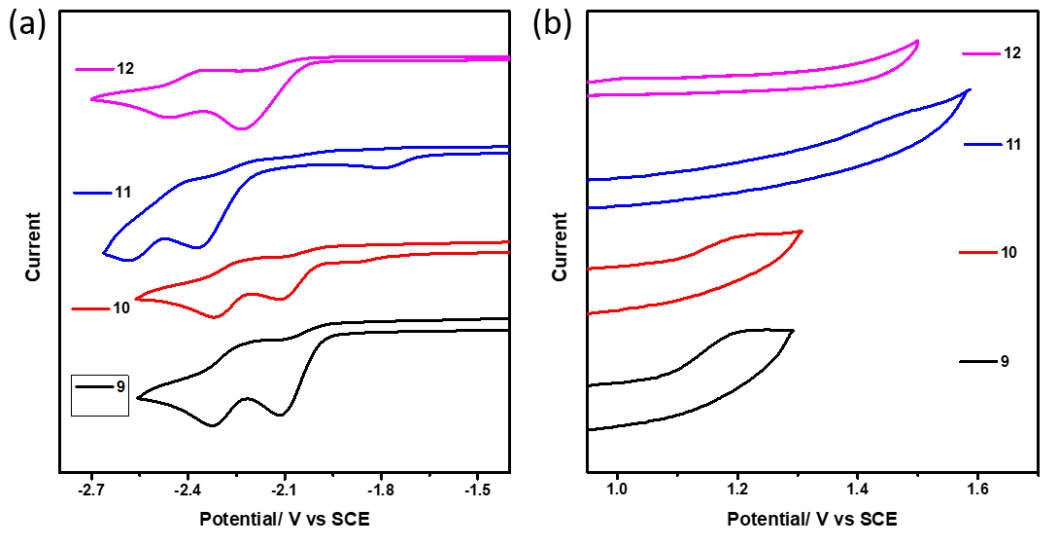

Figure S15. Cyclic voltammograms of **9–12** measured in DMF solution with 0.1 M $^{n}Bu_4NPF_6$ as supporting electrolyte at room temperature. (a) Reductive sweep and (b) oxidative sweep at a scan rate of 100 mV s^{-1}.

Estimation of Förster Radius

The Förster Radius (R_{FRET}) can be calculated by the following equation:

$$R_{FRET} = \sqrt[6]{\left\{\frac{9000ln10(\kappa^2)\Phi_d J}{128\pi^5\eta^4 N_A}\right\}}$$

where Φ_d is the donor's emission quantum yield (in this case, **11** in PMMA (10 wt%)), κ is the orientation factor, n is the refractive index of the medium and J is the overlap integral. We used Φ_d = 0.85, κ = 0.476,[20] and n = 1.49, respectively.

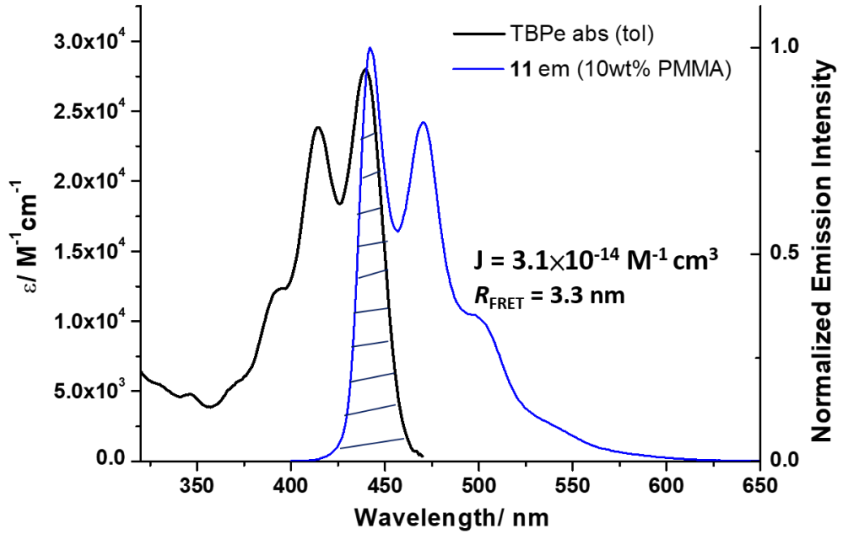

Figure S16. Spectral overlap of absorption spectrum of TBPe in toluene and emission spectrum of **11** in PMMA (10 wt%). The overlap of these spectra results in an overlap integral of 3.1×10^{-14} M^{-1} cm^3 and R_{FRET} of 3.3 nm, respectively.

DFT Calculations

Table S6. Ground state normal mode frequency, and the corresponding shift vector and Huang-Rhys factors of **11**. The absolute values of calculated shift vectors for high frequency vibrational modes (101-261) are less than 11 a.u. and has not been listed here.

Normal mode	freq / cm^{-1}	shift vector / a.u.	Huang-Rhys factor
1	8.92	-117.758	0.281794054
2	14.44	-167.134	0.918931071
3	17.64	-44.0841	0.078099574
4	22.79	28.4189	0.041931942
5	23.65	20.5703	0.022798093
6	24.96	11.3124	0.007276796
7	26	-30.4933	0.055076753
8	29.48	26.1617	0.045966933
9	33.77	6.27466	0.003028988
10	35.78	-6.43177	0.003371999
11	39.59	-4.74915	0.002034246
12	49.97	-13.6323	0.021156009
13	50.25	-3.77357	0.001630148
14	53.7	-8.0088	0.007846849
15	61.22	4.90128	0.003350414
16	69.89	-10.005	0.015938056
17	71.31	1.86245	0.000563515
18	81.93	15.9377	0.047411138
19	92.4	-5.77503	0.007020476
20	103.76	1.67216	0.000660955
21	109.54	-4.94227	0.006095535
22	116.02	4.1186	0.004483511
23	117.47	-0.914847	0.00022398
24	122.58	0.309657	2.67773E-05
25	126.2	6.22034	0.011124327
26	129.9	-4.64991	0.006398591
27	133	-6.94596	0.014618484
28	140	-0.924915	0.000272846
29	141.2	1.26377	0.000513756
30	144.9	7.82251	0.020199786
31	146.1	0.498587	8.27405E-05
32	154.3	3.08943	0.003355126
33	159	-0.10357	3.88554E-06
34	160.7	-1.89048	0.001308417
35	166.1	0.134765	6.87242E-06
36	173.3	0.334597	4.42007E-05
37	175	-1.37243	0.000750939

38	179.6	-0.794321	0.000258157
39	183.2	-0.247658	2.55986E-05
40	201.9	-7.1005	0.023189977
41	216.5	-10.6901	0.056364747
42	219.8	0.420375	8.84887E-05
43	227.6	-1.35973	0.000958658
44	229	1.98825	0.002062356
45	232	4.47098	0.010565245
46	233.6	0.118758	7.50559E-06
47	235.9	0.323054	5.60873E-05
48	248	-0.421448	0.000100352
49	260.1	0.779583	0.000360123
50	264.2	0.231755	3.23279E-05
51	265	-0.607194	0.00022258
52	266	0.212787	2.74383E-05
53	267.9	-1.19939	0.00087797
54	272.9	-0.440643	0.000120716
55	276.2	0.364651	8.3669E-05
56	277.4	-0.294864	5.4946E-05
57	282.7	-0.699892	0.000315482
58	287	0.950139	0.000590259
59	287.9	-0.465405	0.000142066
60	298.2	0.416529	0.000117865
61	305.2	-1.0825	0.000814754
62	310.2	-0.0750786	3.98346E-06
63	311.2	-0.110734	8.69336E-06
64	315.5	-0.181388	2.36484E-05
65	323.1	0.191283	2.69324E-05
66	340.9	-2.46248	0.004709324
67	343.4	0.664449	0.00034539
68	345.7	-0.794752	0.000497449
69	347.5	-3.65627	0.010583211
70	351.3	-0.982591	0.000772698
71	352.8	0.178825	2.57023E-05
72	367.7	0.246187	5.07703E-05
73	370.4	-1.57038	0.002080974
74	391.8	-10.7979	0.104070865
75	400.8	0.877443	0.000702994
76	405.5	0.151659	2.12478E-05
77	408.8	-0.125318	1.46259E-05
78	411.4	0.229941	4.95545E-05
79	416.7	-0.83403	0.000660348
80	421.9	-0.200578	3.86689E-05

81	451.4	2.78613	0.007982712
82	455.3	0.00192968	3.86237E-09
83	456.3	-0.884389	0.000813061
84	457.3	0.717855	0.00053686
85	462.1	-5.78481	0.035228998
86	474.5	-0.685672	0.000508224
87	481.9	0.0375285	1.5462E-06
88	487.1	-0.387846	0.000166926
89	497.5	-0.0648081	4.76034E-06
90	510.4	-0.567186	0.000374066
91	512.6	-1.14671	0.001535578
92	517.2	0.616131	0.000447292
93	520.5	0.273773	8.88767E-05
94	537.3	-0.220614	5.95757E-05
95	554	0.217414	5.96583E-05
96	580	-0.0209361	5.7917E-07
97	581.5	-0.201065	5.35561E-05
98	585	-0.0089673	1.07168E-07
99	591.1	3.42258	0.015774453
100	581.5	1.55678	0.003210631

Table S7. Ground state normal mode frequency, and the corresponding shift vector and Huang-Rhys factors of **2**. The absolute values of calculated shift vectors for high frequency vibrational modes (101-261) are less than 11 a.u. and has not been listed here.

Normal mode	freq / cm^{-1}	shift vector / a.u.	Huang-Rhys factor
1	10.73	-98.9957	0.239562321
2	18.38	30.0249	0.037748072
3	23.86	-9.44182	0.004845828
4	27.39	-16.1502	0.016275486
5	31.8	26.2217	0.04981211
6	42.42	13.1096	0.016608701
7	60.59	12.9029	0.02298062
8	87.33	8.98746	0.016070283
9	98.76	0.73962	0.000123079
10	85.9	8.01801	0.012580922
11	87.33	-3.24645	0.002096848
12	98.76	2.31532	0.001206116
13	123.65	4.32468	0.005268515
14	125.05	14.6217	0.060906769
15	149.97	0.979478	0.000327778
16	151.43	-3.90919	0.005271954
17	164.98	-1.00407	0.000378918
18	200.79	-14.7722	0.09982023

19	207.7	5.2975	0.013278975
20	21.29	-3.13317	0.000476135
21	228.04	-2.35521	0.002881751
22	238.17	1.1482	0.000715333
23	247.39	0.191925	2.07602E-05
24	251.66	-1.12819	0.000729734
25	255.8	-0.179824	1.88444E-05
26	265.3	-7.31307	0.032323832
27	277.83	-3.68712	0.008604781
28	295.9	0.347645	8.1471E-05
29	297.2	-5.61721	0.021363689
30	305.8	-0.65514	0.000299014
31	330.1	-2.54395	0.004866859
32	331.5	0.24945	4.69934E-05
33	340.9	0.735292	0.000419887
34	376.4	0.70603	0.000427447
35	388.1	-13.6252	0.164140421
36	430.8	0.839086	0.000690995
37	442.7	1.30361	0.001713922
38	464.4	6.31384	0.042176009
39	508.1	-0.82662	0.000790947
40	522.3	-0.971671	0.001123426
41	525.4	-0.335534	0.000134756
42	569.2	-0.319435	0.000132317
43	586.81	2.121	0.006014021
44	591.7	2.63937	0.00939049
45	633.96	0.0204131	6.01819E-07
46	652.1133	0.713958	0.000757277
47	658.2	-0.466377	0.000326151
48	678.21	1.26976	0.002491114
49	690	-0.0366153	2.10747E-06
50	691.62	1.76755	0.004922629
51	700.55	0.130214	2.70608E-05
52	714.6	0.667109	0.000724507
53	716.13	-10.5991	0.183280379
54	733.34	0.267628	0.000119662
55	741.44	0.108159	1.976E-05
56	758.87	-0.00212028	7.77213E-09
57	761.11	0.349627	0.000211955
58	769.1	-0.686217	0.000825072
59	799.1	-0.247359	0.000111389
60	834	0.0960741	1.75374E-05
61	835.3	0.0937736	1.67336E-05

62	846.7	-2.86706	0.01585584
63	847.6	0.264552	0.000135145
64	854.83	-8.3984	0.137359593
65	887.4	-0.657446	0.000873828
66	891.8	-0.156277	4.96185E-05
67	898.1	-0.296477	0.000179843
68	898.4	0.865698	0.001533871
69	968.8	-0.373856	0.000308481
70	1020	0.214877	0.000107292
71	1056.4	-0.265016	0.000169028
72	1073.3	0.0960527	2.25593E-05
73	1074.9	1.3617	0.00454064
74	1089.5	0.255237	0.000161697
75	1091.99	0.458071	0.000522
76	1096.5	-3.94999	0.038975057
77	1126.2	7.98445	0.163565484
78	1127.7	0.608266	0.000950532
79	1147.7	5.94832	0.092513084
80	1148.3	4.12428	0.044497722
81	1148.8	2.01628	0.01063977
82	1156.3	-0.447347	0.000527164
83	1161.4	0.707729	0.001325263
84	1184.97	0.625101	0.001054858
85	1192.1	4.29009	0.049984071
86	1215.5	0.305808	0.000258964
87	1230.6	5.19211	0.075577202
88	1250.8	-1.38823	0.005491574
89	1251.5	0.649102	0.001201276
90	1230.6	-0.660309	0.001222355
91	1250.77	1.96375	0.010988438
92	1251.897	1.59953	0.007296919
93	1279.37	-0.24828	0.000179666
94	1283.83	-1.64409	0.007905782
95	1292.4	0.131366	5.081E-05
96	1295	-0.212887	0.000133707
97	385	0.550014	0.000265335
98	1330.7999	-1.12084	0.003808782
99	1333.9	-7.72819	0.181495133
100	1341.8	-0.224706	0.000154349

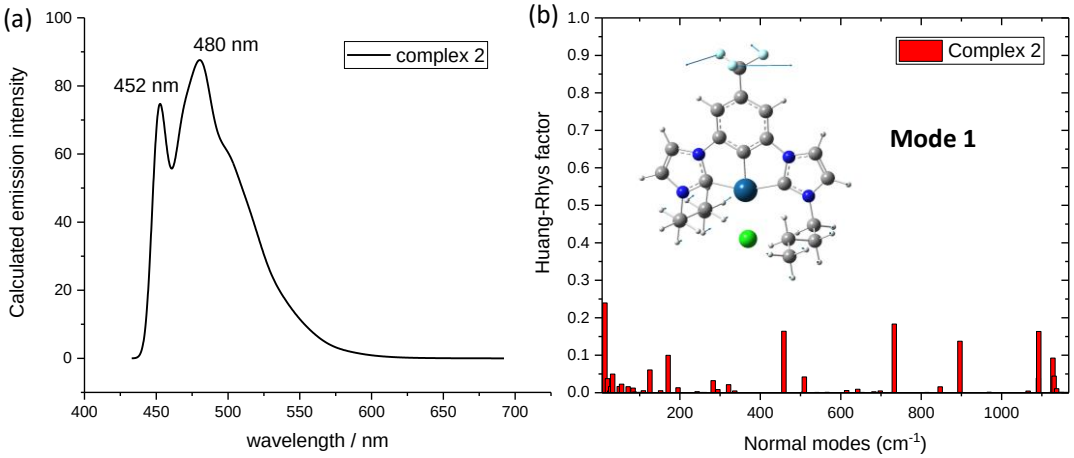

Figure S17. a) Simulated vibronically-resolved emission spectrum and b) Huang-Rhys factors of the $T_1 \rightarrow S_0$ transition versus normal modes of **2**. The inset of (b) depicts vibrational mode 1 of **2**.

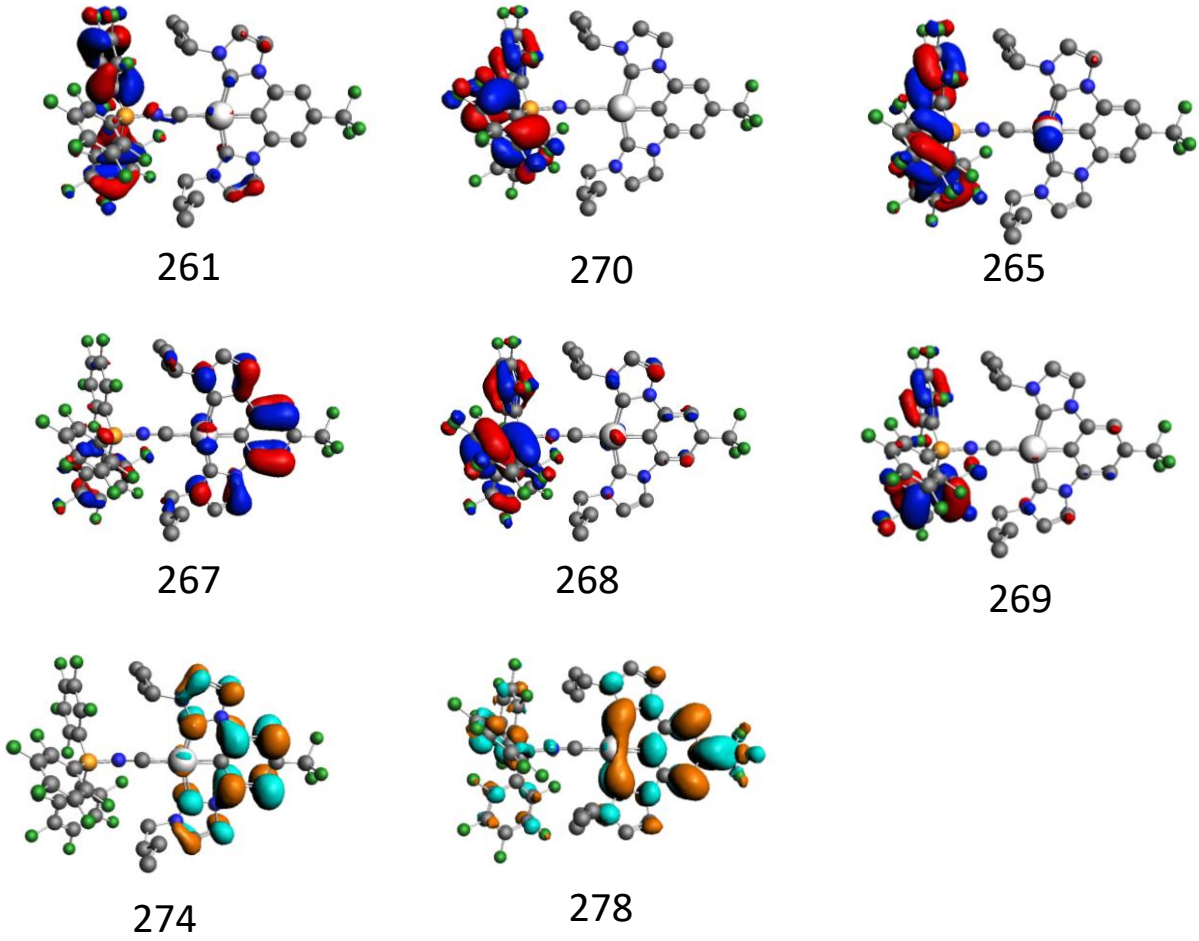

Figure S18. Calculated frontier molecular orbitals of **11**.

Table S8. Calculated spin-free (singlet and triplet) excited states of **11** at the optimized T_1 structure, together with the spin-orbit coupling matrix element ($<S_m|H_{so}|T_1>$) between S_m and T_1.Orbital 272 is HOMO and 273 is LUMO.

	E/eV	oscillator strength	Major contribution (%)	Minor contribution (%)	$<S_m\|H_{so}\|T_1>$/cm^{-1}
S_1	3.328	0.10835	272->273 (0.95)	271->273(0.03)	91.35
S_2	3.381	0.059419	271->273(0.95)	272->273(0.03)	389.62
S_3	3.931	0.059802	266->273(0.72), 264->273(0.12)	265->273(0.1)	1115.6
S_4	4.201	0.026857	272->274(0.41),267->273(0.39)	268->273(0.07), 269->273(0.07)	109.49
S_5	4.422	0.16037	264->273(0.57), 263->273(0.14)	266->273(0.08), 268->273(0.07)	117.45
S_6	4.496	0.10544	261->273(0.42), 270->273(0.25)	267->273(0.09), 272->274 (0.07)	422.12
S_7	4.518	0.59698	272->274(0.44), 267->273 (0.18), 269->273 (0.13)	268->273(0.09), 270->273(0.06)	254.03
S_8	4.556	0.00615	270->273(0.65), 261->273(0.18)	268->273(0.09), 270->273(0.06)	265.68
S_9	4.632	0.02046	269->273 (0.76), 267->273(0.15)	268->273(0.02)	73.74
S_{10}	4.686	0.01828	268->273(0.61), 261->273 (0.12)	267->273(0.1), 263->273 (0.06)	179.43
T_1	2.46	0	272->273(0.88)	272->278(0.03)	

Major single group excitation contributions for the above excitations

Excitation Nr.	Single group excited states	Excitation energy /eV	weight (sum=1)	Contribution to f
1:	Triplet 1A	2.4586	0.4240	
1:	Triplet 1A	2.4586	0.4240	
1:	Triplet 1A	2.4586	0.1349	
1:	Triplet 3A	3.5779	0.0094	
1:	Triplet 3A	3.5779	0.0018	
1:	Triplet 3A	3.5779	0.0018	
1:	Triplet 2A	3.0612	0.0008	
1:	Triplet 2A	3.0612	0.0008	
1:	Singlet 6A	4.4961	0.0007	0.7762E-04
2:	Triplet 1A	2.4586	0.7178	
2:	Triplet 1A	2.4586	0.1326	
2:	Triplet 1A	2.4586	0.1326	
2:	Triplet 3A	3.5779	0.0059	
2:	Triplet 3A	3.5779	0.0059	
2:	Triplet 3A	3.5779	0.0019	
2:	Singlet 2A	3.3814	0.0009	0.5181E-04
2:	Triplet 12A	4.3542	0.0005	
3:	Triplet 1A	2.4586	0.4284	
3:	Triplet 1A	2.4586	0.4284	
3:	Triplet 1A	2.4586	0.1308	
3:	Singlet 3A	3.9313	0.0073	0.4339E-03
3:	Triplet 2A	3.0612	0.0014	
3:	Triplet 2A	3.0612	0.0014	

Figure S19. Major singlet state contributions to the T_I, T_{II} and T_{III} state transition of the T_1 state of **11**.

OLED performances

Table S9. EL properties of OLEDs based on the emission of **7**, **11,** or **12** with different host/HBL combinations.

EML/hole blocking layer	Host E_t (eV)	ETL E_t (eV)	λ_{max} [nm]	EQE_{max} [%]	CE_{max} [cd A^{-1}]	CIE [x,y]	Blue index
CzSi:**12**(6 wt%)/TSPO1	3.02	3.39	436	11.2	12.2	0.16, 0.12	101.7
TCTA:**12**(6 wt%)/TmPyPb	2.76	2.78	396	0.49	0.23	0.16, 0.07	3.29
CzSi:**12**(6 wt%)/DPEPO	3.02	3.30	438	9.63	9.11	0.15, 0.12	75.9
CzSi:**12**(6 wt%)/TmPyPb	3.02	2.78	437	1.28	1.37	0.16, 0.13	10.5
PYD2: **7** (4)/DPEPO [a)]	2.93	3.30	484	15.33	32.2	0.17, 0.32	100.6
PYD2: **11** (4)/DPEPO [a)]	2.93	3.30	448	14.72	15.54	0.16, 0.19	81.8

[a]Device structure is ITO/PEDOT: PSS/PYD2: emitter/DPEPO/TPBi/LiF/Al and fabricated by solution process.

Table S10. EL properties of blue phosphorescent sensitized fluorescence (PSF) and TADF-sensitized fluorescence (TSF) OLEDs in literature.

Sensitizer:florophore	λ_{max} [nm]	EQE_{max} [%]	CE_{max} [cdA^{-1}]	CIE [x,y]	Blue index	Ref.
11:TBPe	461	15.89	24.34	0.15, 0.20	121.7	**this work**
$Ir(dppi)_3$:BBDPAPe	475	11.6[a]	~28[a]	0.15, 0.28[a]	~100	[21]
$Ir(dfpysipy)_2(mpic)$:TBPe	~460	15.3	18.0	0.14, 0.19	94.7	[22]
CzAcSF:TBPe	~460	15.4	23.7[a]	0.15, 0.23[a]	103.0	[23]
CzAcSF:TBPe	465	18.1	24.3[b]	0.15, 0.22[b]	110.5	[24]
DMAC-DPS:TBPe	~460	13.5[a]	~21[a]	0.14, 0.25[a]	~84	[25]
5CzCN:TBPe	~460	16.8[c]	26.9[c]	0.15, 0.23[c]	116.9	[26]
DMAC-DMT:BPPyA	~460	17.5[b]	17.2[b]	0.14, 0.15[b]	114.7	[27]
PtNON:TBPe	466	16.9	/	0.16, 0.25	/	[28]
PtON7-dtp:TBPDP	478	16.9	28.9	0.13, 0.27	107.0	[29]

[a]At 1000 cd m^{-2}. [b]At 500 cd m^{-2}. [c]At 100 cd m^{-2}.

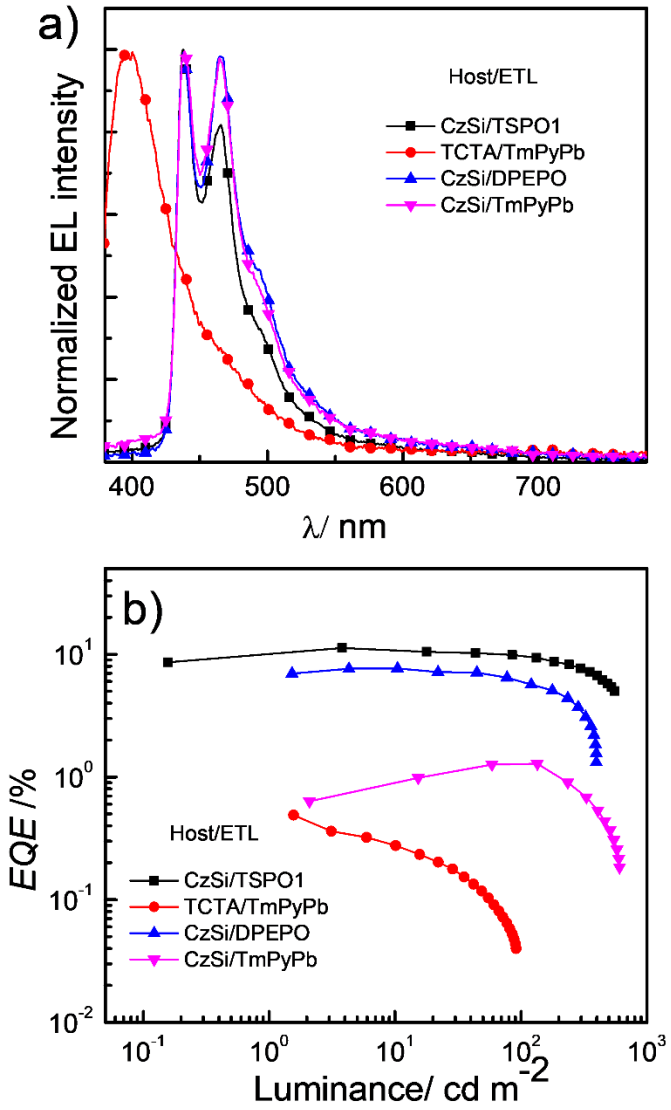

Figure S20. a) Normalized EL spectra and b) EQE-luminance characteristics of OLEDs based on **12** with different host/HBL combinations.

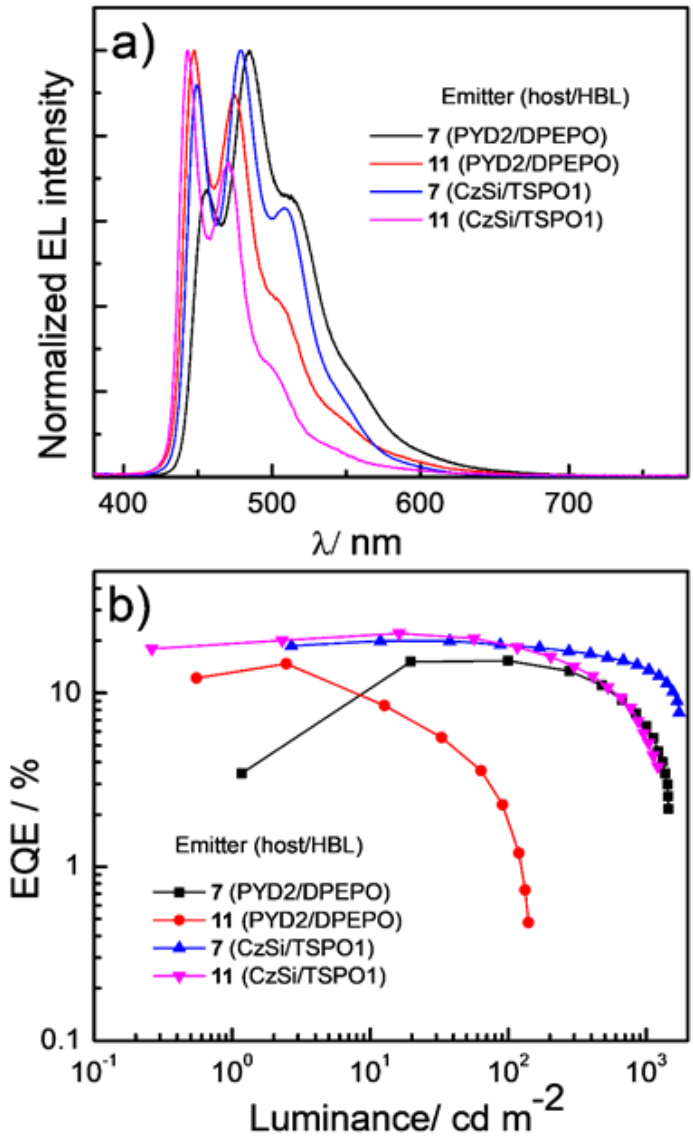

Figure S21. a) Normalized EL spectra and b) EQE-luminance characteristics of OLEDs based on **7** or **11** with different host/HBL combinations.

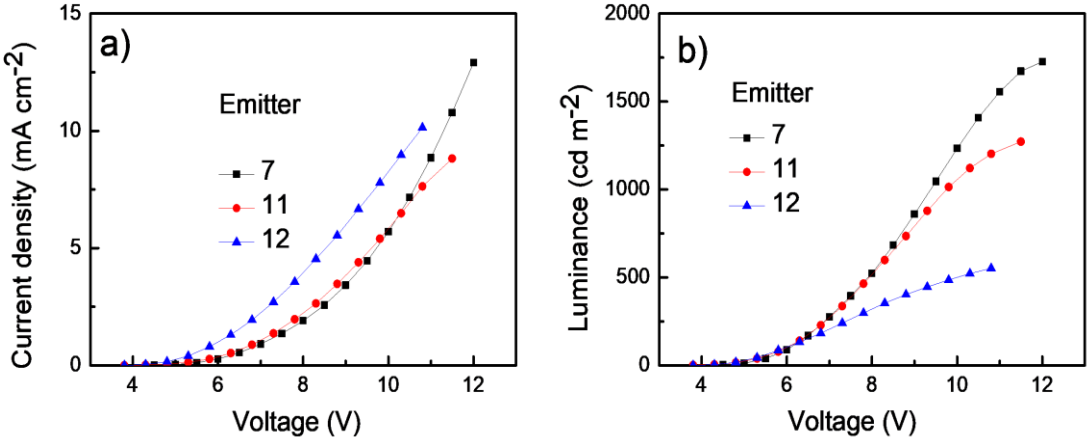

Figure S22. a) Current density-voltage and b) luminance-voltage characteristics of OLEDs with **7**, **11**, and **12**.

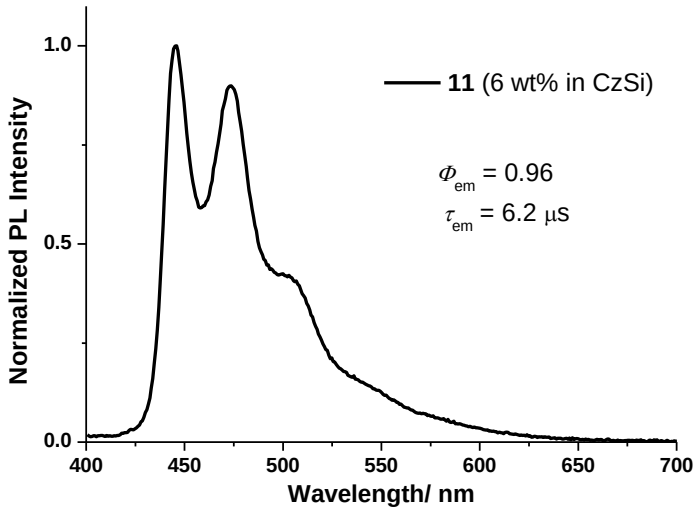

Figure S23. Emission spectrum of vapor-deposited CzSi thin film doped with 6 wt% of **11**. The PLQY of the film is 0.96.

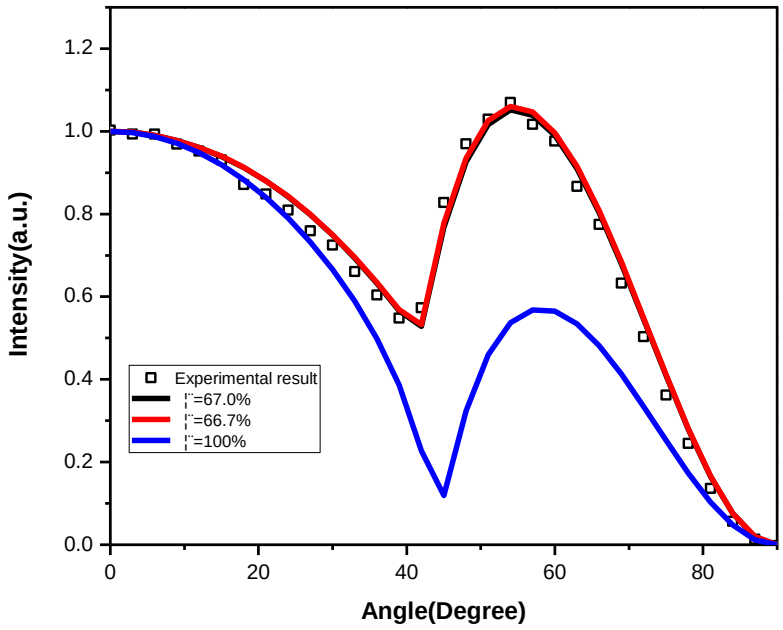

Figure S24. Angular-dependent PL intensities of *p*-polarized light of **11** (6 wt%) doped in CzSi thin films (30 nm). Measured intensities are compared with the simulated values.

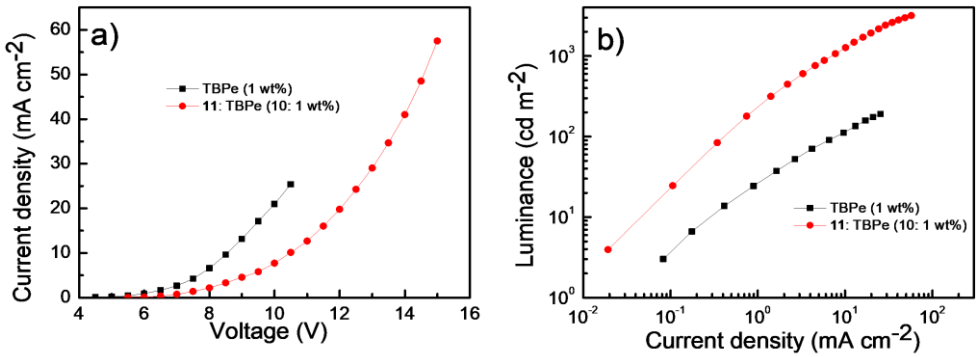

Figure S25. a) Current density-voltage and b) luminance-voltage characteristics of **11**-based OLED and **11**-based PSF OLED.

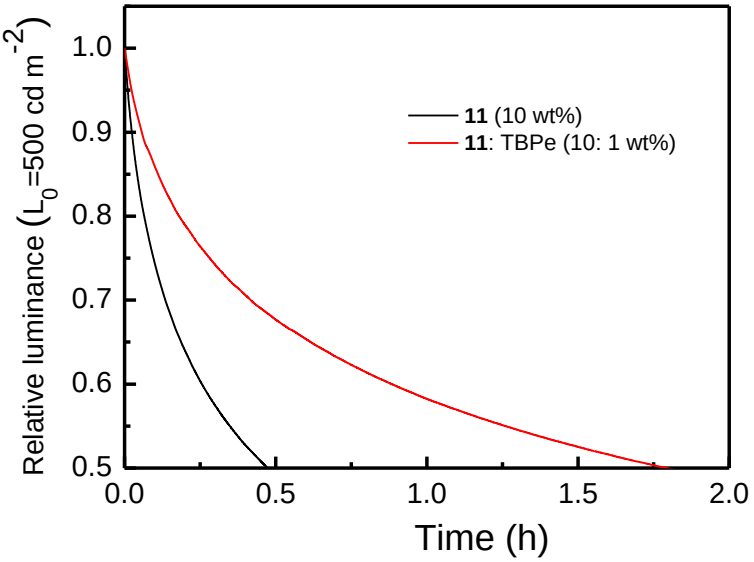

Figure S26. Relative luminance-operational time of **11**-based OLED and **11**-based PSF OLED.

References

1. Gaussian 09, Revision A.02, M. J. Frisch, G. W. Trucks, H. B. Schlegel, G. E. Scuseria, M. A. Robb, J. R. Cheeseman, G. Scalmani, V. Barone, G. A. Petersson, H. Nakatsuji, X. Li, M. Caricato, A. Marenich, J. Bloino, B. G. Janesko, R. Gomperts, B. Mennucci, H. P. Hratchian, J. V. Ortiz, A. F. Izmaylov, J. L. Sonnenberg, D. Williams-Young, F. Ding, F. Lipparini, F. Egidi, J. Goings, B. Peng, A. Petrone, T. Henderson, D. Ranasinghe, V. G. Zakrzewski, J. Gao, N. Rega, G. Zheng, W. Liang, M. Hada, M. Ehara, K. Toyota, R. Fukuda, J. Hasegawa, M. Ishida, T. Nakajima, Y. Honda, O. Kitao, H. Nakai, T. Vreven, K. Throssell, J. A. Montgomery, Jr., J. E. Peralta, F. Ogliaro, M. Bearpark, J. J. Heyd, E. Brothers, K. N. Kudin, V. N. Staroverov, T. Keith, R. Kobayashi, J. Normand, K. Raghavachari, A. Rendell, J. C. Burant, S. S. Iyengar, J. Tomasi, M. Cossi, J. M. Millam, M. Klene, C. Adamo, R. Cammi, J. W. Ochterski, R. L. Martin, K. Morokuma, O. Farkas, J. B. Foresman, D. J. Fox, Gaussian, Inc., Wallingford CT.
2. C. Adamo and V. Barone, *J. Chem. Phys.*, 1999, **110**, 6158.
3. S. Grimme, J. Antony, S. Ehrlich and H. Krieg, *J. Chem. Phys.*, 2010, **132**, 154104.
4. W. R. Wadt and P. J. Hay, *J. Chem. Phys.*, 1985, **82**, 284.
5. P. J. Hay and W. R. Wadt, *J. Chem. Phys.*, 1985, **82**, 299.
6. M. J. Frisch, J. A. Pople and J. S. Binkley, *J. Chem. Phys.*, 1984, **80**, 3265.
7. L. Radom, P. Hariharan, J. Pople and P. Schleyer, *J. Am. Chem. Soc.*, 1973, **95**, 6531.
8. M. Cossi, G. Scalmani, N. Rega and V. Barone, *J. Chem. Phys.*, 2002, **117**, 43.
9. G. t. Te Velde, F. M. Bickelhaupt, E. J. Baerends, C. Fonseca Guerra, S. J. van Gisbergen, J. G. Snijders and T. Ziegler, *J. Comput. Chem.*, 2001, **22**, 931.
10. C. F. Guerra, J. Snijders, G. t. te Velde and E. J. Baerends, *Theor. Chem. Acc.*, 1998, **99**, 391.
11. E. van Lenthe, A. Ehlers and E.-J. Baerends, *J. Chem. Phys.*, 1999, **110**, 8943.
12. E. van Lenthe, E.-J. Baerends and J. G. Snijders, *J. Chem. Phys.*, 1993, **99**, 4597.
13. E. van Lenthe, E.-J. Baerends and J. G. Snijders, *J. Chem. Phys.*, 1994, **101**, 9783.
14. E. Van Lenthe and E. J. Baerends, *J. Comput. Chem.*, 2003, **24**, 1142.
15. K. Mori, T. Goumans, E. van Lenthe and F. Wang, *Phys. Chem. Chem. Phys.*, 2014, **16**, 14523.
16. V. C. Vargas, R. J. Rubio, T. K. Hollis and M. E. Salcido, *Org. Lett*, 2003, **5**, 4847-4849.
17. T. A.K. and Al-Allaf, *J. Organomet. Chem.*, 2002, **654**, 21.
18. X. Zhang, A. M. Wright, N. J. DeYonker, T. K. Hollis, N. I. Hammer, C. E. Webster and E. J. Valente, *Organometallics*, 2012, **31**, 1664.
19. W.-K. Chu, S.-M. Yiu and C.-C. Ko, *Organometallics*, 2014, **33**, 6771.
20. J. Baumann and M. D. Fayer, *J. Chem. Phys.*, 1986, **85**, 4087.
21. P. Heimel, A. Mondal, F. May, W. Kowalsky, C. Lennartz, D. Andrienko, R. Lovrincic, *Nat. Commun.*, 2018, **9**, 4990.
22. H.-G. Kim, H. Shin, Y. H. Ha, R. Kim, S.-K. Kwon, Y.-H. Kim, J.-J. Kim, *ACS Appl. Mater. Interfaces*, 2019, **11**, 26.
23. W. Song, I. Lee, J. Y. Lee, *Adv. Mater.*, 2015, **27**, 4358.
24. I. H. Lee, W. Song, J. Y. Lee, S. H. Hwang, *J. Mater. Chem. C*, 2015, **3**, 8834.
25. S. H. Han, J. Y. Lee, *J. Mater. Chem. C*, 2018, **6**, 1504.
26. S. K. Jeon, H. J. Park, J. Y. Lee, *ACS Appl. Mater. Interfaces*, 2018, **10**, 5700.
27. D. H. Ahn, J. H. Jeong, J. Song, J. Y. Lee, J. H. Kwon, *ACS Appl. Mater. Interfaces*, 2018, **10**, 10246.
28. K. Klimes, Z.-Q. Zhu, J. Li, *Adv. Funct. Mater.*, 2019, 193068.
29. S. Nam, J. W. Kim, H. J. Bae, Y. M. Maruyama, D. Jeong, J. Kim, J. S. Kim, W.-J. Son, H. Jeong, J. Lee, S.-G. Ihn, H. Choi, *Adv. Sci.*, 2021, 2100586.

NMR spectra

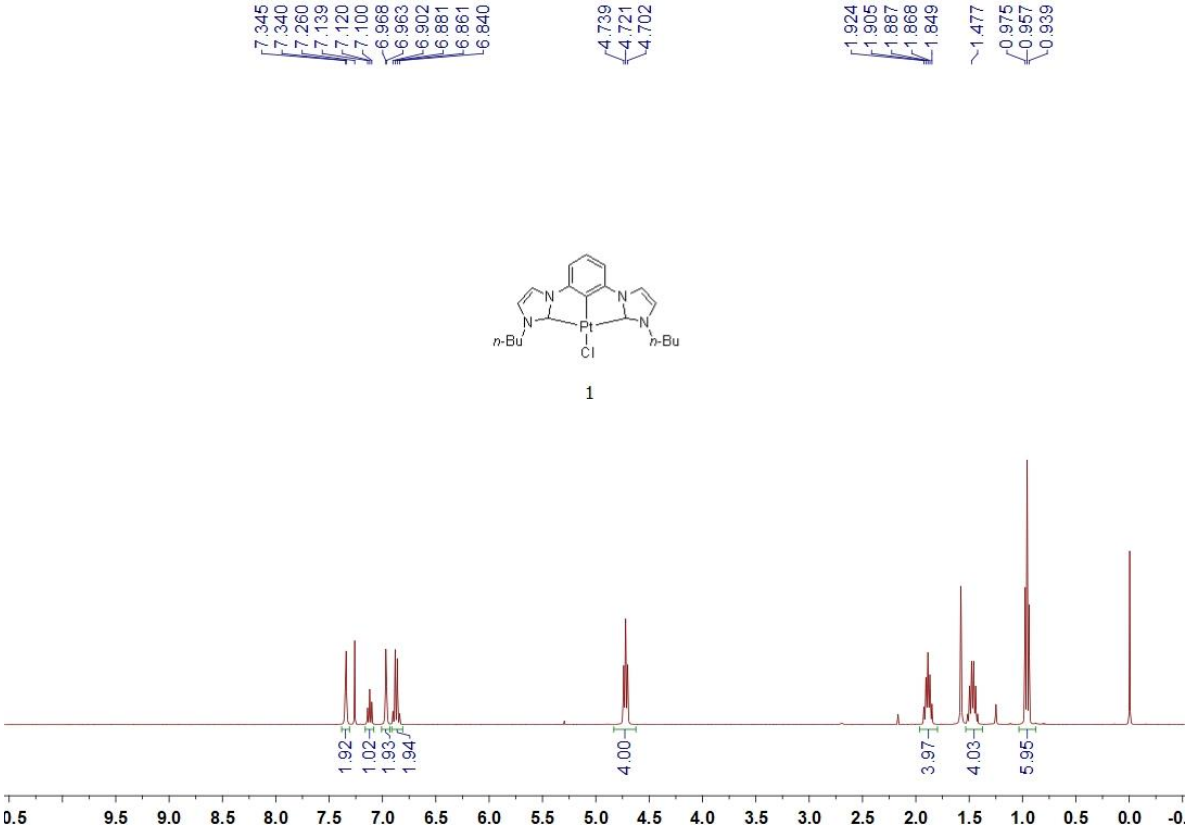

^{1}H NMR (400 MHz) spectrum of **1** in $CDCl_3$.

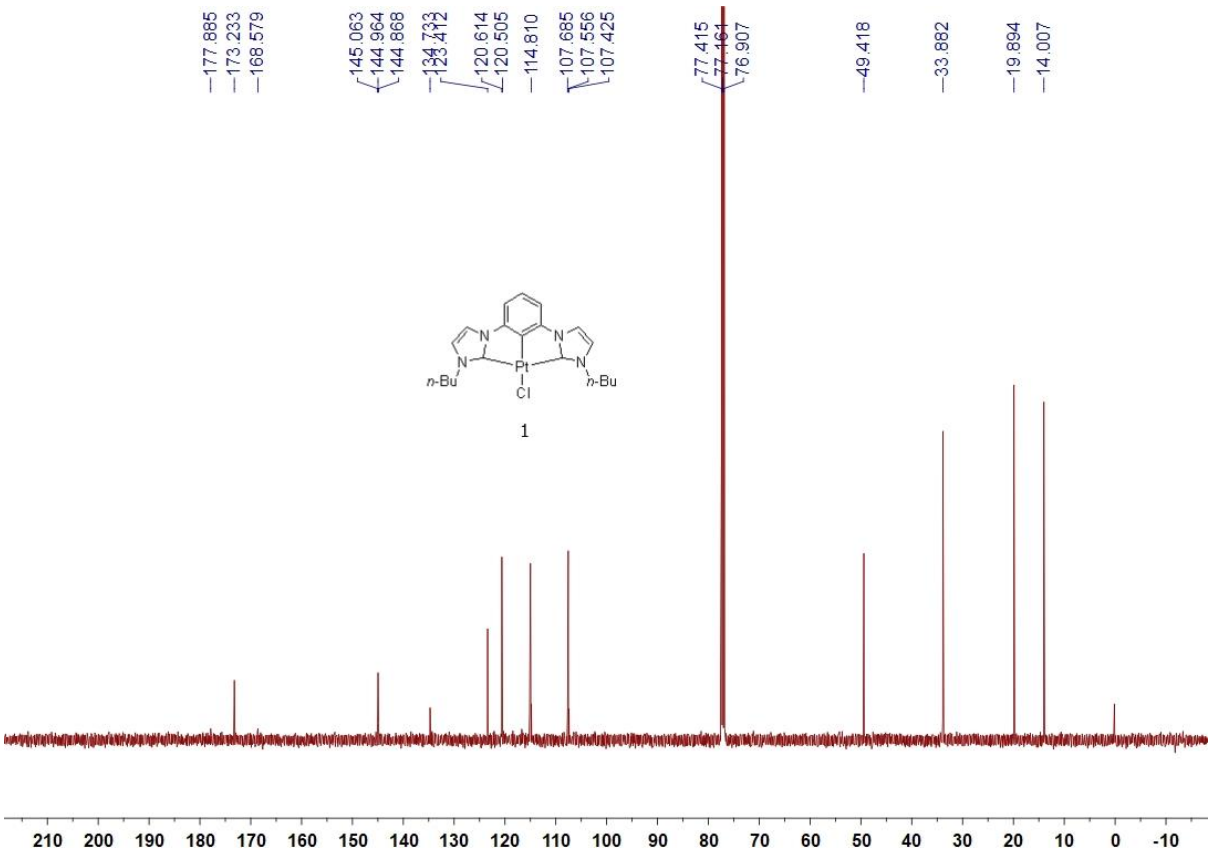

^{13}C NMR (126 MHz) spectrum of **1** in $CDCl_3$.

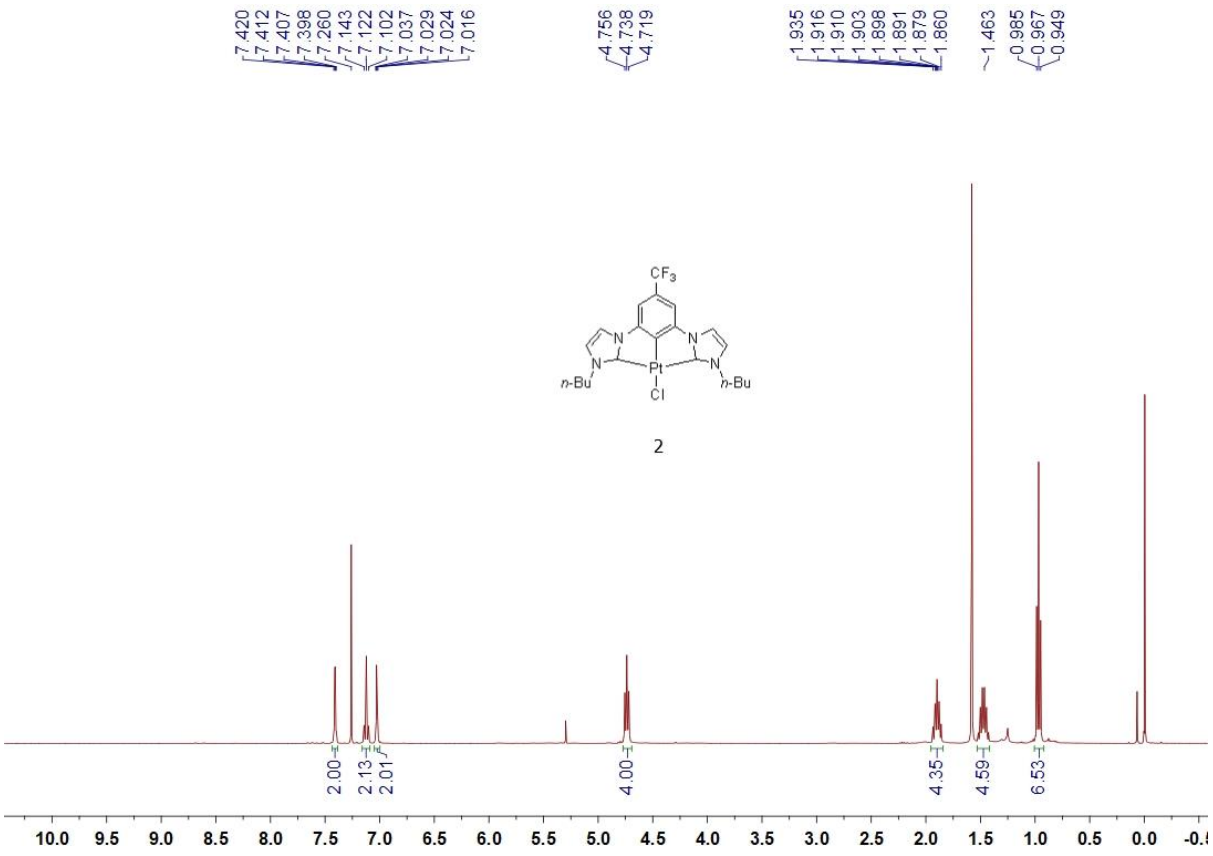

^{1}H NMR (400 MHz) spectrum of **2** in $CDCl_3$.

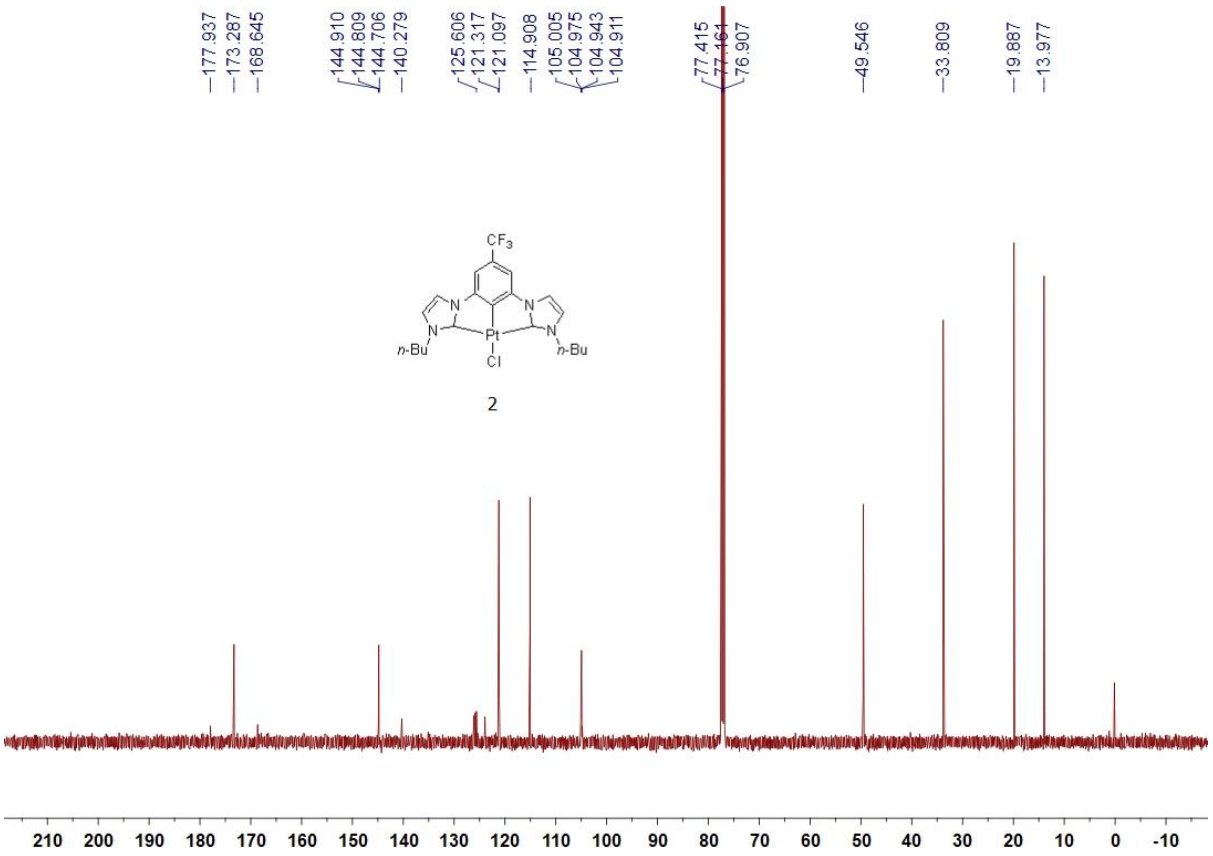

^{13}C NMR (126 MHz) spectrum of **2** in $CDCl_3$.

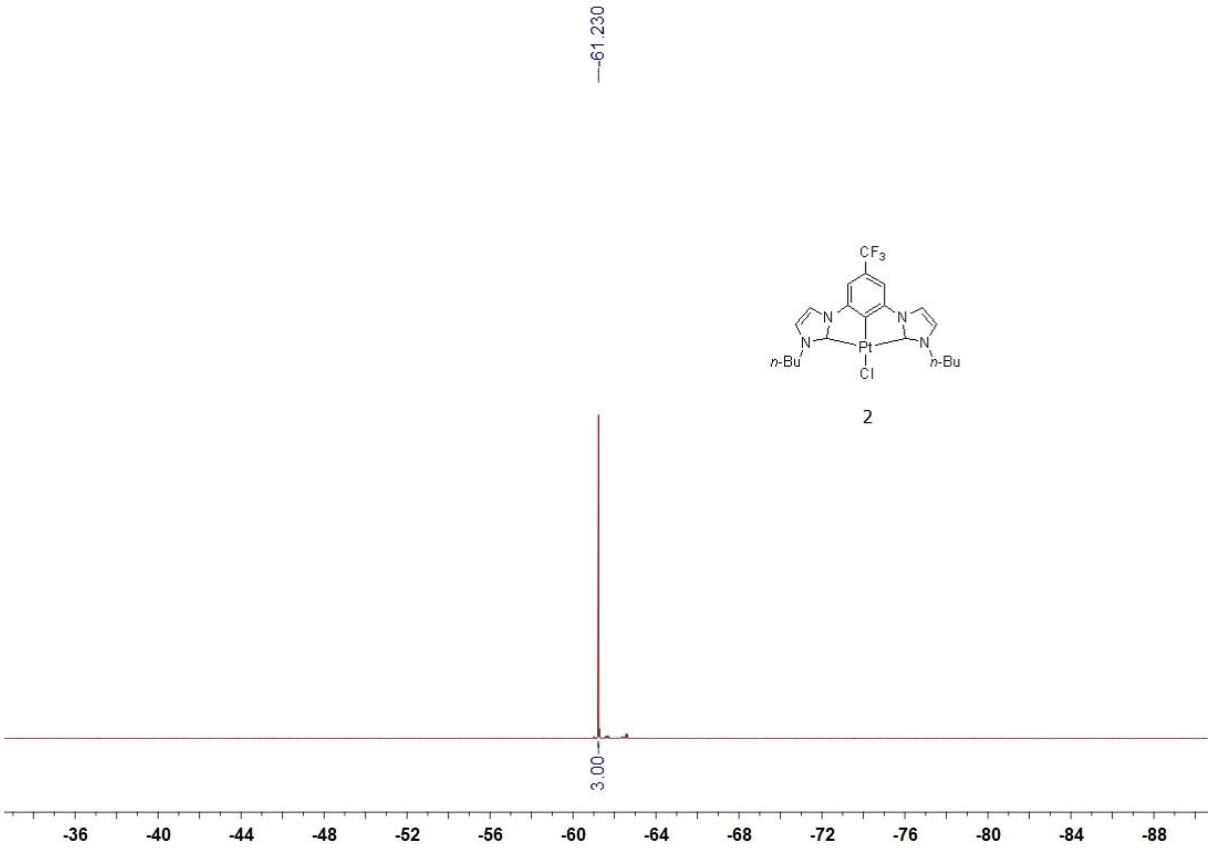

^{19}F NMR (377 MHz) spectrum of **2** in $CDCl_3$.

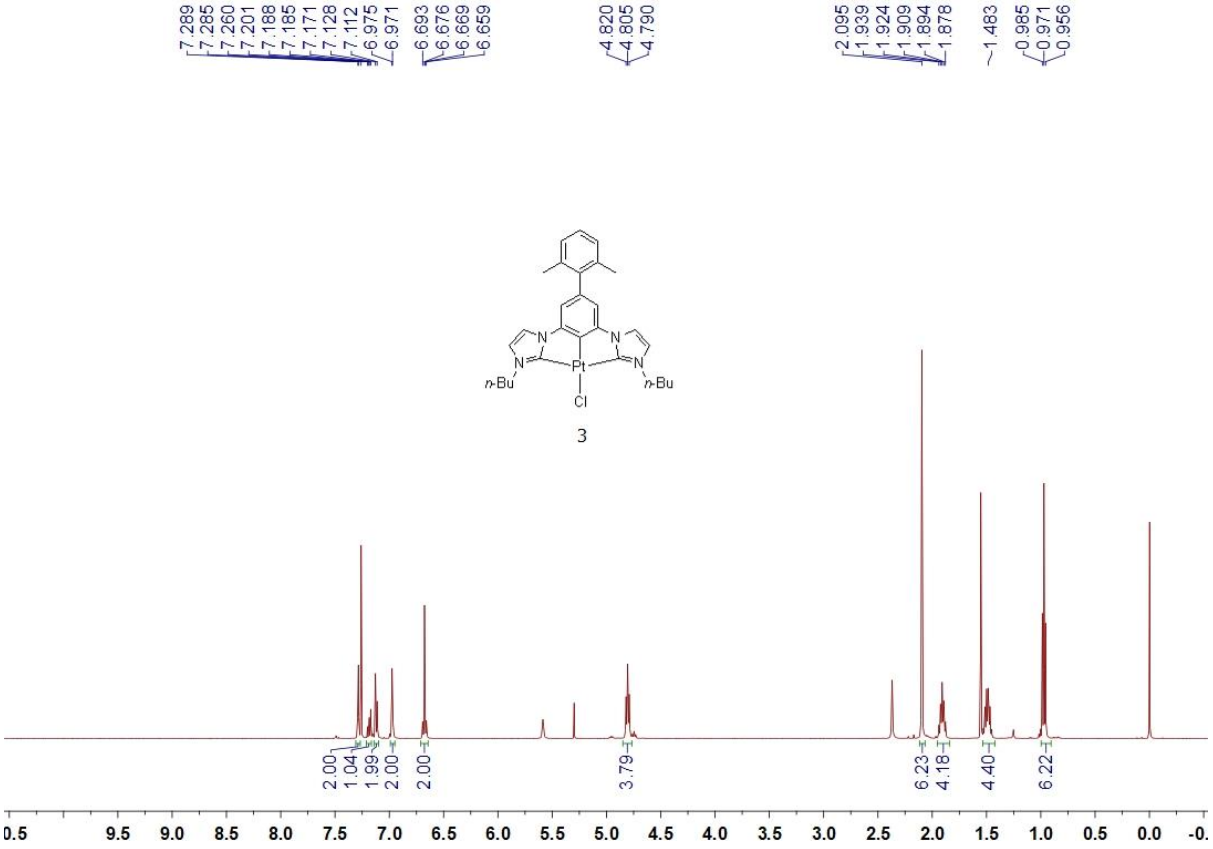

^{1}H NMR (500 MHz) spectrum of **3** in $CDCl_3$.

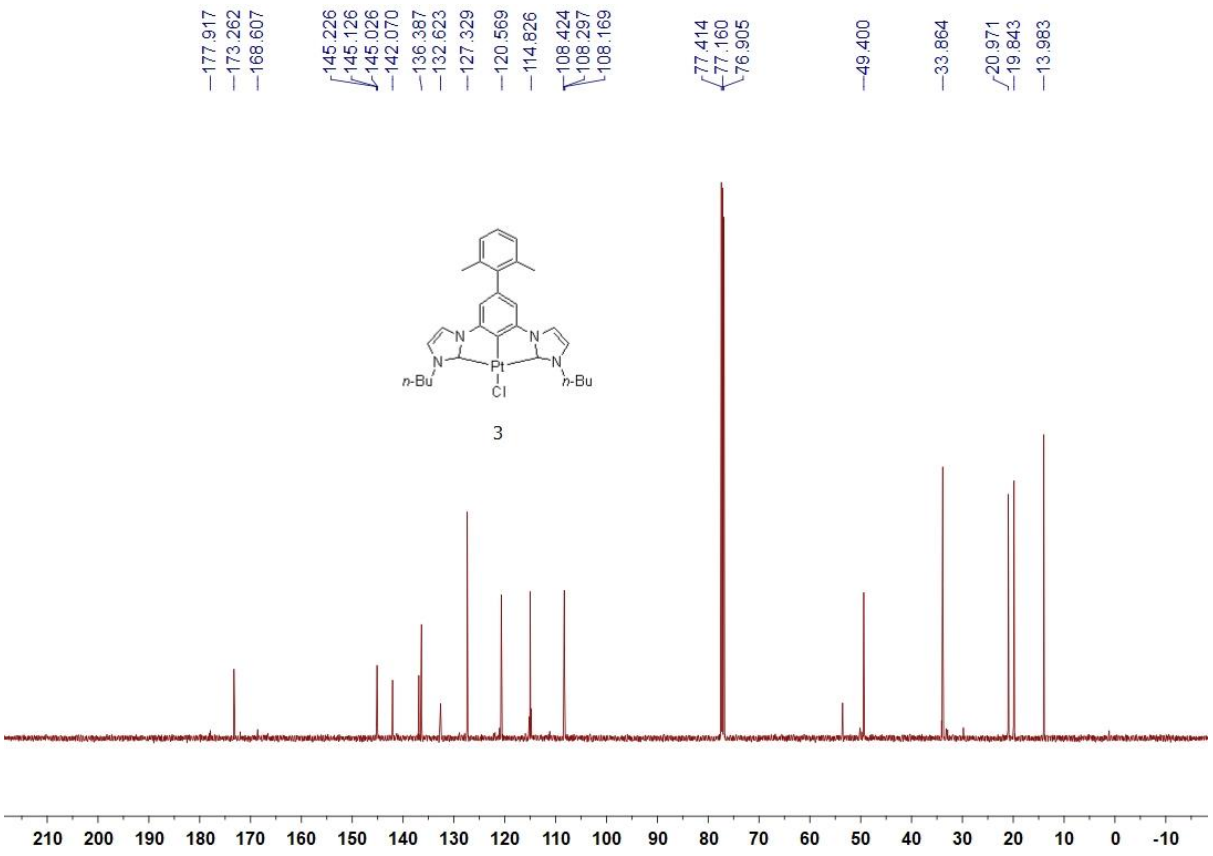

^{13}C NMR (126 MHz) spectrum of **3** in $CDCl_3$.

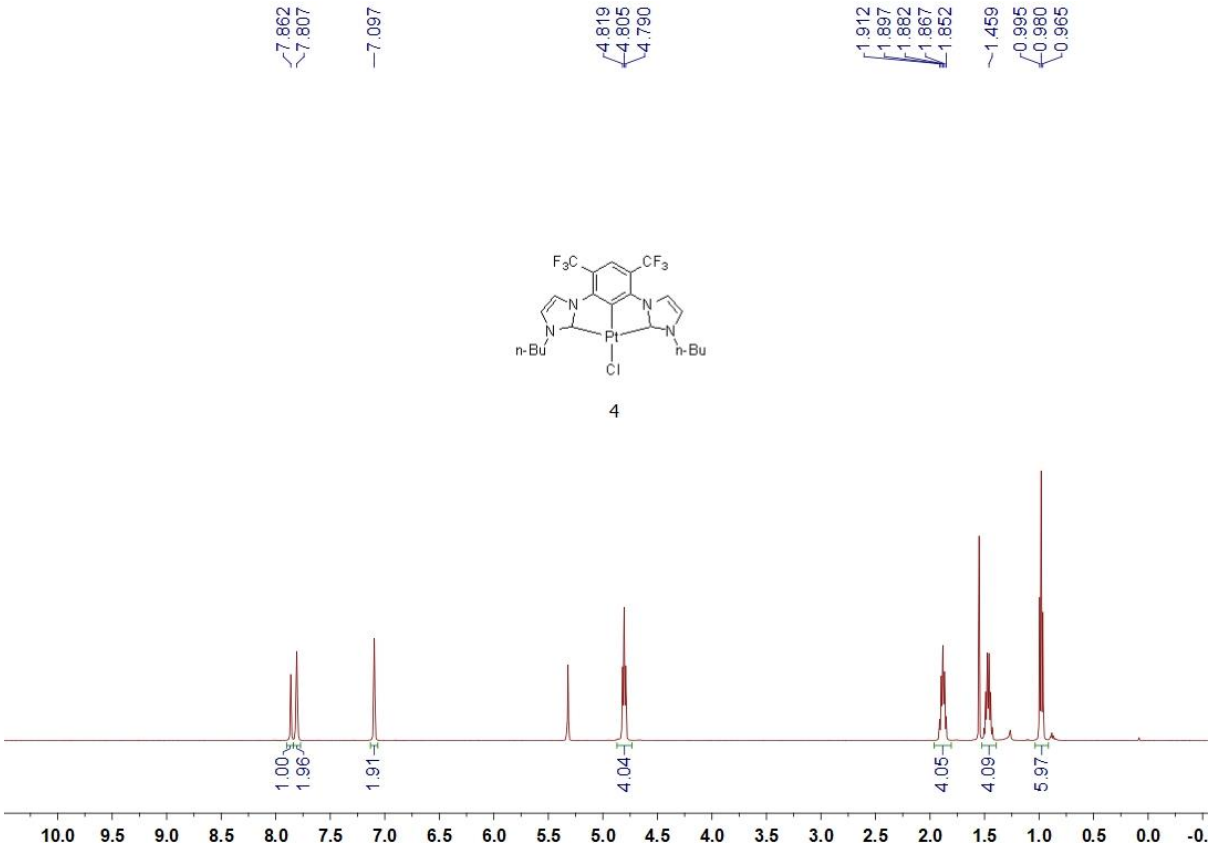

^{1}H NMR (500 MHz) spectrum of **4** in CD_2Cl_2.

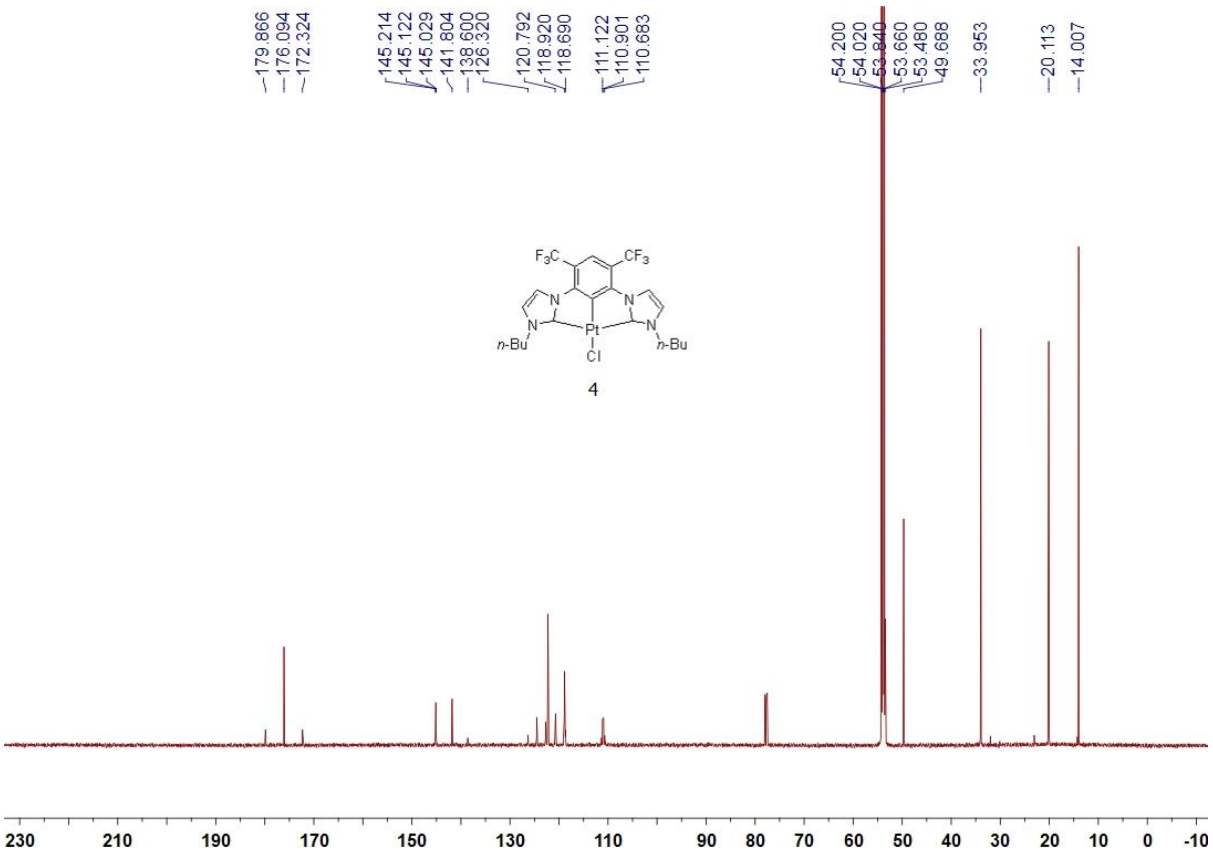

^{13}C NMR (126 MHz) spectrum of **4** in CD_2Cl_2.

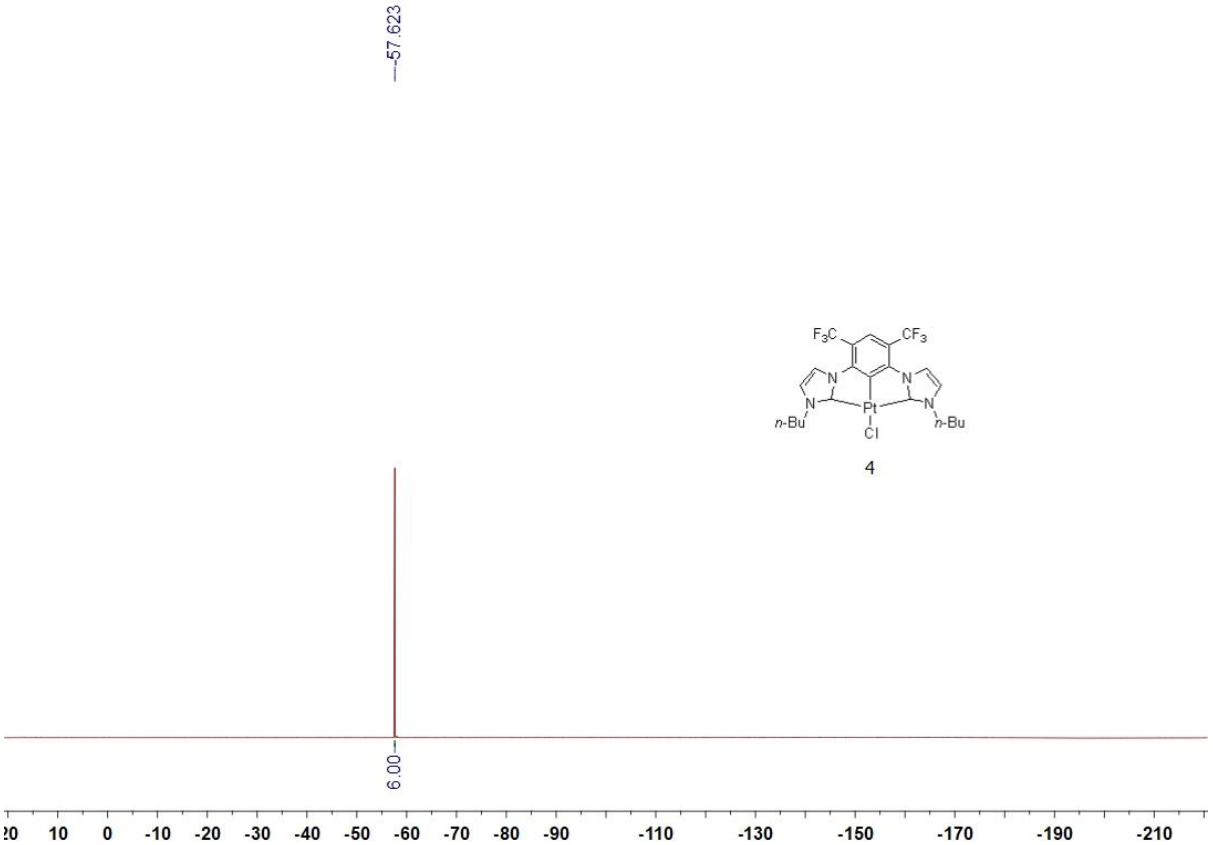

^{19}F NMR (471 MHz) spectrum of **4** in CD_2Cl_2.

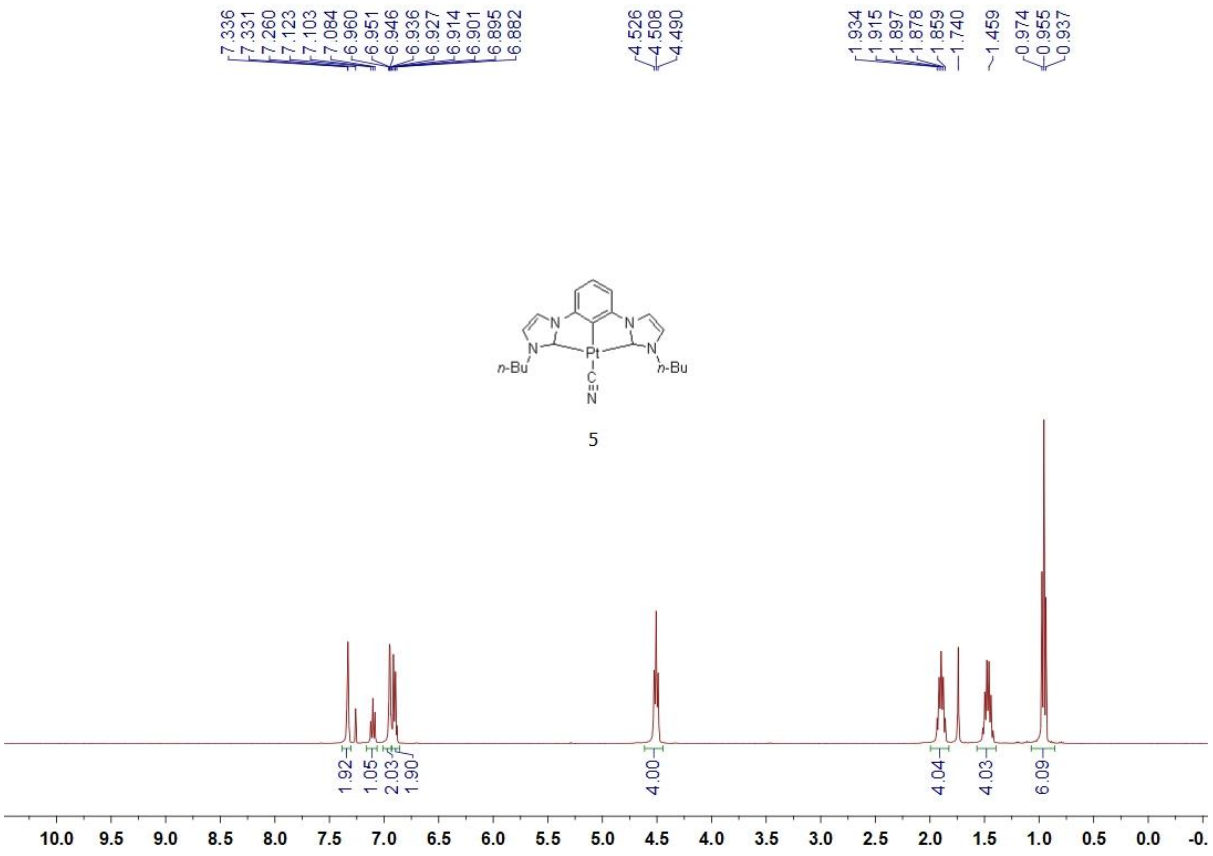

5

^{1}H NMR (400 MHz) spectrum of **5** in $CDCl_3$.

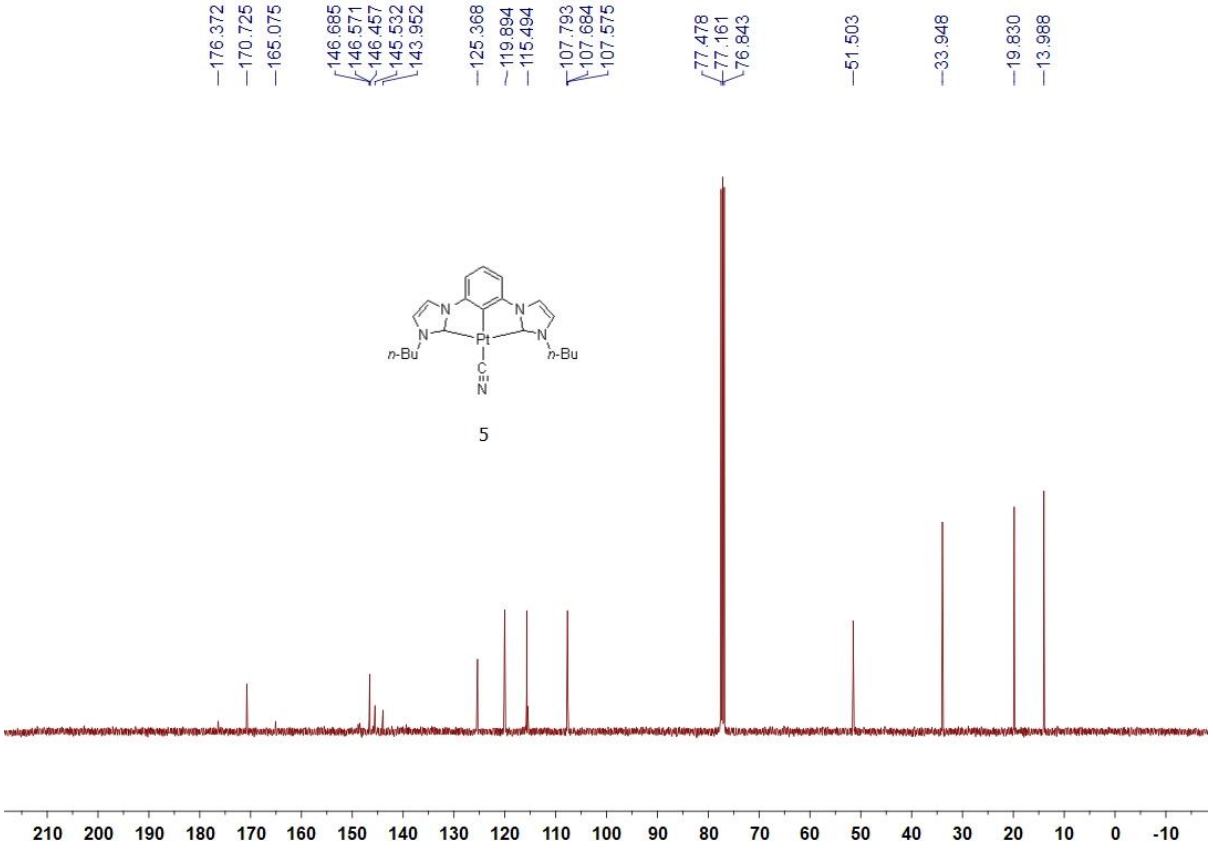

5

^{13}C NMR (101 MHz) spectrum of **5** in $CDCl_3$.

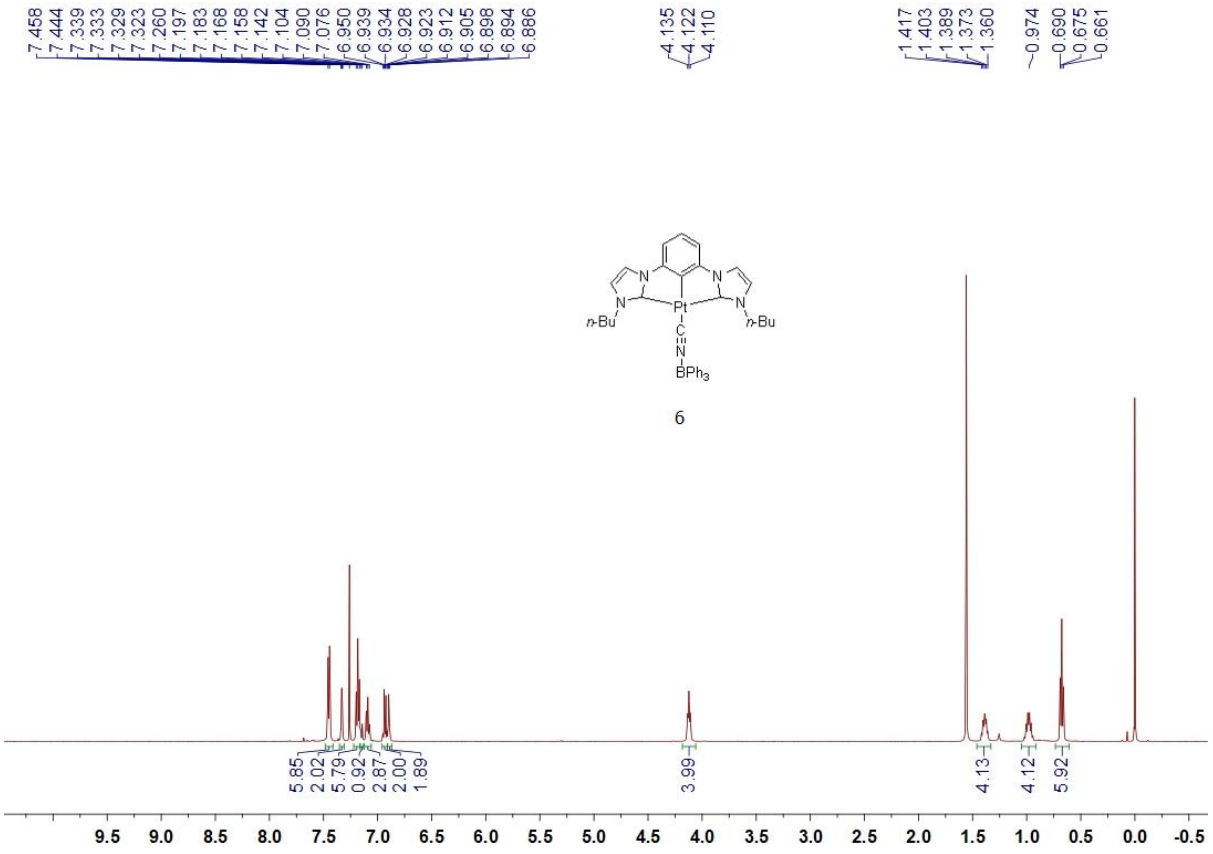

6

^{1}H NMR (500 MHz) spectrum of **6** in $CDCl_3$.

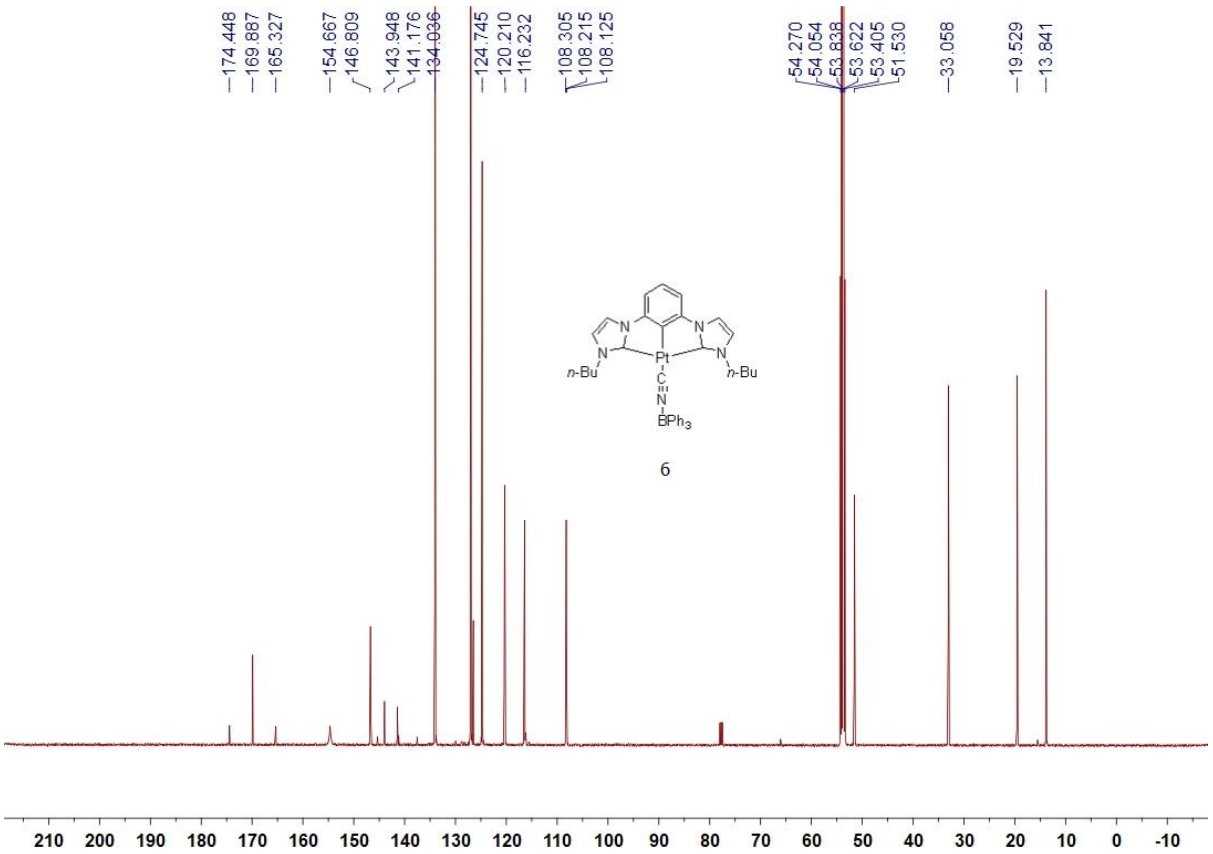

6

^{13}C NMR (126 MHz) spectrum of **6** in CD_2Cl_2.

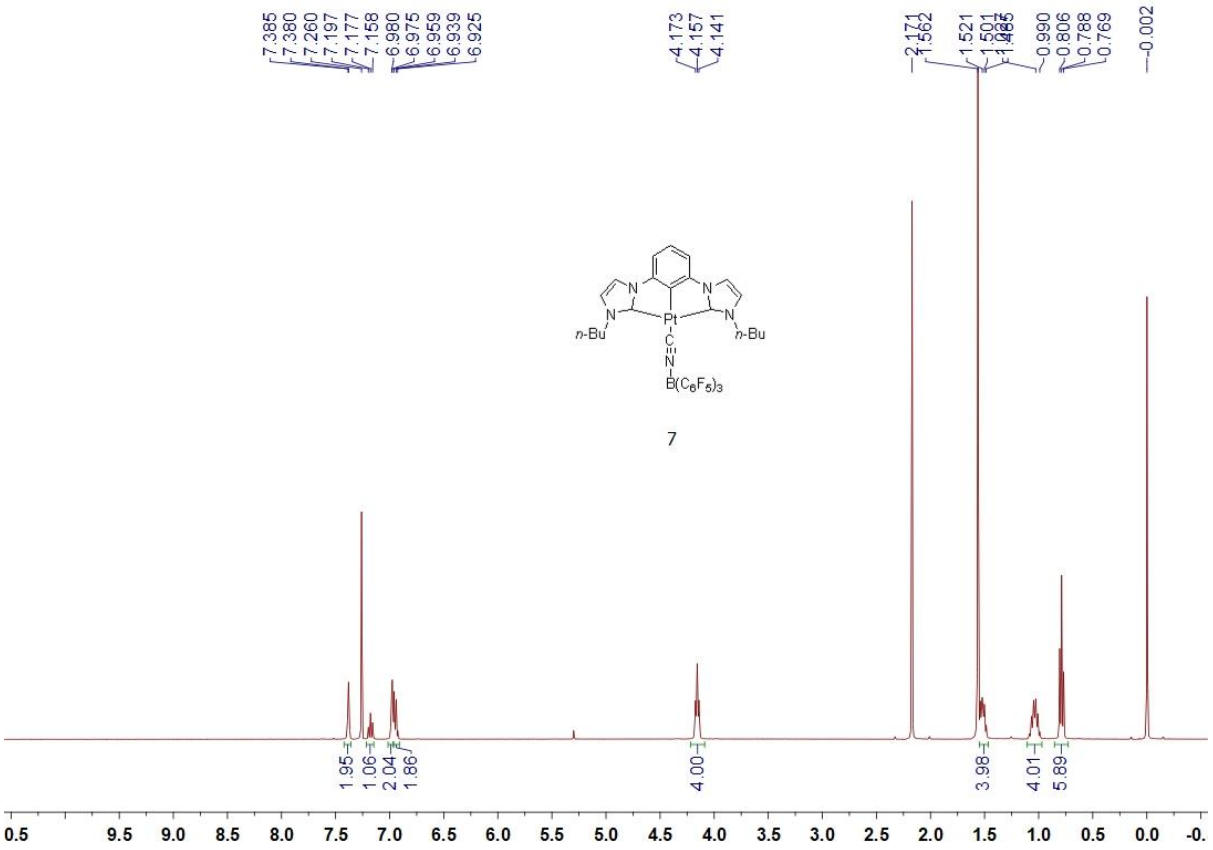

^{1}H NMR (400 MHz) spectrum of **7** in $CDCl_3$.

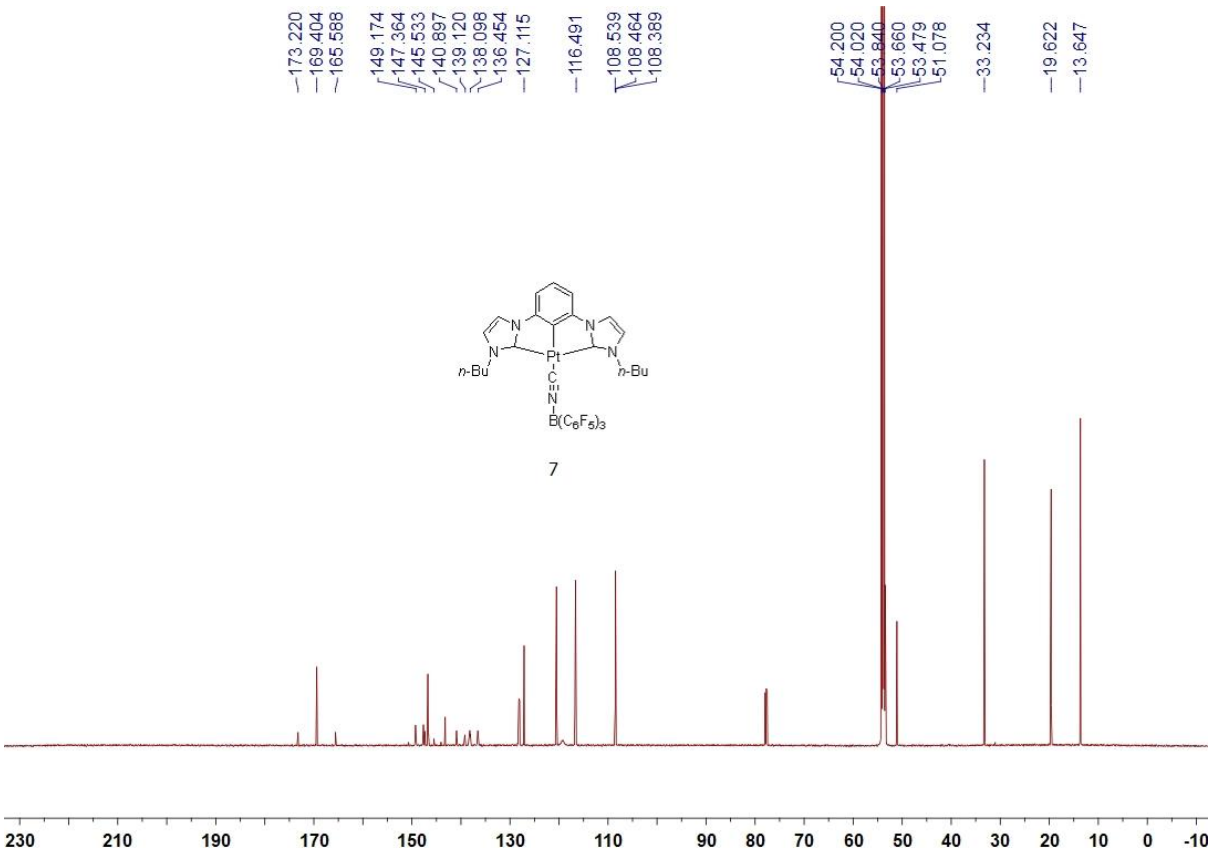

^{13}C NMR (151 MHz) spectrum of **7** in CD_2Cl_2.

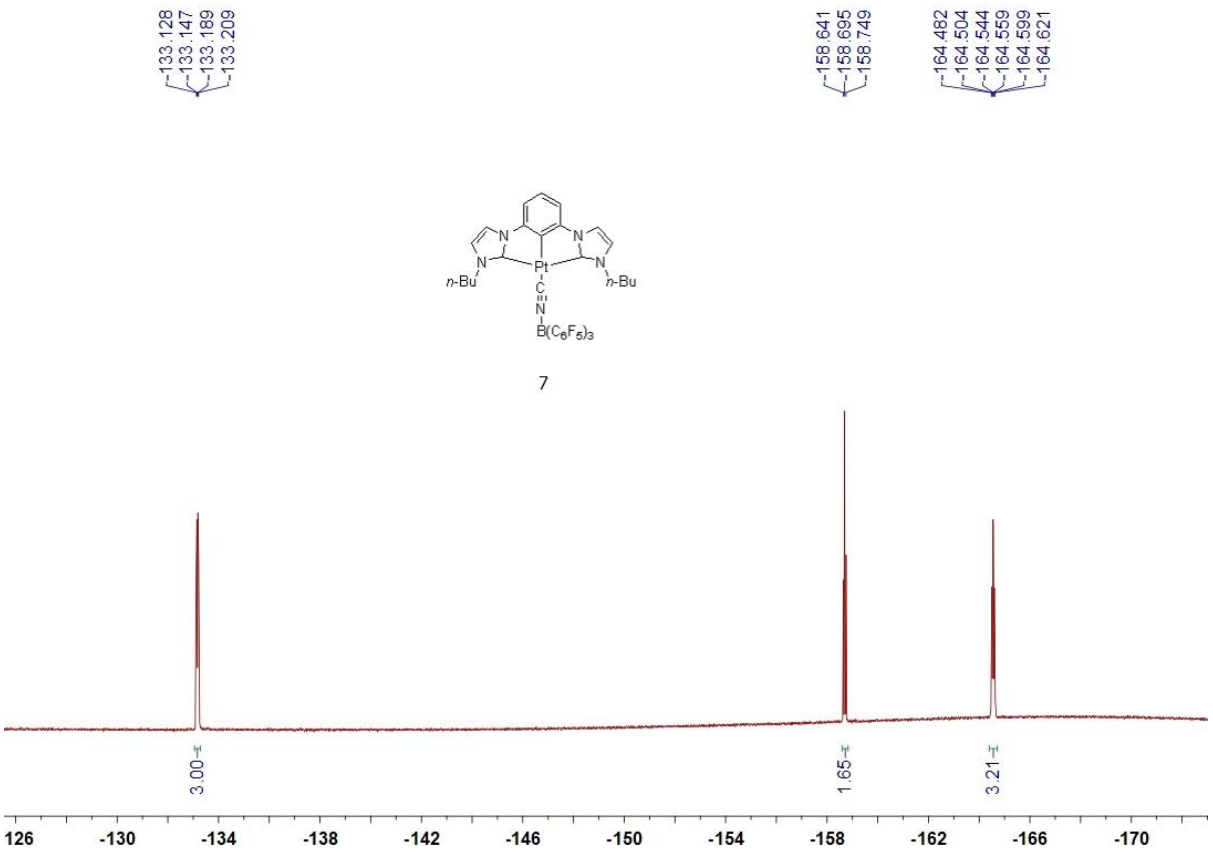

^{19}F NMR (377 MHz) spectrum of **7** in $CDCl_3$.

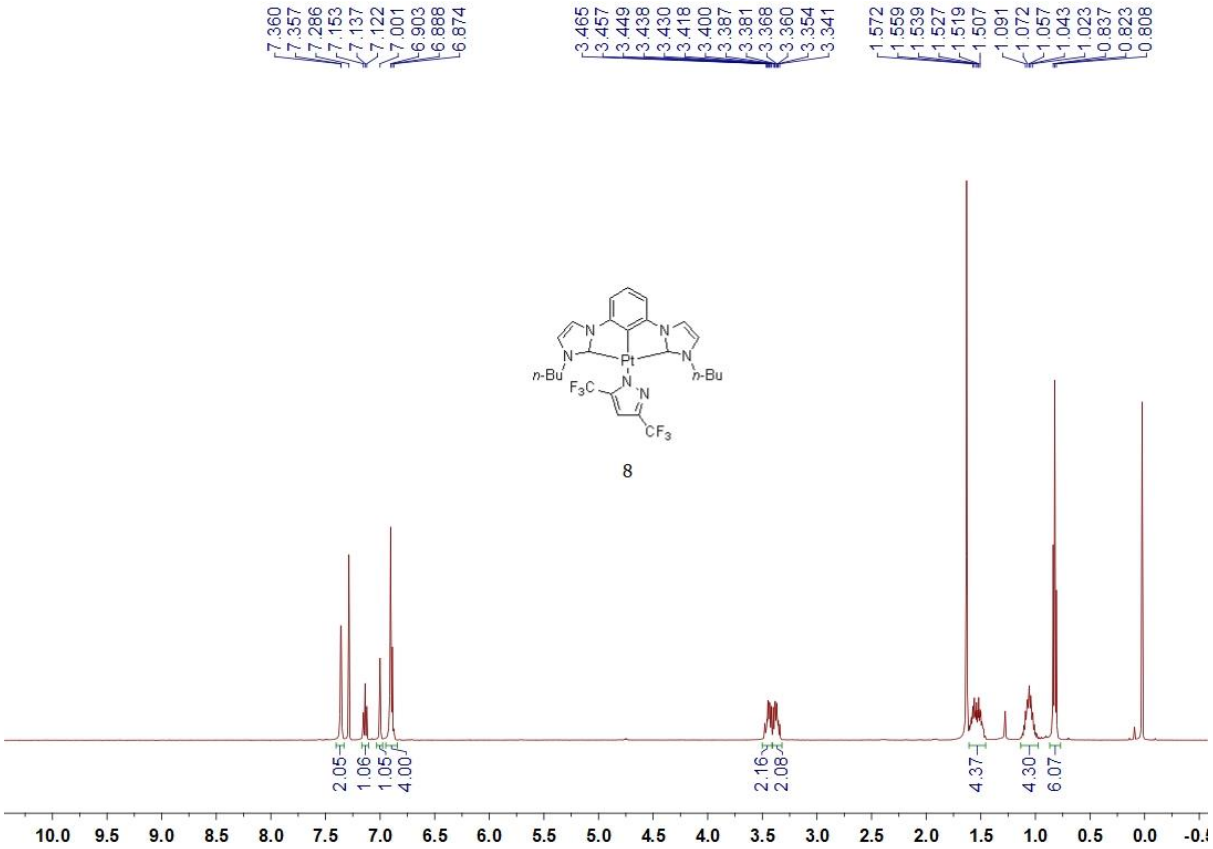

^{1}H NMR (500 MHz) spectrum of **8** in $CDCl_3$.

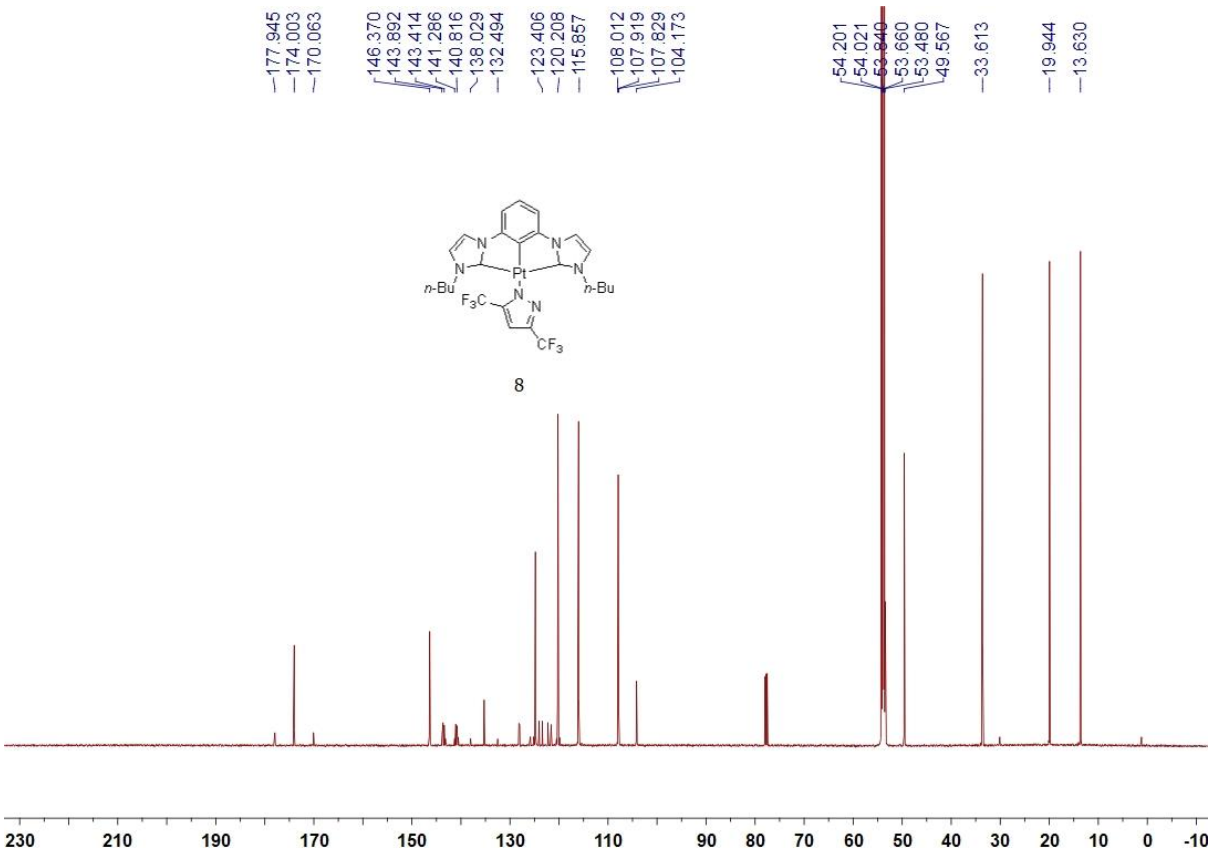

8

^{13}C NMR (151 MHz) spectrum of **8** in CD_2Cl_2.

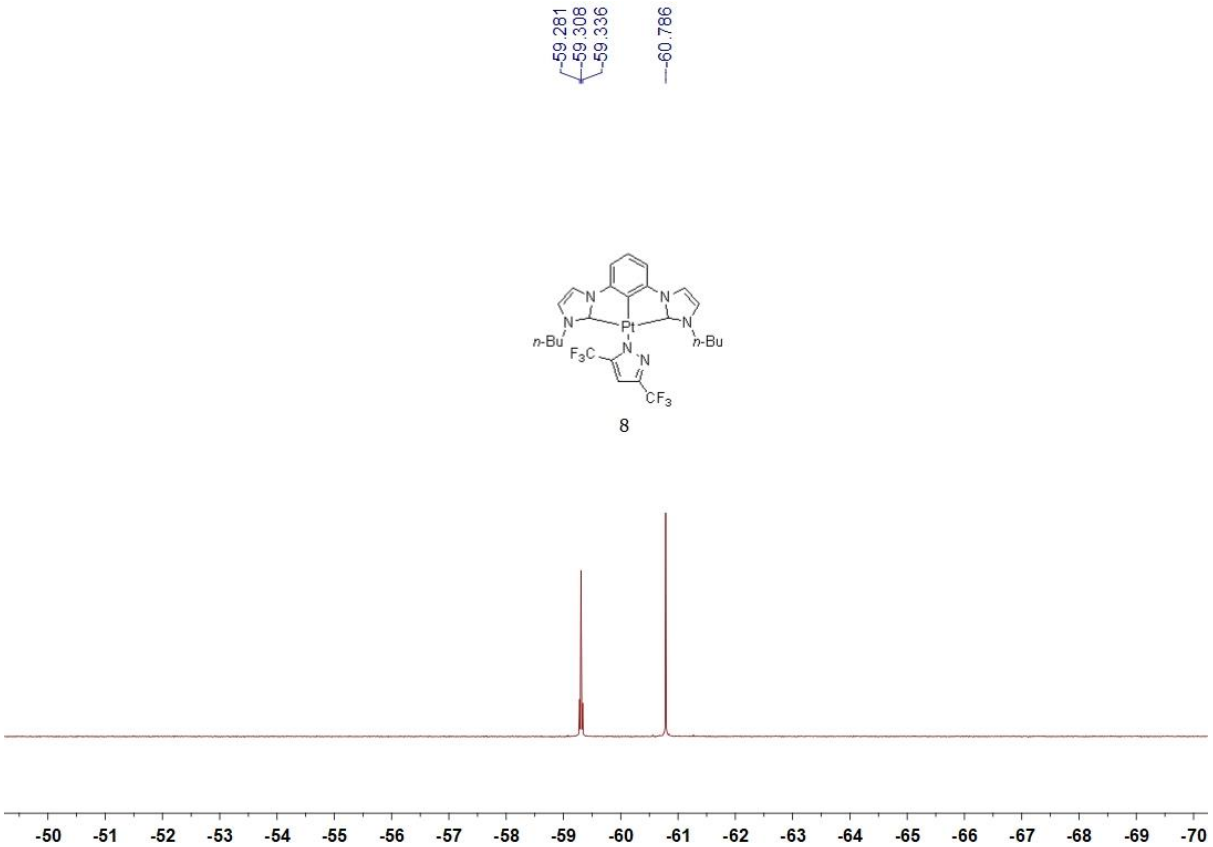

8

^{19}F NMR (377 MHz) spectrum of **8** in $CDCl_3$.

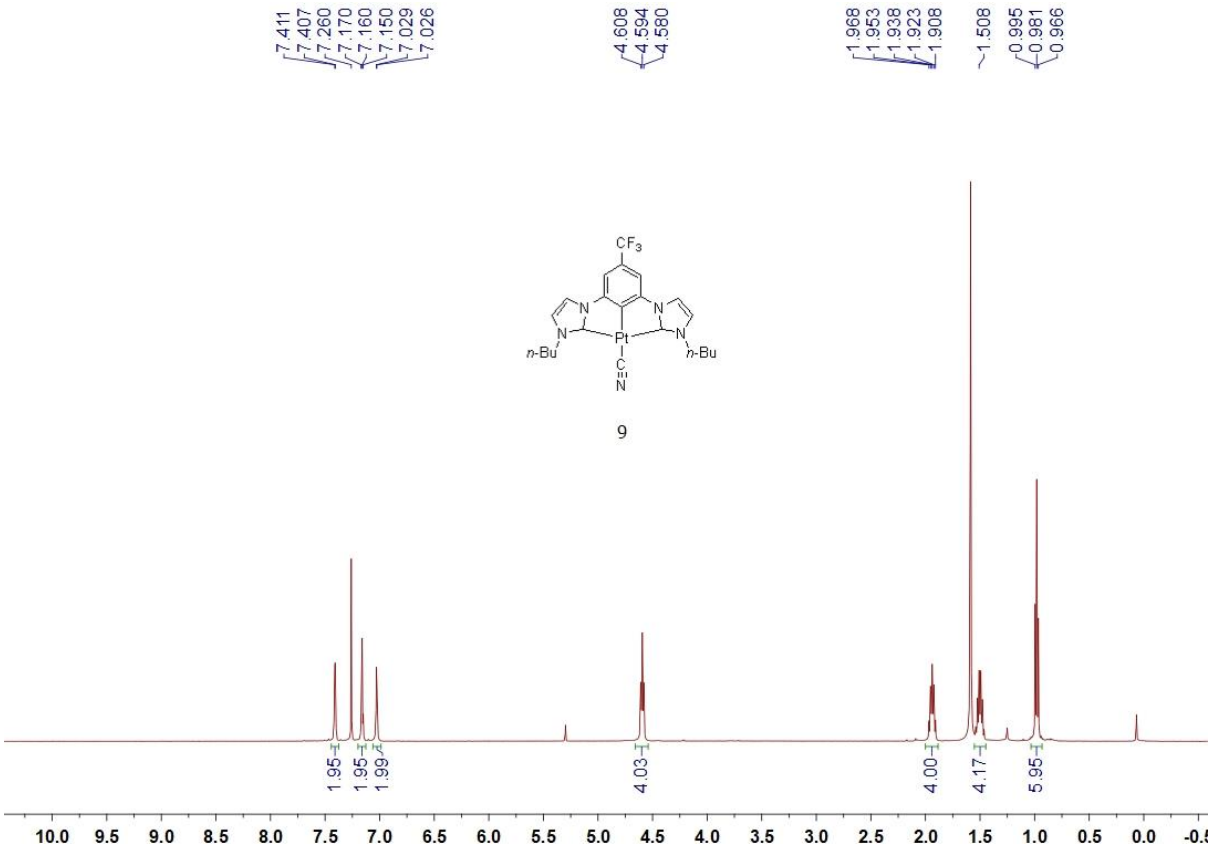

^{1}H NMR (500 MHz) spectrum of **9** in $CDCl_3$.

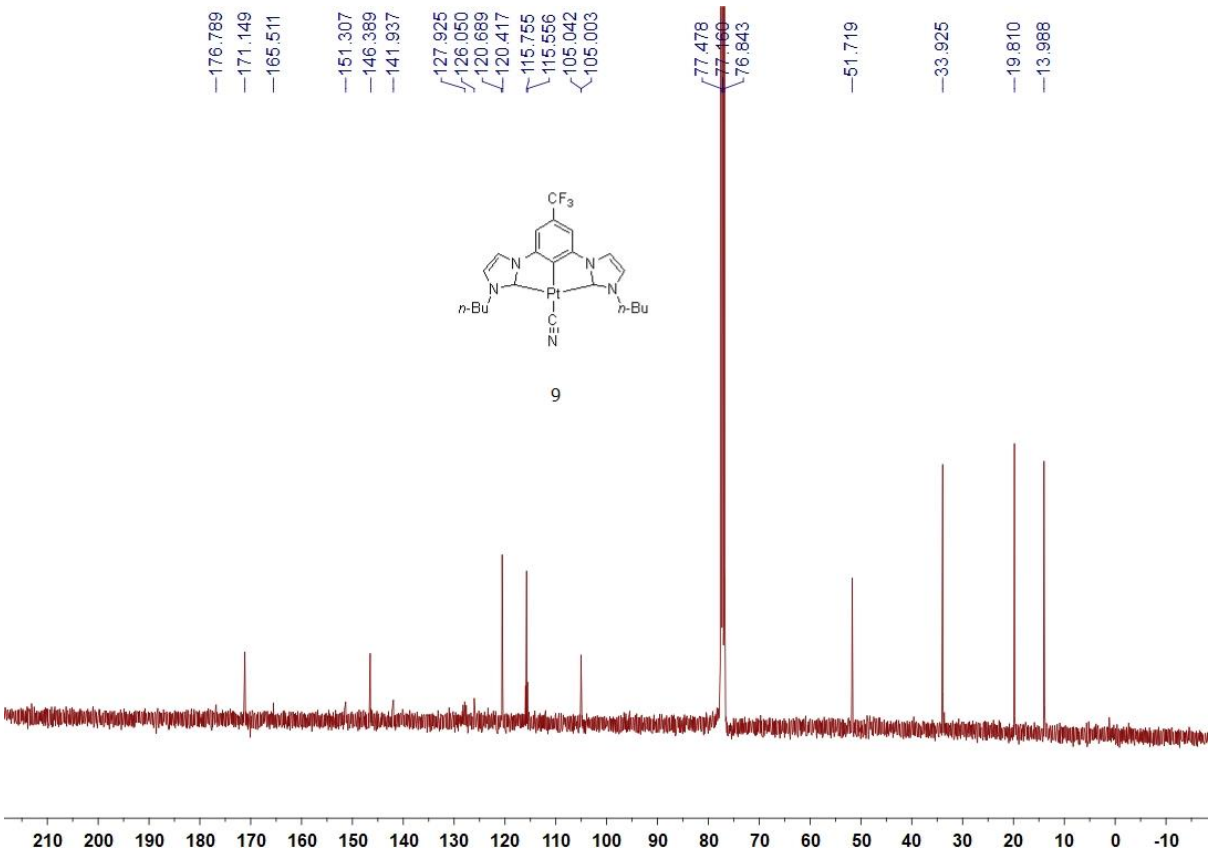

^{13}C NMR (101 MHz) spectrum of **9** in $CDCl_3$.

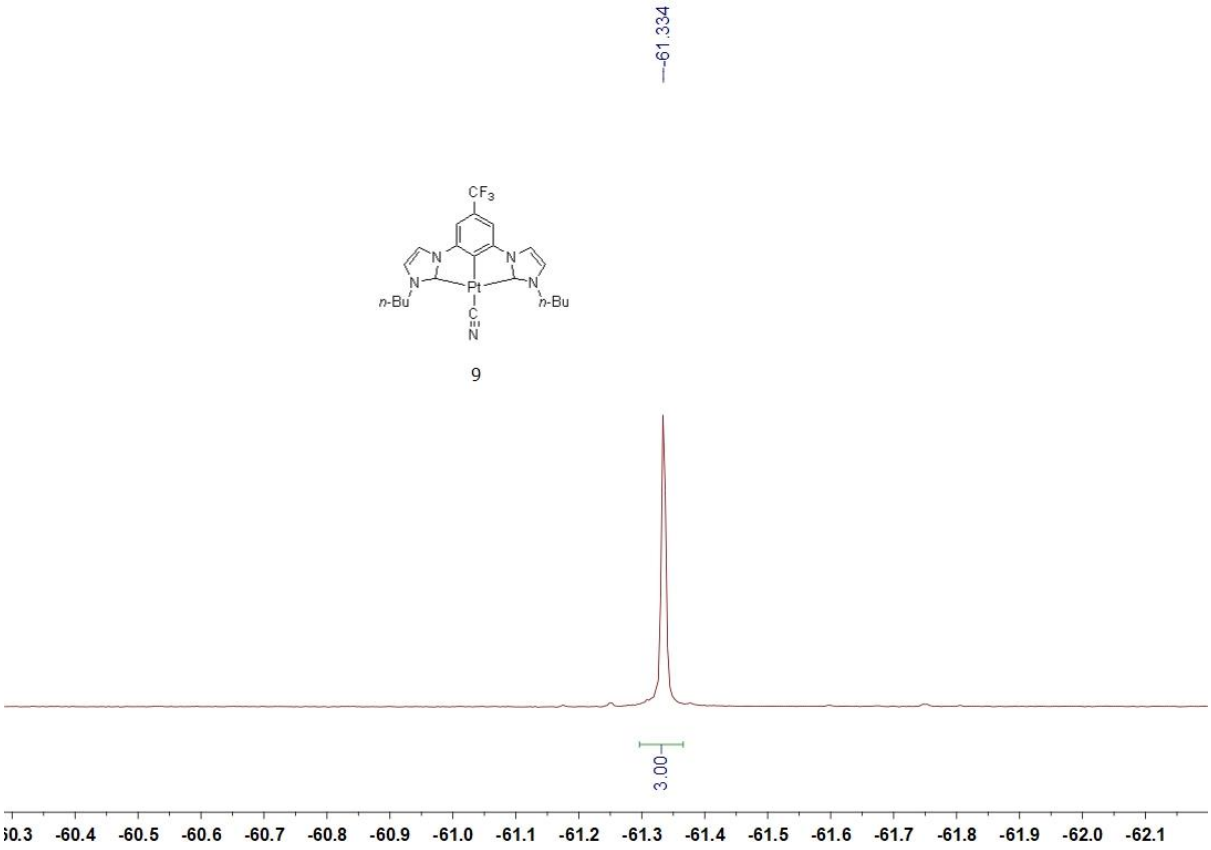

9

^{19}F NMR (471 MHz) spectrum of **9** in $CDCl_3$.

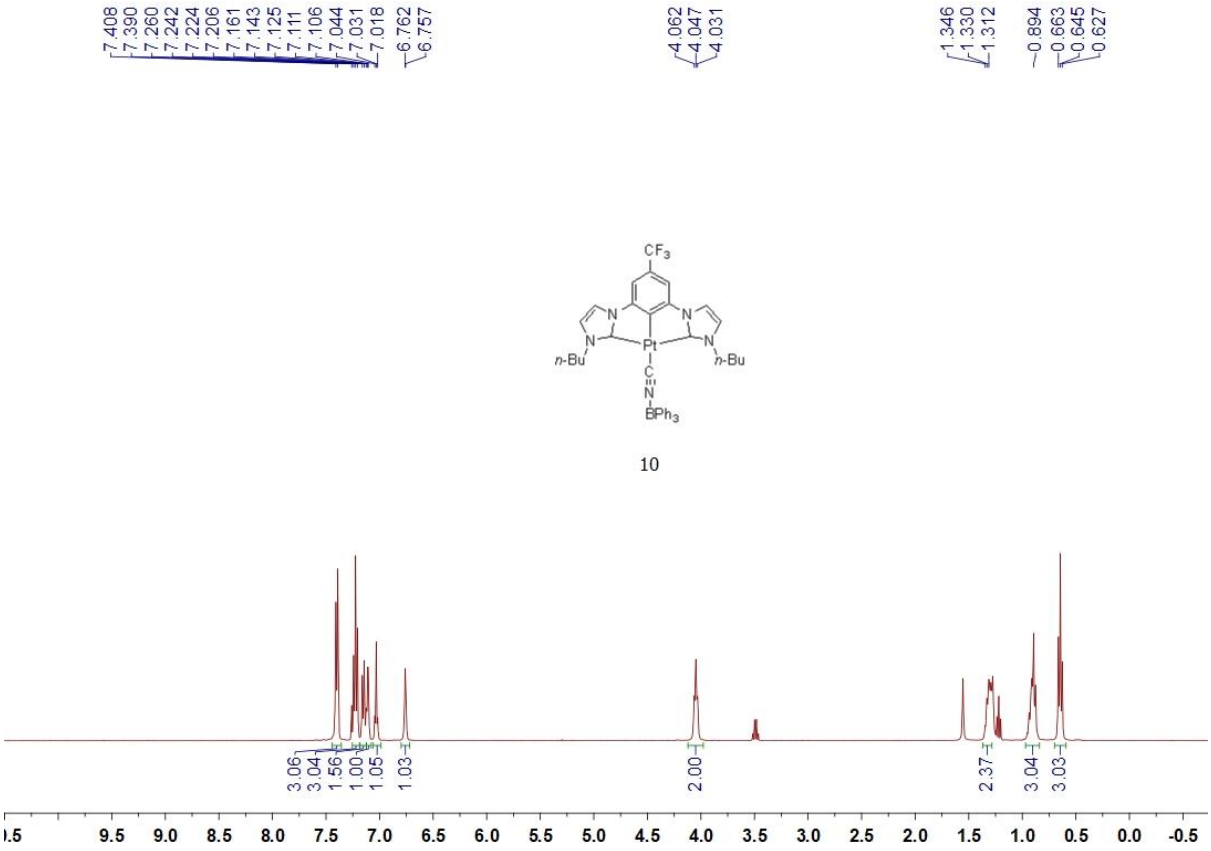

10

^{1}H NMR (400 MHz) spectrum of **10** in $CDCl_3$.

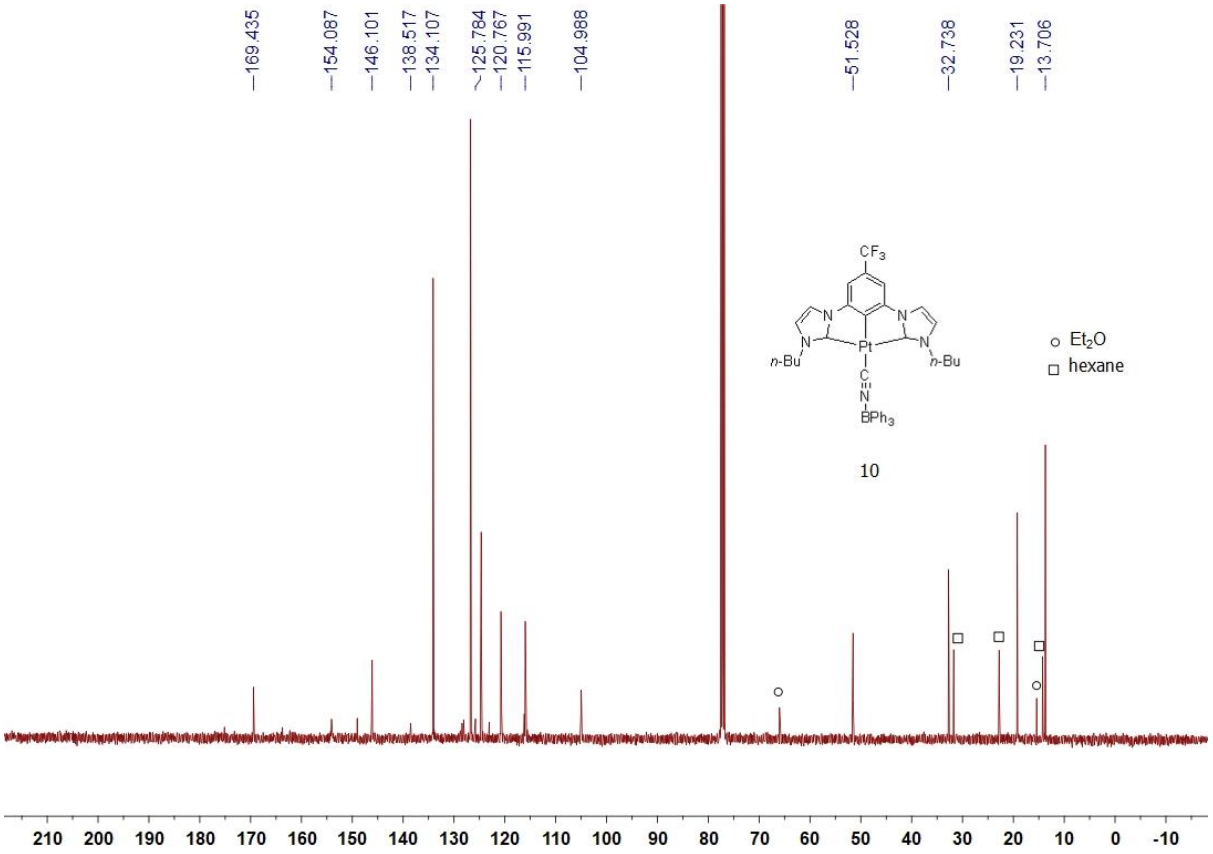

^{13}C NMR (101 MHz) spectrum of **10** in $CDCl_3$.

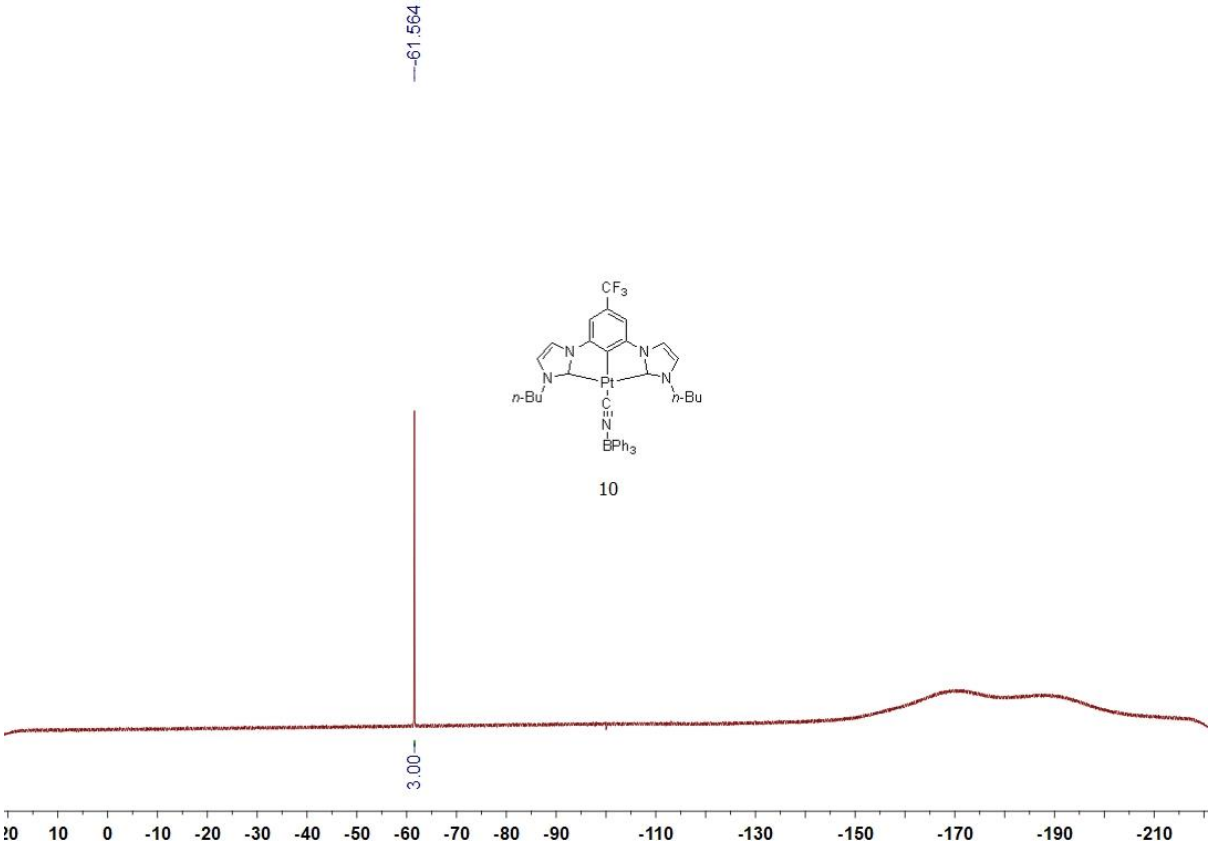

^{19}F NMR (471 MHz) spectrum of **10** in $CDCl_3$.

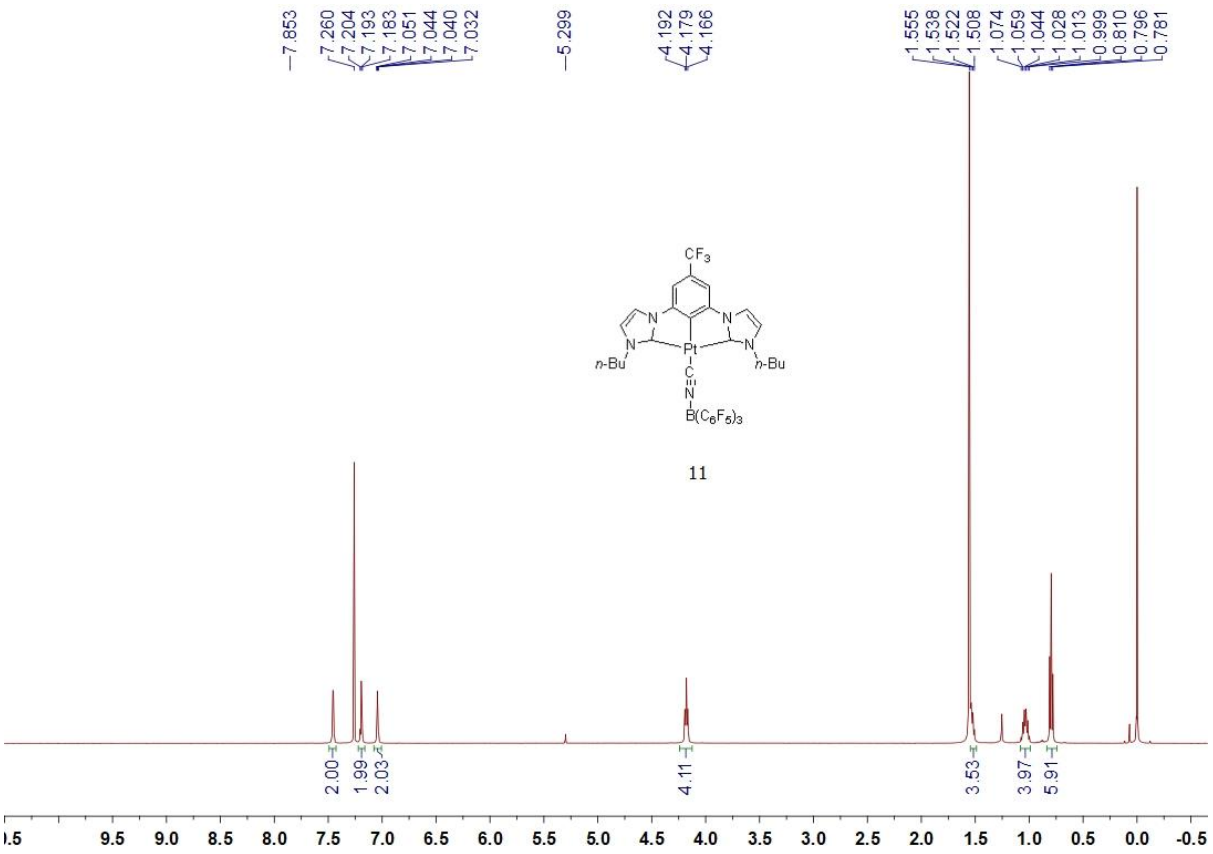

^{1}H NMR (500 MHz) spectrum of **11** in $CDCl_3$.

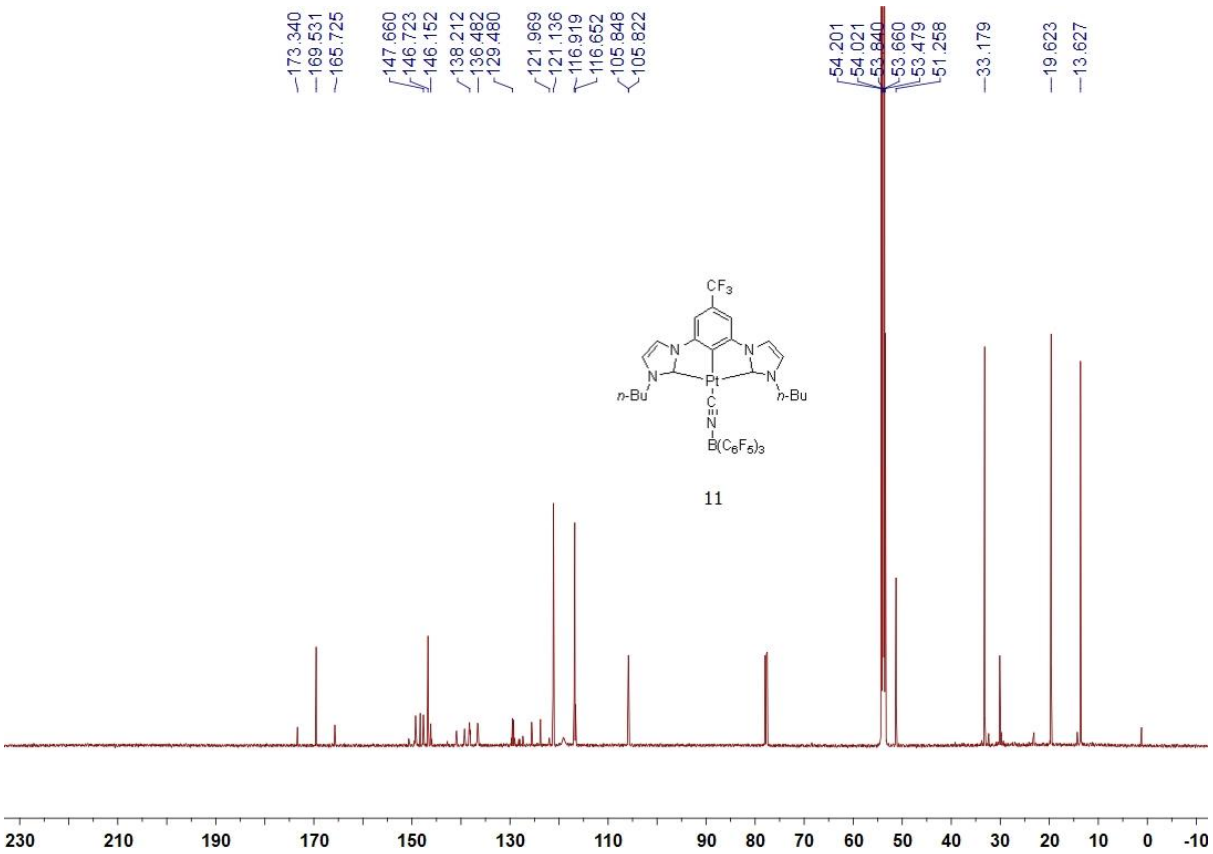

^{13}C NMR (151 MHz) spectrum of **11** in CD_2Cl_2.

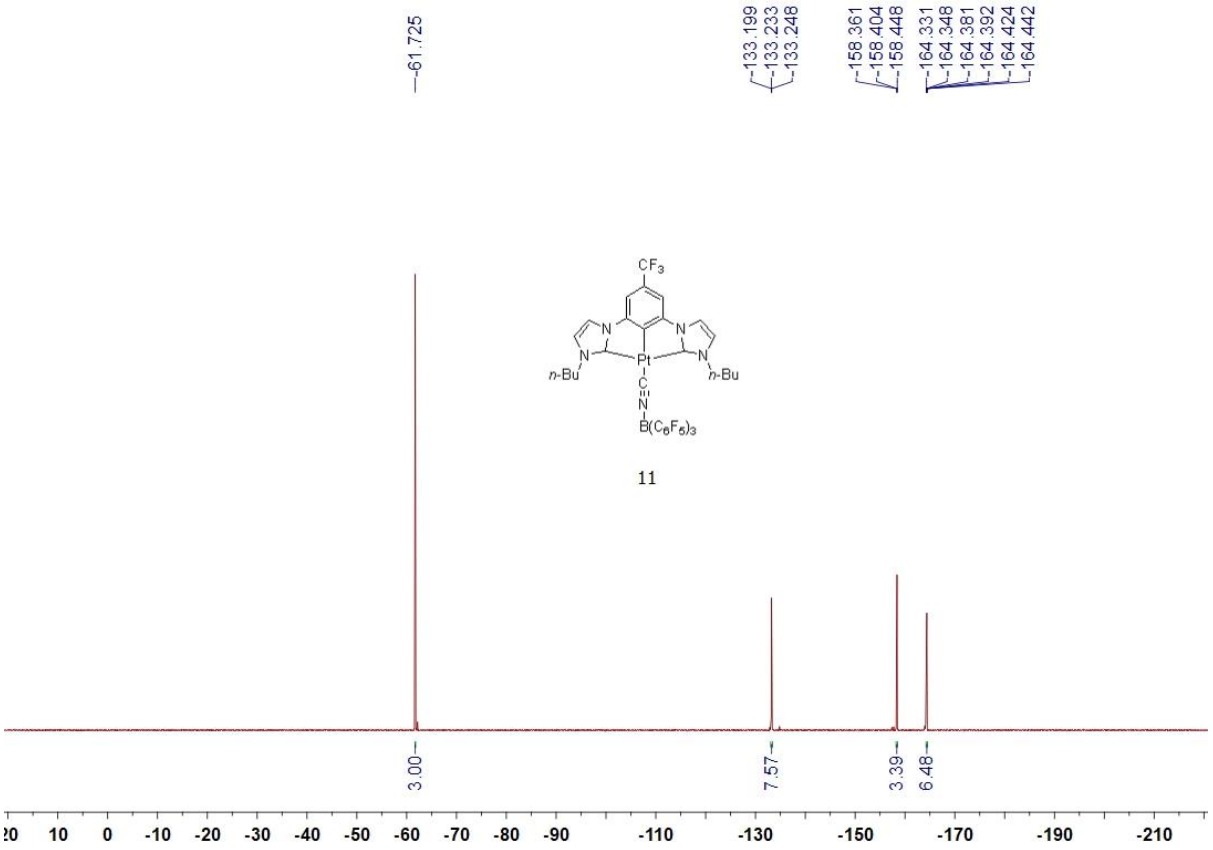

^{19}F NMR (471 MHz) spectrum of **11** in $CDCl_3$.

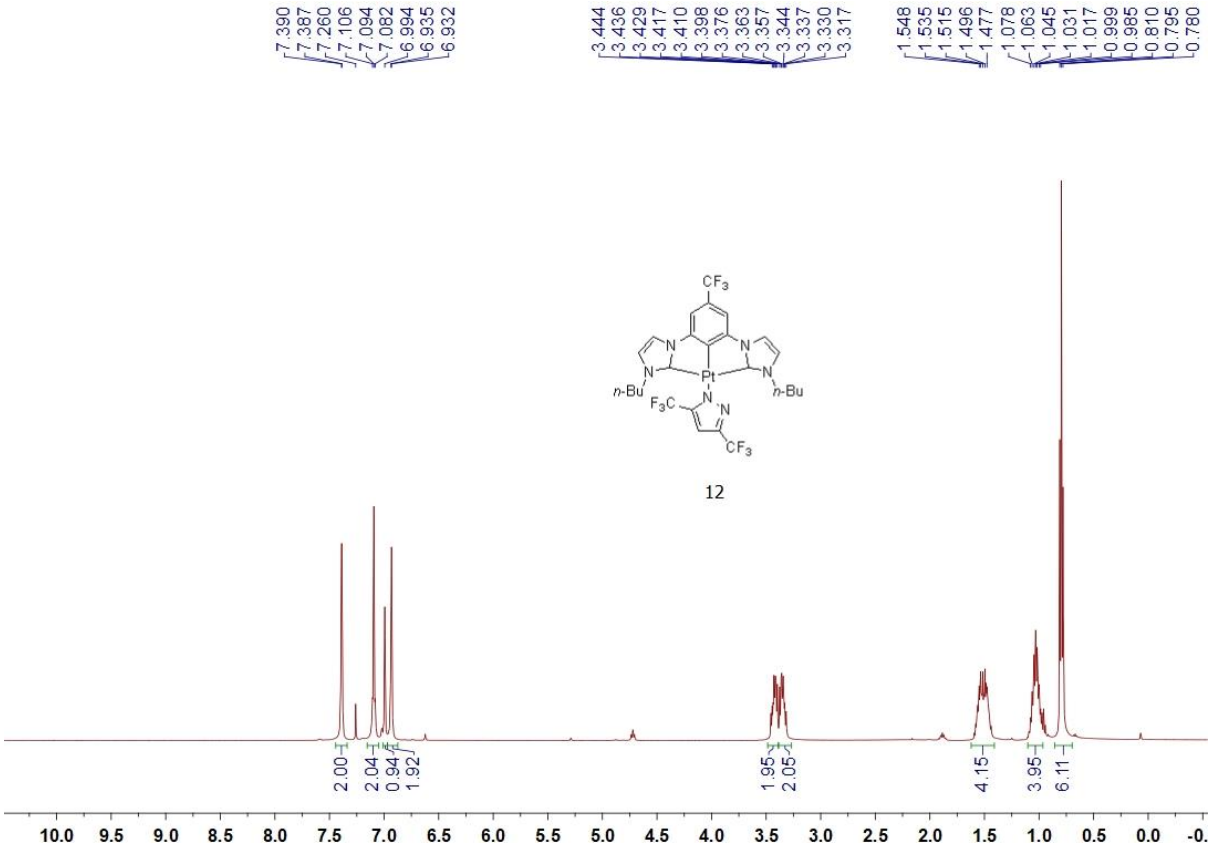

^{1}H NMR (500 MHz) spectrum of **12** in $CDCl_3$.

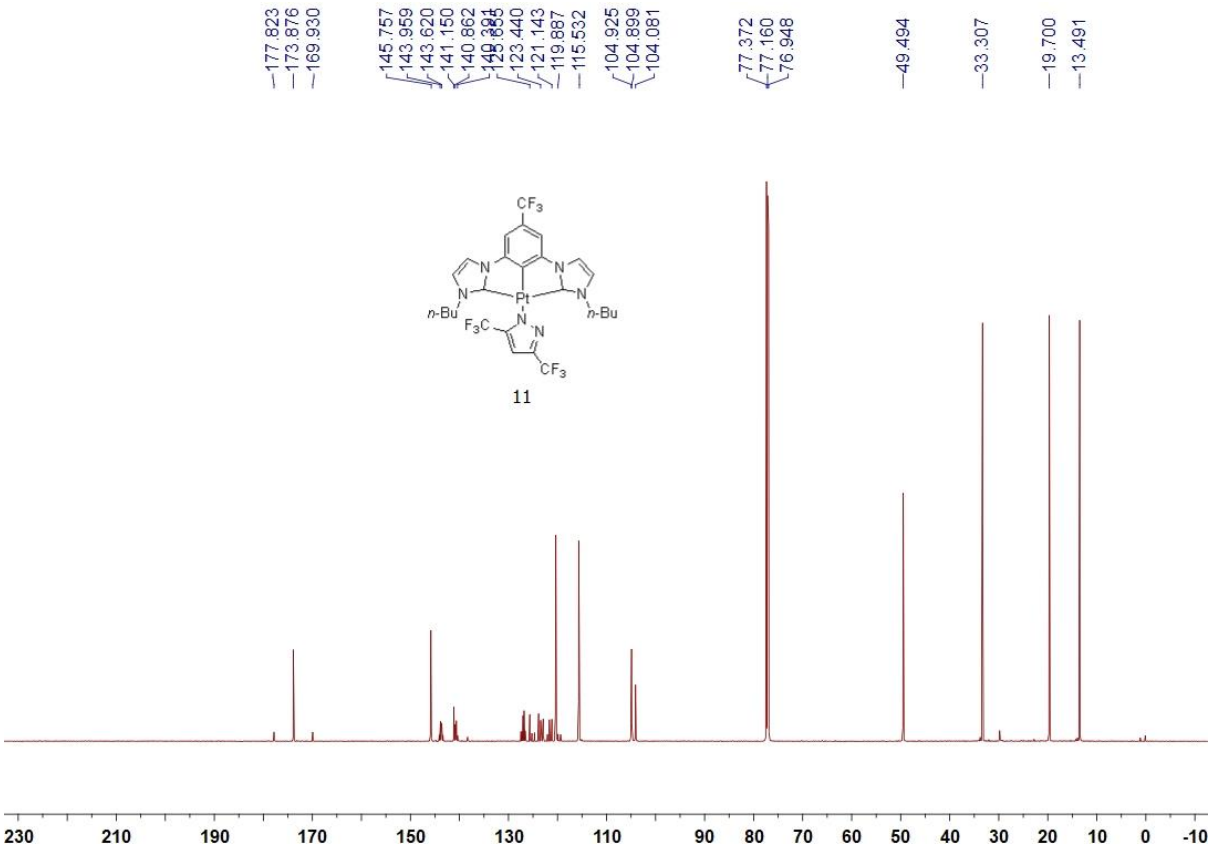

11

^{13}C NMR (151 MHz) spectrum of **12** in $CDCl_3$.

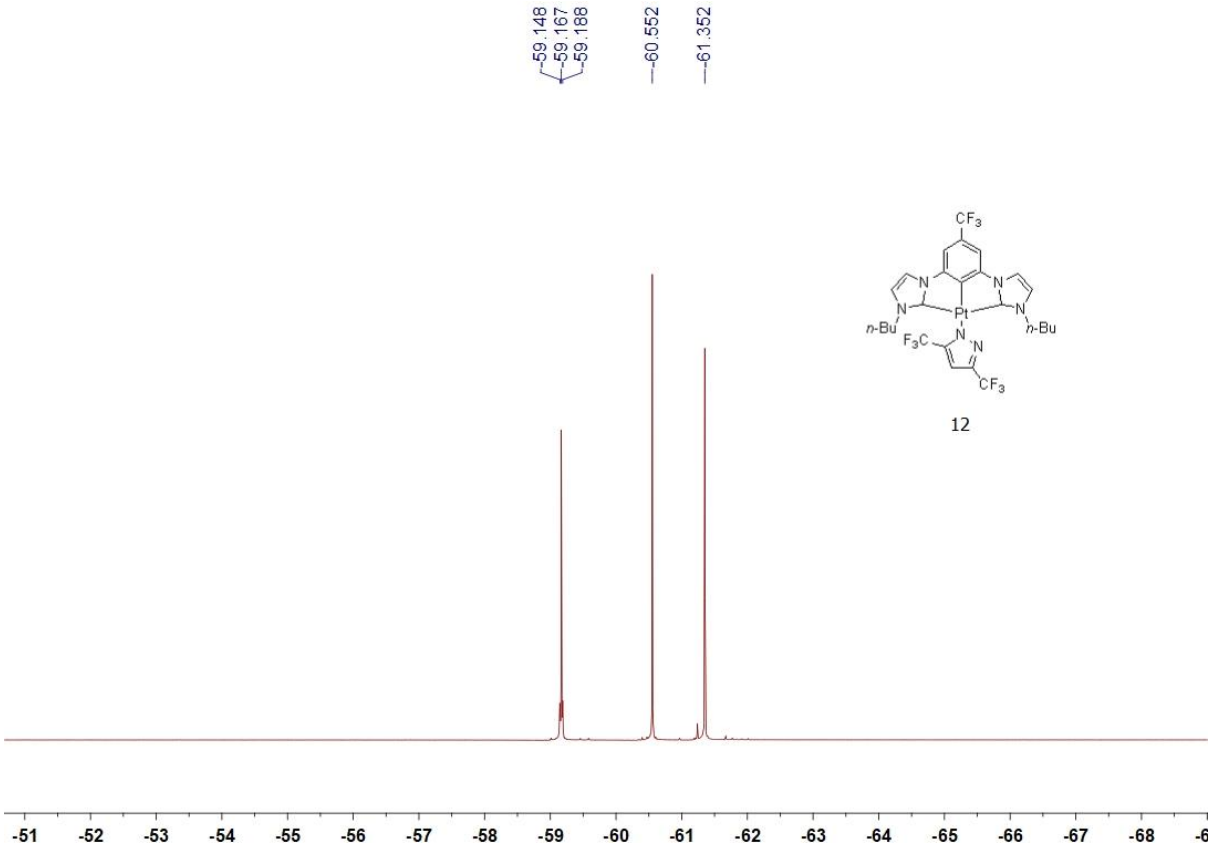

12

^{19}F NMR (471 MHz) spectrum of **12** in $CDCl_3$.

Optimized S_0 of **11**:

Pt	2.05804800	0.07958100	0.13964200
C	2.43286800	-1.80223100	-0.59429500
F	-2.45131200	2.62333800	1.16281500
F	-4.44277200	2.93170400	-3.86326600
C	4.03657200	0.04338500	0.04536300
N	3.91801900	2.16405800	0.92545200
F	-5.06421900	-1.67642000	0.02702000
F	-3.85570500	0.56360400	-2.87209400
F	-1.05721300	-0.98604700	-2.41270300
F	-3.11184600	5.00638600	0.14348000
F	-3.77456500	-4.67618400	-3.30806500
C	4.68925800	-1.06342900	-0.47010900
C	0.04967100	0.13923200	0.11963400
N	3.76380000	-2.07089600	-0.81674100
F	-1.66552100	-1.97586500	1.66335200
F	-5.75632900	0.83892900	3.81483700
N	-1.11240000	0.14742800	0.03708900
F	-4.06798600	5.19624000	-2.38738400
F	-4.97439900	1.39712900	1.35011700
F	-1.51809200	-3.21180200	-3.76871600
C	-4.41833400	-3.16074800	-1.61830100
F	-2.48025500	-2.52725200	4.13958200
F	-4.53557000	-1.12282700	5.25420200
C	6.07216800	-1.09987200	-0.58536500
H	6.60041300	-1.95501300	-0.99247700
N	2.01255100	3.04580600	1.37026200
F	-5.53422300	-3.85523800	-1.39390100
C	4.18899300	3.40785300	1.44449900
H	5.19064600	3.78431200	1.57874200
C	4.77089400	1.14267000	0.45525700
N	1.80722900	-2.94530300	-0.92414400
C	6.78399900	0.02736200	-0.15842900
C	-3.63769900	1.61377400	-2.07104600
C	-2.95537500	2.65179000	-0.08237600
C	-3.12113300	1.46173600	-0.78783900
C	6.15644400	1.16270800	0.36660200
H	6.74771200	2.01704400	0.67684300
C	-2.39150400	-2.82463400	-2.83510200
C	-2.15723400	-1.68149300	-2.08382400
C	3.94645900	-3.35276800	-1.27988500
H	4.91601300	-3.75784600	-1.52263000
C	-2.98503900	-1.25363700	-1.04957800
C	-2.65911700	-1.22516100	2.16799200

C	-4.13573600	-2.01912700	-0.87667400
C	-3.22450700	-0.21277000	1.39853500
C	-3.53166200	-3.57732400	-2.59855700
C	2.98487500	3.96555200	1.72303900
H	2.73488200	4.92619700	2.14569900
B	-2.65156000	0.04798900	-0.11559300
C	2.70955800	-3.90554300	-1.34588100
H	2.39249500	-4.88909500	-1.65626900
C	-4.28972900	0.44772900	2.00125700
C	-3.78553600	4.00199200	-1.87491000
C	-3.96568500	2.85078000	-2.62121300
C	-3.29061400	3.89875600	-0.58265400
C	-4.73378000	0.16398600	3.28730700
C	-4.11863100	-0.83780800	4.02314400
C	-3.07033300	-1.54490100	3.45449500
F	8.73069600	-0.74998400	-1.23576800
C	8.28161400	-0.01227200	-0.20674200
F	8.80078900	-0.55317800	0.91213000
C	2.56362100	1.92503700	0.87402000
C	0.58723400	3.33843600	1.44465700
H	0.37484700	3.69796100	2.45578200
H	0.05562000	2.39796500	1.30158200
C	0.39381500	-3.21771900	-0.70792400
H	-0.01576900	-3.63056900	-1.63371500
H	-0.07922800	-2.25693600	-0.51895800
F	8.81451300	1.21457100	-0.32650800
C	0.17456100	4.36833600	0.40141900
H	-0.86031000	4.65156800	0.61396300
H	0.77408100	5.27957000	0.53278700
C	0.29468000	3.87220400	-1.03496500
H	-0.32009900	2.97083800	-1.15805700
H	1.32929500	3.56398300	-1.23664900
C	0.16857900	-4.14877100	0.47689200
H	-0.91540600	-4.19390100	0.63735300
H	0.49213700	-5.16800500	0.22831200
C	0.86474400	-3.67703500	1.75060600
H	0.70939900	-2.59760700	1.87206300
H	1.94831100	-3.82158700	1.64746300
C	-0.12782700	4.93120100	-2.04548200
H	-1.15517700	5.26809700	-1.86430100
H	-0.07779600	4.54633300	-3.06936900
H	0.52164300	5.81260600	-1.98555900
C	0.35880000	-4.40462800	2.98852500
H	-0.69560600	-4.16870500	3.16705600

H	0.92280400	-4.11009500	3.88013600
H	0.45119400	-5.49187100	2.87795200

Optimized T_1 of **11**:

Pt	2.08048616	0.10352201	0.12047501
C	2.44147619	-1.78503314	-0.58727504
F	-2.42981518	2.59245920	1.26544110
F	-4.57859435	2.97660723	-3.77156629
C	4.01956030	0.08123701	0.00132200
N	3.94659530	2.22639217	0.87465207
F	-5.10802439	-1.58248212	0.01362200
F	-3.90665430	0.56440304	-2.83744222
F	-0.99575008	-0.98474307	-2.40809018
F	-3.17558524	5.01721438	0.30028102
F	-3.86464129	-4.61559535	-3.40198126
C	4.72007536	-1.08151108	-0.51572704
C	0.07917501	0.15831401	0.10630101
N	3.79825929	-2.07115216	-0.82808207
F	-1.56314512	-2.01881515	1.60926513
F	-5.73190344	0.72221806	3.89137430
N	-1.09496708	0.16317701	0.03093200
F	-4.21399832	5.24432040	-2.23580417
F	-4.98560738	1.34146110	1.38843010
F	-1.52498112	-3.20332824	-3.81759129
C	-4.46822234	-3.07695023	-1.67463013
F	-2.34643418	-2.63027020	4.12152131
F	-4.43832534	-1.26269210	5.30231439
C	6.08294349	-1.10652508	-0.62001905
H	6.62865250	-1.95684115	-1.00754108
N	2.00360815	3.08767424	1.32198210
F	-5.64038441	-3.75652329	-1.46878011
C	4.19284132	3.49599527	1.38468911
H	5.18238340	3.89770330	1.50936312
C	4.80182037	1.23416709	0.42045703
N	1.81272114	-2.94278623	-0.90762707
C	6.80469554	0.06626601	-0.19593902
C	-3.68827928	1.63456913	-1.99629715
C	-2.97898123	2.64397820	-0.00267700
C	-3.13659924	1.46483811	-0.72916406
C	6.16742346	1.24079810	0.33357903
H	6.77237053	2.08690516	0.63193505
C	-2.41983719	-2.78937621	-2.86245622
C	-2.15166917	-1.66940512	-2.08927116
C	3.96232130	-3.36862126	-1.30003510

H	4.92113437	-3.78407829	-1.55358512
C	-2.97734523	-1.22981209	-1.05729908
C	-2.58964720	-1.27231210	2.15797316
C	-4.15585532	-1.95992615	-0.91135607
C	-3.18318224	-0.25849302	1.41045411
C	-3.58574127	-3.50607727	-2.65150220
C	2.97778023	4.03203931	1.66227013
H	2.71702321	4.99091538	2.07496916
B	-2.62617220	0.04750900	-0.10076901
C	2.71968421	-3.91187630	-1.34749110
H	2.39789419	-4.89317337	-1.64929112
C	-4.25315832	0.37187203	2.03906016
C	-3.88388630	4.01221631	-1.74232413
C	-4.05596231	2.87484722	-2.50911219
C	-3.35385726	3.89217530	-0.46701904
C	-4.67449236	0.05866300	3.32427625
C	-4.03157431	-0.94162007	4.03569231
C	-2.97964023	-1.61949812	3.44279126
F	8.77964065	-0.77853906	-1.22312810
C	8.28046261	0.01055700	-0.19849202
F	8.80072466	-0.53079804	0.97995507
C	2.56438220	1.95409115	0.83351006
C	0.57149705	3.36553326	1.42152511
H	0.36762703	3.72299129	2.43509419
H	0.04516900	2.42160418	1.28598910
C	0.39256003	-3.21925224	-0.70395505
H	-0.02781200	-3.55782527	-1.65482213
H	-0.07151801	-2.27393417	-0.43345003
F	8.86072870	1.26216110	-0.32432703
C	0.13371401	4.39408833	0.38152203
H	-0.89789307	4.67980536	0.60940704
H	0.73461305	5.30741142	0.49503804
C	0.23387802	3.89107530	-1.05930808
H	-0.37231703	2.98148023	-1.16954409
H	1.26878010	3.59261727	-1.27580210
C	0.16594401	-4.24083932	0.40820203
H	-0.91685707	-4.29240233	0.57676504
H	0.48189604	-5.24059540	0.08078001
C	0.87397207	-3.87051129	1.71429113
H	0.72666506	-2.80174921	1.91416514
H	1.95609615	-4.01960531	1.59741112
C	-0.21742702	4.94465638	-2.07003216
H	-1.24461910	5.27340140	-1.87185114
H	-0.18131101	4.55587235	-3.09274524

H	0.42508203	5.83179745	-2.02362716
C	0.35997003	-4.68413736	2.90003122
H	-0.69039305	-4.44536534	3.09923124
H	0.93087907	-4.46615034	3.80885429
H	0.43567503	-5.76090341	2.70620121

Optimized S_0 of **2**:

Pt	0.80814600	0.01812800	-0.00186100
C	0.37205000	1.89219200	-0.68422900
C	-1.13120100	-0.02201400	-0.01016700
N	-0.89656100	-2.17649100	0.76799500
C	-1.84967900	1.08988600	-0.43150200
N	-0.97932400	2.13610800	-0.79893500
C	-3.23708900	1.08171000	-0.45743700
H	-3.81460400	1.93692400	-0.79190700
N	1.06309600	-3.00037700	1.07268300
C	-1.09162800	-3.46306400	1.21619500
H	-2.06932500	-3.89307100	1.36566200
C	-1.80624800	-1.16590200	0.39565200
N	0.94726500	3.04219300	-1.07968300
C	-3.88802500	-0.08611100	-0.04035200
C	-3.19330000	-1.22197300	0.39199600
H	-3.73785900	-2.10699200	0.70248200
C	-1.22307500	3.41263800	-1.25209700
H	-2.21621400	3.79980800	-1.41604800
C	0.14655700	-3.98331000	1.40536700
H	0.45496200	-4.95716100	1.75303700
C	-0.00569400	3.98485500	-1.42601900
H	0.26577500	4.97050700	-1.77119400
F	-5.92255000	0.65951900	-0.96835200
C	-5.38414400	-0.09125300	0.00843700
F	-5.84964700	0.40402800	1.17258100
C	0.44467500	-1.87498400	0.67143900
C	2.50618400	-3.21045700	1.07216900
H	2.78121900	-3.63289300	2.04358900
H	2.96434900	-2.22422400	0.97442400
C	2.37983500	3.31292500	-1.05619800
H	2.64929900	3.76215900	-2.01703900
H	2.87757000	2.34521300	-0.96775400
F	-5.89010800	-1.33024800	-0.11185300
C	2.94768200	-4.12443700	-0.06507000
H	4.03375900	-4.25443600	0.02911700
H	2.50500200	-5.12219400	0.06514900
C	2.61166600	-3.58280600	-1.44969200

H	3.03462800	-2.57517400	-1.55166000
H	1.52366700	-3.46672600	-1.54406300
C	2.76833500	4.22528600	0.10153500
H	3.85096700	4.39302700	0.02958400
H	2.29435900	5.20922200	-0.02342300
C	2.42550200	3.65272000	1.47215700
H	2.86916400	2.65291700	1.56358500
H	1.33913700	3.51122900	1.54892000
C	3.12443400	-4.48575500	-2.56373600
H	4.21496600	-4.59096600	-2.51653300
H	2.86989500	-4.08383900	-3.55027700
H	2.69093000	-5.49063400	-2.48989100
C	2.90220100	4.54803400	2.60815400
H	3.99087700	4.67642200	2.57949800
H	2.64117900	4.12505300	3.58414500
H	2.44902500	5.54485300	2.54357900
Cl	3.27100500	0.06577700	-0.00019200

Optimized T_1 of **2**:

Pt	0.79064000	0.03163900	-0.00827500
C	0.32632700	1.90263500	-0.68537400
C	-1.10822000	-0.05483400	-0.04106800
N	-0.86488000	-2.22458200	0.74916400
C	-1.88704600	1.08707300	-0.46481400
N	-1.03819700	2.13126600	-0.81268000
C	-3.24875800	1.04578200	-0.48087300
H	-3.86192300	1.88100000	-0.80015600
N	1.13248400	-2.97737200	1.06387500
C	-1.00947500	-3.52294500	1.19971500
H	-1.97033400	-3.98993000	1.34546300
C	-1.79393500	-1.26495100	0.38479000
N	0.88651500	3.06422000	-1.07076300
C	-3.88488900	-0.18258500	-0.05367600
C	-3.15851700	-1.33831000	0.38545500
H	-3.70097600	-2.22356900	0.69626100
C	-1.29073600	3.41180800	-1.26373900
H	-2.28670900	3.78728300	-1.43638400
C	0.24538800	-3.99123300	1.39223100
H	0.58737700	-4.95359400	1.74129900
C	-0.07999500	3.99542100	-1.42153500
H	0.18234000	4.98614900	-1.75961800
F	-5.92811300	0.42827400	-1.03827700
C	-5.37268800	-0.18873400	0.02178500
F	-5.82270200	0.46360400	1.11575700

C	0.48000600	-1.87099800	0.65822300
C	2.58050100	-3.14258200	1.07746000
H	2.86079700	-3.54569700	2.05585000
H	3.00893100	-2.14384200	0.97333600
C	2.31326600	3.35969600	-1.04001200
H	2.57983000	3.81335500	-1.99981800
H	2.82747400	2.40095700	-0.94972400
F	-5.87718100	-1.43158000	0.07554900
C	3.06119500	-4.05415700	-0.04578500
H	4.15001800	-4.14876700	0.05905600
H	2.64953200	-5.06429500	0.09099400
C	2.71977300	-3.53796500	-1.43873700
H	3.11099300	-2.51838400	-1.54784700
H	1.62949300	-3.45748200	-1.54266000
C	2.68187400	4.27871400	0.11897500
H	3.76164900	4.46574900	0.05079800
H	2.19121000	5.25436100	-0.00720600
C	2.34399600	3.69945100	1.48797800
H	2.80546900	2.70785400	1.58066000
H	1.26016000	3.53769000	1.55963000
C	3.27053700	-4.43524700	-2.53911100
H	4.36344200	-4.50503800	-2.48191100
H	3.01166700	-4.05179100	-3.53184900
H	2.86878100	-5.45271600	-2.45828900
C	2.79934200	4.60265000	2.62644700
H	3.88554000	4.75143900	2.60221400
H	2.54243400	4.17417300	3.60113300
H	2.32791800	5.59091600	2.56075900
Cl	3.26222300	0.13804600	0.00523800